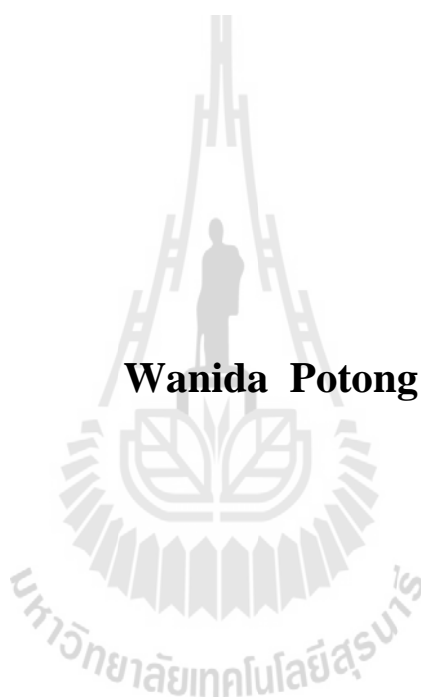


**STUDY OF SOLID-LIQUID EQUILIBRIUM OF
PALMITIC ACID IN N-DECANE – OLEIC ACID**

Wanida Potong



**A Thesis Submitted in Partial Fulfillment of the Requirements for the
Degree of Master of Engineering in Chemical Engineering
Suranaree University of Technology
Academic Year 2011**

การศึกษาสมดุลของแข็ง-ของเหลวของกรดปาล์มมิติก
ในเดคะนสายโซ่ตรง – กรดโอเลอิก



นางสาววนิดา โปธิ์ทอง

วิทยานิพนธ์นี้เป็นส่วนหนึ่งของการศึกษาตามหลักสูตรปริญญาวิศวกรรมศาสตรมหาบัณฑิต
สาขาวิชาวิศวกรรมเคมี
มหาวิทยาลัยเทคโนโลยีสุรนารี
ปีการศึกษา 2554

**STUDY OF SOLID–LIQUID EQUILIBRIUM OF
PALMITIC ACID IN N-DECANE – OLEIC ACID**

Suranaree University of Technology has approved this thesis submitted in partial fulfillment of the requirements for a Master’s Degree.

Thesis Examining Committee

(Assoc. Prof. Dr. Adrian Flood)

Chairperson

(Asst. Prof. Dr. Panarat Rattanaphanee)

Member (Thesis Advisor)

(Dr. Terasut Sookkumnerd)

Member

(Asst. Prof. Dr. Atichat Wongkoblaph)

Member

(Prof. Dr. Sukit Limpijumnong)

Vice Rector for Academic Affairs

(Assoc. Prof. Flt. Lt. Dr. Kontorn Chamniprasart)

Dean of Institute of Engineering

วนิดา โพธิ์ทอง : การศึกษาสมดุลของแข็ง-ของเหลวของกรดปาล์มมิติกในเดเคน
สายโซ่ตรง – กรดโอเลอิก (STUDY OF SOLID-LIQUID EQUILIBRIUM OF
PALMITIC ACID IN N-DECANE – OLEIC ACID) อาจารย์ที่ปรึกษา :
ผู้ช่วยศาสตราจารย์ ดร.พนารัตน์ รัตนพานิช, 125 หน้า.

ปัญหาหนึ่งที่มีกพบในอุตสาหกรรมการผลิตฮาร์ดดิสค์คือ การมีสารตกค้างบนชิ้นงาน
เกินค่าที่ยอมรับได้ ทำให้มีการส่งผลิตภัณฑ์กลับจากลูกค้า และการทิ้งผลิตภัณฑ์ที่ไม่ผ่านมาตรฐาน
เป็นจำนวนมาก ส่งผลให้ต้นทุนต่อหน่วยผลิตภัณฑ์เพิ่มสูงขึ้น และผลกำไรจากการประกอบการ
ลดลงอย่างต่อเนื่อง ผลการวิเคราะห์กลุ่มตัวอย่างชิ้นงานที่มีสารตกค้างจากโรงงานแห่งหนึ่งพบว่า
สารที่ตกค้างบนชิ้นงานเป็นสารประกอบไฮโดรคาร์บอนแบบโซ่ตรง เมื่อวิเคราะห์ขั้นตอนการผลิต
ชิ้นงานดังกล่าว จึงสันนิษฐานว่า สารประกอบชนิดนี้อาจเกิดจากการตกค้างของน้ำมันหล่อเย็น ซึ่ง
ประกอบด้วย น้ำมันแร่ (mineral oil) 95.29% โดยโมล และกรดไขมัน (fatty acids) 4 ชนิดคือ กรด
ปาล์มมิติก (palmitic acid) 2.19% กรดโอเลอิก (oleic acid) 1.66% กรดสเตียริก (stearic acid)
0.33% และกรดไลโนเลอิก (linoleic acid) 0.53% โดยโมล หรือเกิดจากการตกค้างของสารล้าง ซึ่ง
ประกอบด้วย เดเคนสายโซ่ตรง (n-decane) 98.82% และออกเทนสายโซ่ตรง (n-octane) 1.18%
โดยโมล ผลการศึกษาความสามารถในการละลายระหว่างองค์ประกอบของน้ำมันหล่อเย็น และของ
สารล้าง ที่อุณหภูมิระหว่าง 5 ถึง 50 องศาเซลเซียส พบว่าน้ำมันหล่อเย็นกับสารล้างสามารถละลาย
เข้าด้วยกันได้อย่างสมบูรณ์ (completely miscible) ตลอดช่วงอุณหภูมิที่ทำการศึกษา แต่กรดไขมัน
ในน้ำมันหล่อเย็นสามารถละลายในสารละลายไฮโดรคาร์บอนได้ที่บางอุณหภูมิเท่านั้น

งานวิจัยนี้มีจุดมุ่งหมายเพื่อศึกษาพฤติกรรมทางความร้อนในการเปลี่ยนแปลงเฟสด้วย
เครื่องดีฟเฟอเรนเชียลสแกนนิ่งแคลอริมิเตอร์ ของกรดไขมันบริสุทธิ์ และสารผสมที่ประกอบด้วย
เดเคนสายโซ่ตรง กรดปาล์มมิติก และกรดโอเลอิก ในกระบวนการหลอมเหลวจะเป็นการเปลี่ยนแปลง
เฟสระหว่างของแข็งเป็นของเหลว โดยแสดงด้วยเส้นกราฟความร้อน (heating curve) สำหรับการ
เปลี่ยนแปลงเฟสระหว่างของเหลวเป็นของแข็งจะเกิดขึ้นในกระบวนการทำความเย็น ซึ่งแสดงด้วย
เส้นกราฟความเย็น (cooling curve) ผลการศึกษาการเปลี่ยนแปลงเฟสของกรดปาล์มมิติกบริสุทธิ์
พบว่า อุณหภูมิการหลอมเหลว และเอนทัลปีของการหลอมเหลวแสดงค่าสอดคล้องกับค่า
ที่รายงานไว้ในวรรณกรรมต่างๆ สำหรับกรดโอเลอิกบริสุทธิ์ในกระบวนการหลอมเหลวแสดงการ
เปลี่ยนแปลงเฟสแบบผันกลับได้ระหว่างของแข็ง-ของแข็ง และสำหรับสารผสมสามองค์ประกอบ
พบว่า การเปลี่ยนแปลงเฟสจะขึ้นอยู่กับปริมาณของกรดไขมันในสารผสม ในขณะที่ปริมาณของ
เดเคนสายโซ่ตรงไม่มีผลต่อการเปลี่ยนแปลงเฟส ณ อุณหภูมิที่ทำการวิเคราะห์ ผลการศึกษาค่า
ความจุความร้อนจำเพาะในสถานะของเหลวสำหรับกรดไขมันบริสุทธิ์ และสารผสมสาม

องค์ประกอบพบว่า แสดงค่าสอดคล้องกับค่าที่คำนวณได้ นอกจากนี้ค่าความจุความร้อนจำเพาะของสารผสมสามองค์ประกอบแสดงพฤติกรรมเชิงเส้นตรงกับช่วงอุณหภูมิที่ทำการศึกษาในสถานะของเหลว

จากพฤติกรรมการเปลี่ยนแปลงเฟสของสารผสมสามองค์ประกอบ จึงทำการศึกษาความสัมพันธ์ระหว่างของแข็ง-ของเหลวของ เดคเคนสายโซ่ตรง + กรดปาล์มมิติก + กรดโอเลอิก ในช่วงอุณหภูมิระหว่าง 305.15 ถึง 323.15 องศาเซลวิน ซึ่งข้อมูลที่ได้จากการทดลองจะนำมาอธิบายกลไกการเกิดสารตกค้างบนชิ้นงานในกระบวนการที่เกี่ยวข้องกับสารผสมระหว่างสารไฮโดรคาร์บอนกับกรดไขมัน ผลการศึกษาพบว่า กรดปาล์มมิติกเป็นองค์ประกอบหลักในเฟสของแข็ง และผลการคำนวณสัมประสิทธิ์แอกทิวิตี้ของกรดปาล์มมิติกในสารผสม พบว่ามีค่ามากกว่าหนึ่งซึ่งบ่งบอกว่าการละลายของกรดปาล์มมิติกมีค่าต่ำกว่าค่าการละลายในทางอุดมคติ ข้อมูลการทดลองของการละลายของกรดปาล์มมิติกในสารผสมนำมาเปรียบเทียบกับสมการ NRTL และ UNIQUAC ซึ่งพบว่า สมการ UNIQUAC มีความเหมาะสมสำหรับอธิบายความสัมพันธ์ระหว่างของแข็ง-ของเหลวของกรดปาล์มมิติกในสารผสมของเดคเคนสายโซ่ตรงกับกรดโอเลอิก มากกว่าสมการ NRTL โดยการเปรียบเทียบจากค่าเบี่ยงเบนมาตรฐานของอุณหภูมิ



สาขาวิชา วิศวกรรมเคมี

ปีการศึกษา 2554

ลายมือชื่อนักศึกษา _____

ลายมือชื่ออาจารย์ที่ปรึกษา _____

ลายมือชื่ออาจารย์ที่ปรึกษาร่วม _____

WANIDA POTONG : STUDY OF SOLID–LIQUID EQUILIBRIUM OF
PALMITIC ACID IN N-DECANE – OLEIC ACID. THESIS ADVISOR :
ASST. PROF. PANARAT RATTANAPHANEE, Ph.D., 125 PP.

SOLID–LIQUID EQUILIBRIUM/UNIQUAC/NRTL/CUTTING FLUID/HARD
DISK DRIVE

A problem normally encountered in manufacturing of hard disk drive components is the surface contamination of the product, which results in product rejection prolonged production time, increasing production cost, and thus decreasing profit of the production. Sample analysis showed that the residues on the specimen were aliphatic hydrocarbons. This residue could be from two possible sources in the production lines, i.e. the cutting fluid and the cleaning solvent. Component analysis of these two fluids showed that the cutting fluid composed of 95.29% mineral oil, 2.19% palmitic acid, 1.66% oleic acid, 0.33% stearic acid, and 0.53% linoleic acid by mole, while the cleaning solvent was found to compose of 98.82% n-decane and 1.18% n-octane by mole. Preliminary study of solubility for the cutting fluid and cleaning solvent at the temperature range of 5–50°C showed that the mixtures were completely miscible, but fatty acids could dissolve in hydrocarbon solvents only a limited temperature range.

This research aims to analyze the thermal behavior of pure fatty acids and ternary mixtures containing n-decane, palmitic acid and oleic acid using differential scanning calorimetry (DSC). Solid–liquid and liquid–solid phase transitions were observed on the DSC heating and cooling curves. Melting temperature and enthalpy of melting for pure palmitic acid were in good agreement with the values previously

reported in the literatures. For pure oleic acid, two endothermic peaks appeared on heating curve, which could relate to a reversible solid–solid phase transition of this acid. Phase transition of the ternary mixtures was found to depend on the quantities of fatty acids in the mixtures, while the quantity of n-decane did not affect the phase transition at the studied temperature range. The liquid specific heat capacity for pure fatty acids and ternary mixtures were in good agreement with the estimated values. The specific heat capacity for the liquid phase of the ternary mixtures was observed to depend linearly on the temperature in the range studied here.

Solid–liquid equilibria of ternary mixtures were determined in the temperature range of 305.15–323.15 K. The co-existing solid and liquid phases were found to contain substantial different compositions. Palmitic acid was the major component in the solid phase, which was likely the result of its positive deviation behavior in the ternary mixtures. Activity coefficient larger than unity emphasized that the observed solubility of palmitic acid was lower than the value predicted for the case of ideal solution. The experimental data of the palmitic acid solubility were correlated with the NRTL and UNIQUAC models. The best description of solid–liquid equilibrium of palmitic acid in n-decane – oleic acid was obtained from UNIQUAC model.

School of Chemical Engineering

Academic Year 2011

Student's Signature _____

Advisor's Signature _____

Co-advisor's Signature _____

ACKNOWLEDGEMENT

First and foremost, I would like to express my sincere thanks to my thesis advisors, Asst. Prof. Dr. Panarat Rattanaphanee and Dr. Terasut Sookkumnerd for their limitless patience, invaluable help and constant encouragement throughout the course of this research. I am most grateful for their advice involving the research and living. I would not have achieved this far, and this thesis would not have been completed if I had not received the supports from them.

I would also like to acknowledge the valuable suggestions provided to me by all the faculty members in school of chemical engineering, especially Assoc. Prof. Dr. Adrian E. Flood, Asst. Prof. Dr. Atichat Wongkoblak for their services as my committee member.

In addition, I gratefully acknowledge the financial support from the Industry/University Cooperative Research Center (I/UCRC) in HDD Component, the Faculty of Engineering, KhonKaen University and National Electronics and Computer Technology Center, National Science and Technology Development Agency.

Finally, I am grateful to my parents and my friends for all their supports throughout the period of my graduate study.

Wanida Potong

TABLE OF CONTENTS

	Page
ABSTRACT (THAI)	I
ABSTRACT (ENGLISH)	III
ACKNOWLEDGEMENTS	V
TABLE OF CONTENTS	VI
LIST OF TABLES	XII
LIST OF FIGURES	XV
SYMBOLS AND ABBREVIATIONS	XIX
 CHAPTER	
I INTRODUCTION	1
1.1 Background and Significance of the Problem	1
1.2 Research Objectives	4
1.3 Scope and Limitations of the Research	4
1.3.1 Thermal Properties of Pure Fatty Acids and Mixtures	4
1.3.2 The Solid–Liquid Equilibria of Mixtures	4
1.3.3 Thermodynamic Models	5
1.4 Outputs	5
1.5 References	5

TABLE OF CONTENTS (Continued)

	Page
II ANALYSIS OF PHASE TRANSFORMATION OF PURE FATTY ACIDS AND ITS MIXTURES BY DIFFERENTIAL SCANNING CALORIMETRY	7
2.1 Abstract	7
2.2 Introduction	8
2.3 Theory	10
2.3.1 Differential Scanning Calorimetry (DSC)	10
2.3.2 Interpretation of the DSC Thermogram	11
2.3.2.1 Glass Transition Temperature, T_g	11
2.3.2.2 Melting Temperature, T_m	12
2.3.2.3 Crystallization Temperature, T_{cryst}	14
2.3.3 Estimation of Specific Heat Capacity by DSC	14
2.3.4 Estimation of Liquid Specific Heat Capacity for Pure Components (n-decane, palmitic acid and oleic acid) and Its Mixtures	15
2.4 Experimental Procedures	18
2.4.1 Chemicals	18
2.4.2 Preparation of Ternary Mixtures	18

TABLE OF CONTENTS (Continued)

	Page
2.4.3 Differential Scanning Calorimetry (DSC)	18
2.5 Results and Discussion	20
2.5.1 Baselines for DSC Analysis	20
2.5.2 Calibration Curve of the DSC Analysis	20
2.5.3 DSC Analysis for Pure Palmitic Acid	21
2.5.4 DSC Analysis for Pure Oleic Acid	24
2.5.5 DSC Analysis of n-Decane – Palmitic Acid – Oleic Acid Mixture with Mass Ratio (D:P:O) of 1:1:1	28
2.5.6 DSC Analysis of n-Decane – Palmitic Acid – Oleic Acid Mixtures with Mass Ratio (D:P:O) of 1:0.5:1	30
2.5.7 DSC Analysis of n-Decane – Palmitic Acid – Oleic Acid Mixtures with Mass Ratio (D:P:O) of 1:0.3:1	33
2.5.8 DSC Analysis of n-Decane – Palmitic Acid – Oleic Acid Mixtures with Mass Ratio (D:P:O) of 1:0.2:1	36

TABLE OF CONTENTS (Continued)

	Page
2.5.9 DSC Analysis of n-Decane – Palmitic Acid – Oleic Acid Mixtures with Mass Ratio (D:P:O) of 1:0.1:1	39
2.6 Conclusion	44
2.7 References	45
III STUDY OF SOLID-LIQUID EQUILIBRIA OF TERNARY N-DECANE + PALMITIC ACID + OLEIC ACID MIXTURES	48
3.1 Abstract	48
3.2 Introduction	49
3.3 Theory	51
3.3.1 Solid-Liquid Equilibria	51
3.3.2 Thermodynamic Models	55
3.3.2.1 The Non-Random Two-Liquid (NRTL) Model	55
3.3.2.2 The UNiversal QUAsi-Chemical (UNIQUAC) Model	56
3.3.3 Broyden's Method	58
3.4 Experimental Procedures	62
3.4.1 Chemicals	62

TABLE OF CONTENTS (Continued)

	Page
3.4.2 Preparation of Ternary Mixtures	62
3.4.3 Solid–Liquid Equilibria	62
3.4.4 Analysis of the Compositions	63
3.4.5 Determination of Components in Liquid and Solid Phases	63
3.5 Results and Discussion	65
3.5.1 Solid–Liquid Equilibria	65
3.5.2 Solid–Liquid Equilibrium Models	70
3.6 Conclusion	75
3.7 References	76
IV CONCLUSIONS AND RECOMMENDATIONS	78
4.1 Conclusions	78
4.2 Recommendations	81
APPENDICES	
APPENDIX A. COMPONENT ANALYSIS OF CUTTING FLUID AND CLEANING SOLVENT SAMPLES	82
APPENDIX B. PROPERTIES OF N-DECANE, PALMITIC ACID AND OLEIC ACID	88

TABLE OF CONTENTS (Continued)

	Page
APPENDIX C. PRELIMINARY STUDY OF MISCIBILITY OF CUTTING FLUID AND CLEANING SOLVENT BY SPECTROPHOTOMETER	94
APPENDIX D. DSC ANALYSIS FOR PURE OLEIC ACID	97
APPENDIX E. EXAMPLE OF COMPONENT ANALYSIS OF N-DECANE + PALMITIC ACID + OLEIC ACID MIXTURE	107
APPENDIX F. ESTIMATION OF LIQUID SPECIFIC HEAT CAPACITY OF PURE FATTY ACIDS AND TERNARY MIXTURES	115
APPENDIX G. SOLID-LIQUID EQUILIBRIUM BY NRTL AND UNIQUAC MODELS	119
BIOGRAPHY	125

LIST OF TABLES

Table	Page
2.1 The significant properties of fatty acids	17
2.2 The values of <i>a</i> , <i>b</i> , <i>c</i> , and <i>d</i> in each group (Rihani et al., 1965)	17
2.3 Thermal properties for phase transition of pure palmitic acid	22
2.4 Specific heat capacities for the solid and liquid phase of pure palmitic acid	24
2.5 Specific heat capacities for the liquid phase of pure oleic acid	27
2.6 Specific heat capacities for the liquid phase of the ternary mixture with mass ratio (D:P:O) of 1:1:1	30
2.7 Specific heat capacities for the liquid phase of the ternary mixture with mass ratio (D:P:O) of 1:0.5:1	33
2.8 Specific heat capacities for the liquid phase of the ternary mixture with mass ratio (D:P:O) of 1:0.3:1	36
2.9 Specific heat capacities for the liquid phase of the ternary mixture with mass ratio (D:P:O) of 1:0.2:1	39

LIST OF TABLES (Continued)

Table	Page
2.10 Thermal properties for phase transition of pure palmitic acid and ternary n-decane – palmitic acid – oleic acid mixtures obtained from the DSC analysis	41
2.11 Specific heat capacities for the liquid phase of the ternary mixture with mass ratio (D:P:O) of 1:0.1:1	43
3.1 Structure parameters for UNIQUAC equation (Abrams et al., 1975)	58
3.2 Temperature program for the analysis	64
3.3 Equilibrium temperature and composition of ternary n-decane (1) + palmitic acid (2) + oleic acid (3) mixtures	69
3.4 Solubility and activity coefficient of palmitic acid in n-decane – oleic acid	71
3.5 Energy parameters of NRTL model for the palmitic acid in n-decane – oleic acid system	74
3.6 Energy parameters of UNIQUAC model for the palmitic acid in n-decane – oleic acid system	74
A.1 Component analysis of fatty acid methyl ester in 1 g of cutting fluid	83
A.2 Quantities of four fatty acids (mg) in 1 g of cutting fluid	85
A.3 Hydrocarbon content of mineral oil	86

LIST OF TABLES (Continued)

Table	Page
A.4	Percent by mole of mineral oil and four fatty acids in cutting fluid86
A.5	Hydrocarbon content of cleaning solvent87
B.1	Chemical and physical properties of n-decane90
B.2	Chemical and physical properties of palmitic acid91
B.3	Chemical and physical properties of oleic acid92
D.1	Thermal properties for liquid–solid phase transition of pure oleic acid at 3, 5, 7, 9 and 10°C/min99
D.2	Specific heat capacity of oleic acid for the liquid phase with the scanning rate of 3°C/min102
D.3	Specific heat capacity of oleic acid for the liquid phase with the scanning rate of 5°C/min103
D.4	Specific heat capacity of oleic acid for the liquid phase with the scanning rate of 7°C/min104
D.5	Specific heat capacity of oleic acid for the liquid phase with the scanning rate of 9°C/min105
D.6	Specific heat capacity of oleic acid for the liquid phase with the scanning rate of 10°C/min106
E.1	Mass ratio of n-decane, palmitic acid and oleic acid in ternary mixture113

LIST OF FIGURES

Figure	Page
1.1 The typical components of a hard disk drive	2
2.1 Schematic diagram of power compensation DSC	12
2.2 Schematic diagram of heat flux DSC	13
2.3 DSC thermogram	13
2.4 Baselines from Perkin-Elmer PYRIS Diamond DSC	20
2.5 Calibration curve of the DSC using indium as the standard sample	21
2.6 The DSC analysis for pure palmitic acid	22
2.7 The DSC curve for specific heat capacity of pure palmitic acid in melting process	23
2.8 DSC analysis for pure oleic acid	25
2.9 A study of polymorphism in oleic acid (Suzuki et al., 1985)	26
2.10 The DSC curve for specific heat capacity of pure oleic acid in melting process	27
2.11 DSC analysis for ternary mixture with n-decane : palmitic acid : oleic acid mass ratio of 1:1:1	28
2.12 Specific heat capacity for ternary mixture with mass ratio of 1:1:1 in melting process	29

LIST OF FIGURES (Continued)

Figure	Page
2.13 DSC analysis for ternary mixture with n-decane : palmitic acid : oleic acid mass ratio of 1:0.5:1	31
2.14 Specific heat capacity for ternary mixture with mass ratio of 1:0.5:1 in melting process	32
2.15 DSC analysis for ternary mixture with n-decane : palmitic acid : oleic acid mass ratio of 1:0.3:1	34
2.16 Specific heat capacity for ternary mixture with mass ratio of 1:0.3:1 in melting process	35
2.17 DSC analysis for ternary mixture with n-decane : palmitic acid : oleic acid mass ratio of 1:0.2:1	37
2.18 Specific heat capacity for ternary mixture with mass ratio of 1:0.2:1 in melting process	38
2.19 DSC analysis for ternary mixture with n-decane : palmitic acid : oleic acid mass ratio of 1:0.1:1	40
2.20 Specific heat capacity for ternary mixture with mass ratio of 1:0.1:1 in melting process	42
3.1 Thermodynamic cycle for calculating the fugacity of pure subcooled liquid	52
3.2 Illustration of temperature program	64

LIST OF FIGURES (Continued)

Figure	Page
3.3	Mole fraction of palmitic acid in liquid phase with mass ratios (D:P:O) of 1:0.3:1, 1:0.5:1 and 1:1:166
3.4	Ternary phase diagram of n-decane + palmitic acid + oleic acid in liquid phase with mass ratio of 0.2:1:1, 1:1:1 and 3:1:167
3.5	Solubility of palmitic acid in n-decane – oleic acid: (—) is experiment and (- -) is ideal solution ($\gamma_2 = 1$) calculated from Eq. (3.22)71
B.1	Molecular structure of n-decane89
B.2	Molecular structure of palmitic acid91
B.3	Molecular structure of oleic acid92
C.1	The absorbance measurement at T = 5–50°C96
D.1	DSC analysis for pure oleic acid with the scanning rate of 3°C/min99
D.2	DSC analysis for pure oleic acid with the scanning rate of 5°C/min100
D.3	DSC analysis for pure oleic acid with the scanning rate of 7°C/min100
D.4	DSC analysis for pure oleic acid with the scanning rate of 9°C/min101

LIST OF FIGURES (Continued)

Figure	Page
D.5 DSC analysis for pure oleic acid with the scanning rate of 10°C/min	101
D.6 The DSC curve for specific heat capacity of oleic acid in melting process with the heating rate of 3°C/min	102
D.7 The DSC curve for specific heat capacity of oleic acid in melting process with the heating rate of 5°C/min	103
D.8 The DSC curve for specific heat capacity of oleic acid in melting process with the heating rate of 7°C/min	104
D.9 The DSC curve for specific heat capacity of oleic acid in melting process with the heating rate of 9°C/min	105
D.10 The DSC curve for specific heat capacity of oleic acid in melting process with the heating rate of 10°C/min	106
E.1 Component analysis in liquid phase	110
E.2 Component analysis in solid phase	113

SYMBOLS AND ABBREVIATIONS

T_g	=	the glass transition, °C or K
T_m	=	the melting temperature, °C or K
T_{im}	=	the onset temperature of melting, °C
T_{cryst}	=	the crystallization temperature, °C or K
$T_{i,cryst}$	=	the onset temperature of crystallization, °C
T_c	=	the critical temperature, K
T_r	=	the reduce temperature, K
$T_{t,i}$	=	the triple-point temperature of component i , °C or K
T	=	the temperature, °C or K
	=	the equilibrium temperature, K
	=	the absolute temperature, K
T_i^{cal}	=	the equilibrium temperature calculated from Eq. (3.22), K
T_i^{exp}	=	the experimental equilibrium temperature, K
\bar{C}_p	=	the specific heat capacity, J/g·K or J/mol·K
\bar{C}_{pm}	=	the specific heat capacity of mixture, J/g·K or J/mol·K
\bar{C}_{pi}	=	the specific heat capacity of component i , J/g·K or J/mol·K
C_p^o	=	the ideal specific heat capacity, J/g·K or J/mol·K
C_p	=	the heat capacity, J/°C or J/K

SYMBOLS AND ABBREVIATIONS (Continued)

$\Delta C_{p,i}$	=	the difference between the heat capacity of the liquid and solid phases, J/°C or J/K
ΔH_f	=	the enthalpy of fusion, J/g or J/mol
$\Delta H_{f,i}$	=	the enthalpy of fusion of component i , J/g or J/mol
ΔH_c	=	the enthalpy of crystallization, J/g or J/mol
ω	=	the acentric factor, -
R	=	the universal gas constant, 8.31451 J·mol ⁻¹ ·K ⁻¹
x_i	=	the mole fraction of component i in liquid phase, -
x_1	=	the mole fraction of n-decane in liquid phase, -
x_2	=	the mole fraction of palmitic acid in liquid phase, -
x_3	=	the mole fraction of oleic acid in liquid phase, -
γ_i	=	the activity coefficient of component i in liquid phase, -
g^E	=	the excess Gibb energy per mole, J/mol
m	=	the number of components, -
n	=	the number of experimental data, -
τ	=	the dimensionless interaction parameter, -
g	=	the interaction energy parameter, J/mol
G	=	the dimensionless interaction energy parameter, -
α	=	the nonrandomness parameter in NRTL equation, -
a	=	the binary interaction parameter in UNIQUAC equation, K

SYMBOLS AND ABBREVIATIONS (Continued)

r	=	the pure component volume parameter, -
q and q'	=	the pure component area parameter, -
Φ_i^*	=	the segment fraction, -
θ_i and θ'_i	=	the area fraction, -
z	=	the lattice coordination number, a constant here set equal to 10
σ	=	the root mean square deviation of temperature, K
	=	standard deviation, mg
J	=	Jacobian matrix
DSC	=	Differential Scanning Calorimetry
SLE	=	Solid-Liquid Equilibrium
D	=	n-decane
P	=	palmitic acid
O	=	oleic acid
NRTL	=	Non-Random Two-Liquid
UNIQUAC	=	UNIversal QUAsi Chemical

CHAPTER I

INTRODUCTION

1.1 Background and Significance of the Problem

Typical components of a hard disk drive are shown in Fig. 1.1 which composes of disk platters, read/write heads, spindle motor (inside platter hub), head actuator mechanism, logic board (controller or printed circuit board), cables and connectors, configuration items (such as jumpers or switches), etc.

The platters, spindle motor, heads, and head actuator mechanism are usually contained in a sealed chamber called the hard disk assembly (HDA). It is considered as a single component, which is rarely opened. Logic board and other configurations are the external parts of HDA, can be disassembled from the drive.

Spindle motor is high precision electric motor that is connected to the spindle on which the platters are mounted in a hard disk drive. It is responsible for rotating the platters at high speed of 3600 to 7200 RPM or more. Production of spindle motor is generally started with metal cutting and machining to obtain a desired shape. This step requires a use of cutting fluids to lubricate and cool the cutting tool during the operations. The fluid is cleaned off afterward by washing with the proper solvents.

There are four primary categories of cutting fluids that differ in terms of their thermophysical properties. Straight oils or cutting oils are composed of a base mineral oil or petroleum-derived oil, and often contains polar components for reducing friction between moving surfaces such as fats, vegetable oils, and trace amounts of other additives. Soluble oils are mixtures of oil and water to increase cooling

capacities over straight oils and offer some rust protection. Semi-synthetic oils are similar to soluble oils in performance characteristics, but differ in composition because 30% or less of the total volume of the concentrate contains inorganic or other compounds that dissolve in water. Synthetic oils are chemical fluids that contain inorganic or other chemicals dissolved in large amount of water and offer superior cooling performance (Adler et al., 2006).

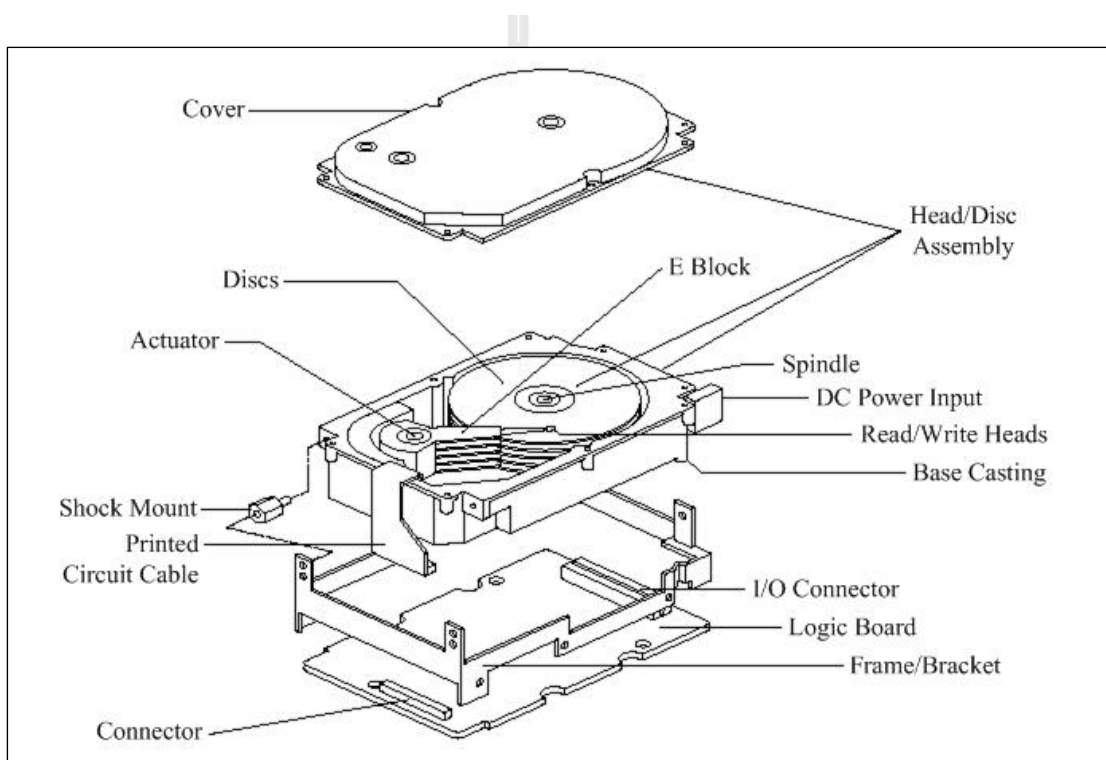


Figure 1.1 The typical components of a hard disk drive.

One of major problem encountered in manufacturing of hard disk drive components is the contamination of the products which results in the product rejection, higher cost of production, and lower profit for the manufacturer. Report from one spindle motor manufacturer revealed that the surface contaminations on the

spindle motor were hydrocarbons of aliphatic structure, which could be from two possible sources in the production line, i.e. the cutting fluids and the washing solvents used during metal cutting and machining.

Component analysis of these two fluids showed that the cutting fluids used in the production of spindle motor was a type of straight oils which composed of 95.29% mineral oil, 2.19% palmitic acid, 1.66% oleic acid, 0.33% stearic acid, and 0.53% linoleic acid by mole, while the washing solvents was found to compose of 98.82% n-decane and 1.18% n-octane by mole.

The four mixed fatty acids are used as an additive to reduce friction of the tool-workpiece interface by adsorbing on metal surfaces and that the adsorbed layer is responsible for the improved lubricating characteristics of the fluids and the rust protection.

Preliminary study on miscibility between the cutting fluids and the washing solvents used in this particular manufacturer in the temperature range of 5–50°C showed that the fatty acids could be dissolved in hydrocarbon solvents only in a few temperature ranges. Furthermore, a study of the solid–liquid equilibrium of palmitic acid in hexane and heptane, the temperature range of 290–325 K (Calvo et al., 2009) shown that the palmitic acid solubilities in linear hydrocarbons were low at low temperatures. It is therefore hypothesized that incomplete dissolution between fatty acids and hydrocarbon might be the cause of the surface contamination of the spindle motor.

1.2 Research Objectives

This research will use the mixtures of n-decane, palmitic acid, and oleic acid. Because of the both acids and n-decane are the main components of the cutting fluids and the washing solvents, respectively. Pure fatty acids and ternary mixtures at various mass ratios will be used for study as follow:

1.2.1 To study the thermal behavior and determine thermal properties of pure fatty acids and mixtures.

1.2.2 To study the solid–liquid equilibria (SLE) of n-decane (D) + palmitic acid (P) + oleic acid (O) mixtures at atmospheric pressure.

1.2.3 To evaluate the activity coefficient of components in the solid–liquid equilibria and correlate the experimental solubility data with thermodynamic models.

1.3 Scope and Limitations of the Research

1.3.1 Thermal Properties of Pure Fatty Acids and Mixtures

Pure fatty acids and ternary mixture of n-decane + palmitic acid (P) + oleic acid with various mass ratios will be studied the solid–liquid and liquid–solid phase transformations using the differential scanning calorimetry (DSC). Mass ratios (D:P:O) studied in this work compose of 1:1:1, 1:0.5:1, 1:0.3:1, 1:0.2:1, and 1:0.1:1. Results of the DSC analysis will report thermal properties of substance such as peak temperature, onset temperature, enthalpy of fusion and solidification as well as specific heat capacity.

1.3.2 The Solid–Liquid Equilibria of Mixtures

Ternary mixtures with mass ratio (D:P:O) of 1:1:1, 1:0.5:1, 1:0.3:1, 3:1:1, 0.2:1:1, and 1:1:0.5 will be determined the solid–liquid equilibrium at

atmospheric pressure in the temperature range of 10–50°C. At equilibrium temperature of each mixture, the quantity of n-decane, palmitic acid, and oleic acid that existed in the liquid and solid phases will be determined by gas chromatograph (GC).

1.3.3 Thermodynamic Models

Experimental results of the solid–liquid equilibria will be used to determine the activity coefficient of each component in the liquid phase which can be calculated by general equation of the solubility of solids in liquids. The interaction parameters of the systems can be evaluated by correlating the experimental results with the NRTL and UNIQUAC models.

1.4 Outputs

1.4.1 Results of the thermal properties of pure fatty acids and mixtures obtained from the DSC analysis.

1.4.2 Experimental results of the solid–liquid equilibria of n-decane + palmitic acid + oleic acid mixtures at atmospheric pressure in the temperature range of 10–50°C.

1.4.3 Interaction parameters for the NRTL and UNIQUAC models that consistent with the solid–liquid equilibria for the system of n-decane + palmitic acid + oleic acid mixtures.

1.5 References

Adler, D.P., Hii, W.W.-S., Michalek, D.J., and Sutherland, J.W. (2006). Examining the role of cutting fluids in machining and efforts to address associated

environmental/health concerns. **Machining Science and Technology**. 10: 23-58.

Calvo, B., Collado, I., and Cepeda, E.A. (2009). Solubilities of palmitic acid in pure solvents and its mixtures. **Journal of Chemical & Engineering Data**. 54(1): 64-68.



CHAPTER II

ANALYSIS OF PHASE TRANSFORMATION OF PURE FATTY ACIDS AND ITS MIXTURES BY DIFFERENTIAL SCANNING CALORIMETRY

2.1 Abstract

Thermal characteristic for pure fatty acids and its mixtures were analyzed by differential scanning calorimetry (DSC). Solid–liquid and liquid–solid phase transitions were observed on the heating and cooling curves. Melting temperature and enthalpy of melting for pure palmitic acid were in good agreement with the values previously reported in the literatures (Cedeño et al., 2001). For pure oleic acid, a reversible solid–solid phase transition from γ to α phase was observed on the heating curve. For the ternary mixtures of palmitic acid, oleic acid and n-decane, the thermal properties of solid–liquid and liquid–solid phase transitions were found to depend on the quantities of palmitic acid and oleic acid in the mixtures. The liquid specific heat capacity obtained for pure fatty acids and ternary mixtures were in good agreement with the estimated values. The specific heat capacity for the liquid phase of the ternary mixtures was observed to depend linearly on the temperature in the range studied here.

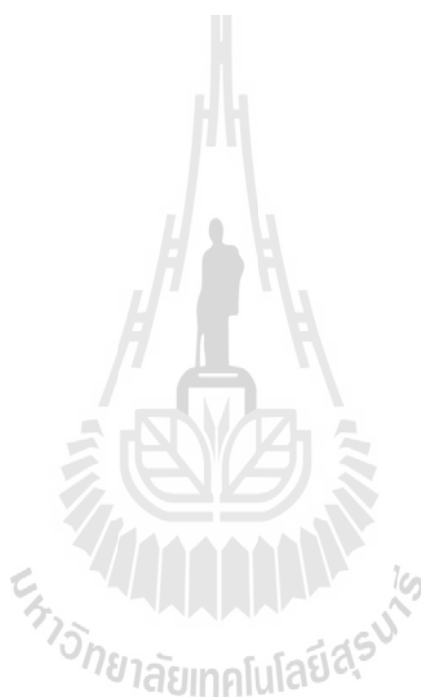
2.2 Introduction

Fatty acids are the most commonly used for friction modifiers to reduce friction between moving surfaces in machining operations. They are classified as the adsorption layer forming friction modifiers where carboxylic acid acts as polar part that can be adsorbed on metal surface (Mang et al., 2007). For example straight oil or neat oil which is one type of cutting fluids. Polar components used as friction modifiers include fats, vegetable oils, ester, and other additives. Neat oil is used in a variety of machining operations from light machining to heavy duty operations such as grinding, turning, milling, tapping, gear cutting etc.

In manufacturing of hard disk drive components, neat oil is as well used. For example production of spindle motor, which is normally started with metal cutting and machining, neat oil is used in this step for lubricating and reducing the heat generated during the operations. However, a problem encountered from one spindle motor manufacturer is surface contamination of the products. This problem results in product rejection and increasing product cost and thus profit of the production decreases.

Analysis of the solid contaminant revealed that its major composition was aliphatic hydrocarbon. Two possible sources of contaminant are neat oil and cleaning solvent used during the machining, since, the main ingredient of neat oil consists of 90% mineral oil and 10% mixed fatty acids where palmitic acid and oleic acid are main components, while the cleaning solvent consists of 98.8% n-decane and 1.2% n-octane. Preliminary study of the solubility between cutting fluid and cleaning solvent in various volume ratios shows that mixed fatty acids in cutting fluid cannot dissolve with hydrocarbons of cleaning solvent in a few temperature ranges.

A study of thermal behaviors of mixed fatty acids and hydrocarbons is needed in order to understand the phase transition which would be useful when working with the fatty acid containing hydrocarbon solution. This research uses mixtures of palmitic acid (C16:0), oleic acid (C18:1), and n-decane at various mass ratios as the modeled systems for studying the thermal properties of the mixture using differential scanning calorimetry (DSC).



2.3 Theory

2.3.1 Differential Scanning Calorimetry (DSC)

Differential scanning calorimetry is one of thermal analysis techniques. It is widely used to measure the heat flow required to raise or lower a sample as it is heated, cooled or held at a constant temperature (isothermal). Applications of DSC include characterization of polymers, fibers, thermosets, elastomers, composites, pharmaceuticals, foods, cosmetics, as well as organics and inorganics. The important properties obtained from analysis by DSC for example glass transition (T_g), melting temperature (T_m), crystallization temperature (T_{cryst}), specific heat capacity (\bar{C}_p), heat of melting (ΔH_f) and crystallization (ΔH_{cryst}), polymorphism, etc. The DSC is commercially available as a power compensation DSC and as a heat-flux DSC.

The structure of a power compensation DSC is shown in Figure 2.1. It has two separate identical holders (sample and reference holders), each equipped with its own heater and sensor. Both holders are covered with a platinum lid. Platinum resistance thermometers (Pt sensor) are used to measure the temperature of the base of the sample and reference holders, which attach into the base of the calorimeter holder. Next to the thermometers, the two individual heaters are also attached into the bottom of the holders. Both furnaces are very lightweight with a mass of only 1 g. This provides exceptionally nimble performance in terms of rapid equilibration and the ability to heat and cool at ultra fast rates. The power compensation DSC records the actual energy as a function of the actual sample temperature.

The structure of a heat flux DSC is shown in Figure 2.2. In this design, sample and reference pans are heated by a single furnace, which is much larger in mass than the furnaces used in a power compensation DSC. The sample and reference

pan are placed on the sample and reference holders. Both holders are independently separate, which connect by the heat sensitive-plate. Thermocouples are attached to the base of the sample and reference holders to measure the heat change occurred. The second series of thermocouples are attached to the furnace and to the heat-sensitive plate.

The differential scanning calorimeter can analyze solid or liquid samples using the different pans. Solid samples may be in powder, crystal, film, or granular form. Proper sample preparation should be in good thermal contact with the base of the pan in order to reduce the resistance of the sample to heat flow through the DSC temperature sensors and obtain the DSC curve in maximum peak sharpness and resolution. The best sample shapes for optimum performance are thin disks or film or fine granules spread in thin layer on the bottom of the pan. Materials such as polymer films can be conveniently prepared by cutting out sections of the film with a standard paper punch or cork borer. Solid materials can be sliced with a razor or knife.

2.3.2 Interpretation of the DSC Thermogram

The graph obtained from DSC measurement is called DSC thermogram or DSC curve. This is a relationship between heat flow (dQ/dt) against temperature (T , °C). An example DSC thermogram is shown in Fig. 2.3. Three characteristics of transition appear in DSC thermogram:

2.3.2.1 Glass Transition Temperature, T_g

When an amorphous polymer is heated, the temperature at which it changes from the glassy to the rubbery form is called the glass transition temperature, T_g . This transition, heat capacity of the substance of both states are at different values. Polymer in the rubbery form has a higher heat capacity at

temperature above T_g . Therefore, heat of polymer at temperature above T_g is slowly increase. A slope of baseline in DSC thermogram of an amorphous polymer shows only the T_g value.

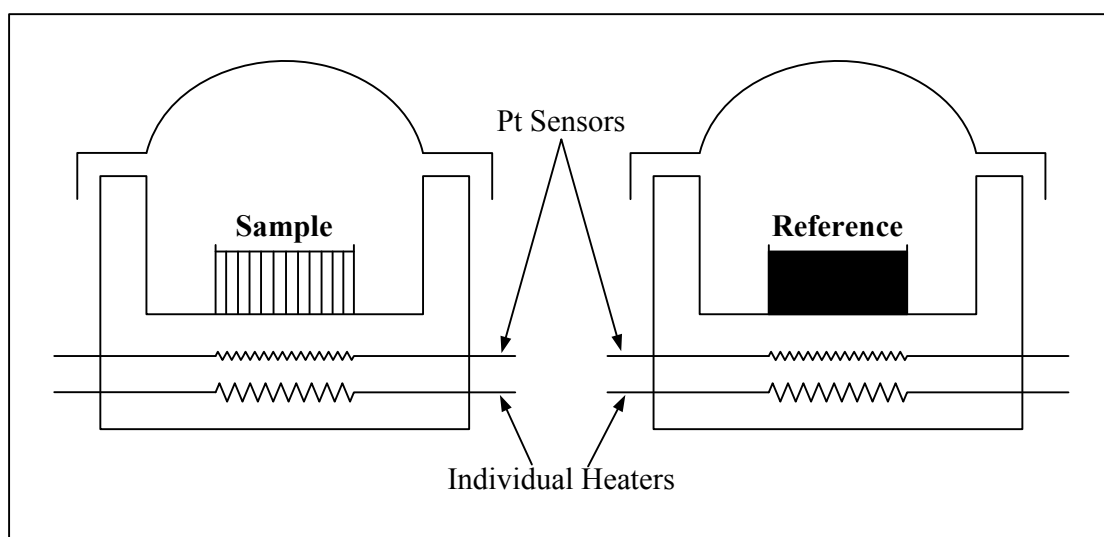


Figure 2.1 Schematic diagram of power compensation DSC.

2.3.2.2 Melting Temperature, T_m

The temperature at the top of peak in endothermic process is taken as the melting temperature (T_m) on DSC thermogram. The extrapolated onset temperature of melting (T_{im}) is defined as the intersection between the extrapolated baseline at the lower temperature and the tangent drawn at the point of greatest slope on the rising side of the melting peak.

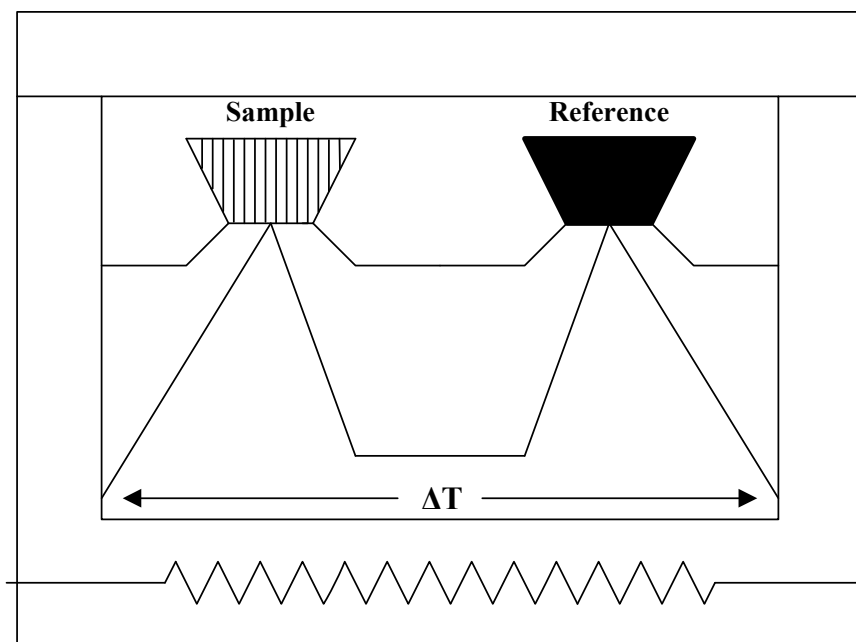


Figure 2.2 Schematic diagram of heat flux DSC.

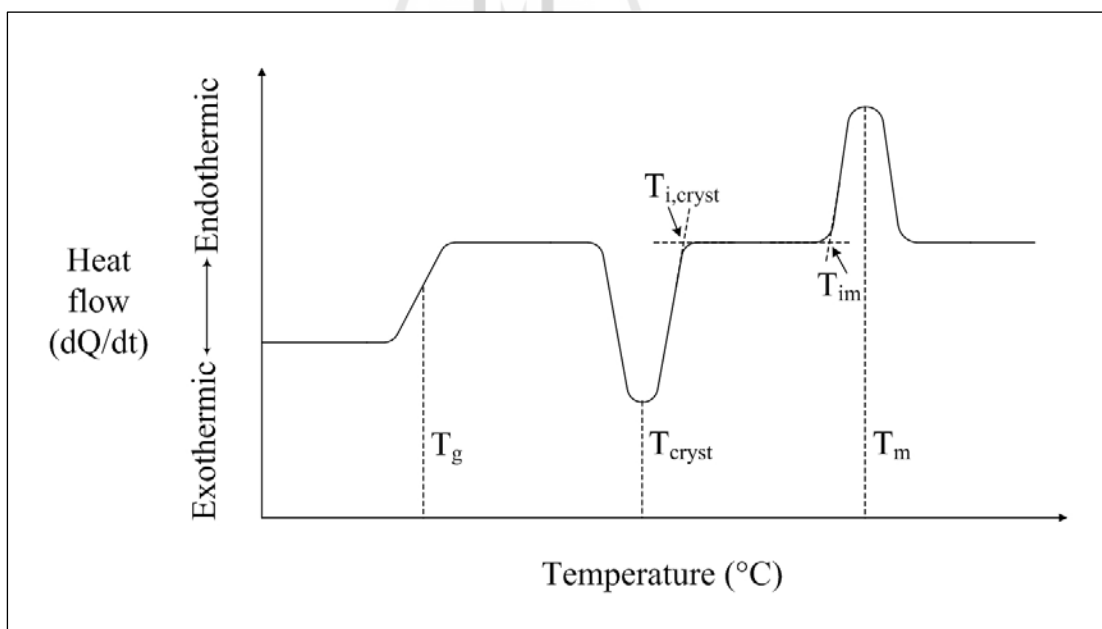


Figure 2.3 DSC thermogram.

2.3.2.3 Crystallization Temperature, T_{cryst}

The peak temperature of crystallization is taken as the temperature of crystallization (T_{cryst}) in exothermic process. The extrapolated onset temperature ($T_{i,\text{cryst}}$) is the temperature at which the extrapolated baseline on the higher temperature side intersects the tangent to the maximum falling slope of the peak.

2.3.3 Estimation of Specific Heat Capacity by DSC

The heat capacity can be estimated using the DSC in the temperature range from -100°C to 600°C with an accuracy of $\pm 2.0\%$. Energy input per unit time or heat flow and the rate of increasing temperature in each experiment or heating rate can be expressed in Eq. (2.1) and (2.2):

$$\frac{\text{Heat difference}}{\text{Time difference}} = \frac{\Delta Q}{\Delta t} = \text{Heat flow} \quad (2.1)$$

$$\frac{\text{Temperature difference}}{\text{Time difference}} = \frac{\Delta T}{\Delta t} = \text{Heating rate} \quad (2.2)$$

Dividing Eq. (2.1) by Eq. (2.2) obtains

$$\frac{\text{Heat flow}}{\text{Heating rate}} = \frac{\Delta Q/\Delta t}{\Delta T/\Delta t} = \frac{\Delta Q}{\Delta T} = C_p \quad (2.3)$$

where C_p is the heat capacity or amount of heat required to change the temperature of a substance by 1 K or 1°C under constant pressure.

Specific heat capacity (\bar{C}_p) is amount of heat required to change the temperature of one unit mass of the substance by 1 K or 1°C :

$$\bar{C}_p = \frac{\Delta Q}{m\Delta T} \quad (2.4)$$

where units of \bar{C}_p are $\frac{\text{cal}}{\text{g}\cdot^{\circ}\text{C}}$ or $\frac{\text{J}}{\text{kg}\cdot\text{K}}$. In case of the molar heat capacity, units of

\bar{C}_p are $\frac{\text{cal}}{\text{mol}\cdot^{\circ}\text{C}}$ or $\frac{\text{J}}{\text{mol}\cdot\text{K}}$.

2.3.4 Estimation of Liquid Specific Heat Capacity for Pure Components (n-decane, palmitic acid and oleic acid) and Its Mixtures

The specific heat capacity of liquid n-decane ($\text{C}_{10}\text{H}_{22}$) can be estimated by the following equation (Huang, et al., 2005):

$$\bar{C}_p \text{ (J/g/K)} = 2.1298 + 2.7920 \times 10^{-3} T + 0.7056 \times 10^{-5} T^2 \quad (2.5)$$

where T is the temperature in unit of $^{\circ}\text{C}$ in the temperature range of -26 to 37°C .

The specific heat capacity of pure liquid fatty acids (palmitic acid and oleic acid) can be accurately estimated using the Rowlinson–Bondi equation (Reid et al., 1987) as follows:

$$\frac{\bar{C}_p - C_p^{\circ}}{R} = 1.45 + 0.45(1 - T_r)^{-1} + 0.25\omega \left[17.11 + 25.2(1 - T_r)^{1/3} T_r^{-1} + 1.742(1 - T_r)^{-1} \right] \quad (2.6)$$

where \bar{C}_p is the specific heat capacity in the liquid phase,

C_p° is the ideal gas specific heat capacity, which is calculated at the same temperature used to calculate \bar{C}_p ,

ω is the acentric factor,

R is the universal gas constant ($8.31451 \text{ J}\cdot\text{mol}^{-1}\cdot\text{K}^{-1}$), and

T_r is the reduced temperature ($T_r = \frac{T}{T_c}$; T_c is the critical temperature).

The value of C_p^o can be estimated by the method of group contribution (Rihani et al., 1965). The contribution from each group to the heat capacity of a compound may be expressed as:

$$C_p^o = a + bT + cT^2 + dT^3 \quad (2.7)$$

where a , b , c , and d are the contributions according to the groups and T is the absolute temperature. The ideal heat capacity of any compound can be determined by the equation,

$$C_p^o = \sum_{i=1}^n a + \sum_{i=1}^n bT + \sum_{i=1}^n cT^2 + \sum_{i=1}^n dT^3 \quad (2.8)$$

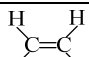
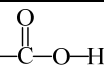
where n is the number of the components/elements in the compound.

Thermodynamic parameters needed for estimation of specific heat capacity of pure fatty acids are listed in Table 2.1 and the values of a , b , c , and d for palmitic acid and oleic acid are summarized in Table 2.2.

Table 2.1 The significant properties of fatty acids.

Fatty acids	Carbon number	T_c (K)	ω	Reference
Palmitic acid	C16:0	799.74	0.728	Cedeño et al., 2000
Oleic acid	C18:1	819.14	1.185	Morad et al., 2000

Table 2.2 The values of a , b , c , and d in each group (Rihani et al., 1965).

Group	a	$b \times 10^2$	$c \times 10^4$	$d \times 10^6$
$-\text{CH}_3$	0.6087	2.1433	-0.0852	0.001135
$-\text{CH}_2$	0.3945	2.1363	-0.1197	0.002596
	-3.1210	3.8060	-0.2359	0.005504
	1.4055	3.4632	-0.2557	0.006886

The liquid specific heat capacity for multicomponent mixtures can be estimated from the equation based on a molar fraction average (Teja, 1983):

$$\bar{C}_{\text{pm}} = \sum_{i=1}^n x_i \bar{C}_{\text{pi}} \quad (2.9)$$

where x_i are the molar fractions of the components and \bar{C}_{pi} are the values of the specific heat capacities of pure compounds, which evaluated at the mixture temperature.

2.4 Experimental Procedures

2.4.1 Chemicals

n-Decane (99+% purity) and palmitic acid (98% purity) were obtained from ACROS. Pure oleic acid used in this work was purchased from CARLO ERBA.

2.4.2 Preparation of Ternary Mixtures

All ternary mixtures samples were prepared by weighing the required amounts of each component on an analytical balance (Sartorius BP 221 model) with an accuracy of ± 0.0001 g. Five different mass ratios of n-decane (D) : palmitic acid (P) : oleic acid (O) used in this work were 1:1:1, 1:0.5:1, 1:0.3:1, 1:0.2:1, and 1:0.1:1. The weighed quantities of each component were contained into a 50 ml SCHOTT DURAN laboratory glass bottles, which were then capped tightly before being immersed in the water bath (NESLAB GP-400) at 60°C and left for thermal equilibration for 1 hour. After that, the mixtures were manually shaken until all the components were completely dissolved and the mixtures were visibly homogeneous. The solutions were kept at room temperature until later use.

2.4.3 Differential Scanning Calorimetry (DSC)

Thermal characteristic of pure palmitic acid and its mixtures were measured by Perkin-Elmer PYRIS Diamond differential scanning calorimetry (DSC-7), which is schematically illustrated in Fig. 2.1. Before each use, the equipment was dehumidified by flowing nitrogen gas at 50°C and a flow rate of 20 ml/min for 2 hours. Then, baselines for the analysis were plotted by placing two identical empty aluminum pans in the reference and sample calorimetric blocks as shown in Fig. 2.1. The equipment was then programmed to heat and cool at temperature range between 0–70°C with the heating and cooling rate of 5°C/min. Each process took

approximately 30 minutes. After that, the calibration was performed in a temperature range from 100–200°C with a heating rate of 10°C/min using indium (99.999% purity) as a standard sample. Melting temperature and enthalpy of fusion of indium reported in the reference are 156.60°C and 28.45 J·g⁻¹, respectively.

A 0.0064 g of pure palmitic acid was analyzed in the solid state. A 0.0081 g of pure oleic acid and approximately 0.0015–0.0025 g of ternary mixtures were analyzed in the liquid state. Liquid samples were introduced into a 40 µl aluminum pan by a micropipette (BIO-RAD, 100 µl). The pans were then sealed with a mechanical sealer and placed in the sample block of DSC. Heating and cooling were then performed from 0–70°C with the same heating and cooling rate as in baselines preparation. A temperature range of -5–30°C with the cooling and heating rate of 1, 3, 5, 7, 9 and 10°C/min was used for the DSC measurement of oleic acid. Data acquisition and processing was done with Perkin-Elmer's PYRIS software. All experiments were duplicated to check reproducibility.

2.5 Results and Discussion

2.5.1. Baselines for DSC Analysis

Baselines for heating and cooling in Perkin-Elmer PYRIS Diamond DSC are shown in Fig. 2.4. Both baselines are straight, which indicate that they can be used as the reference lines for the analysis in this work.

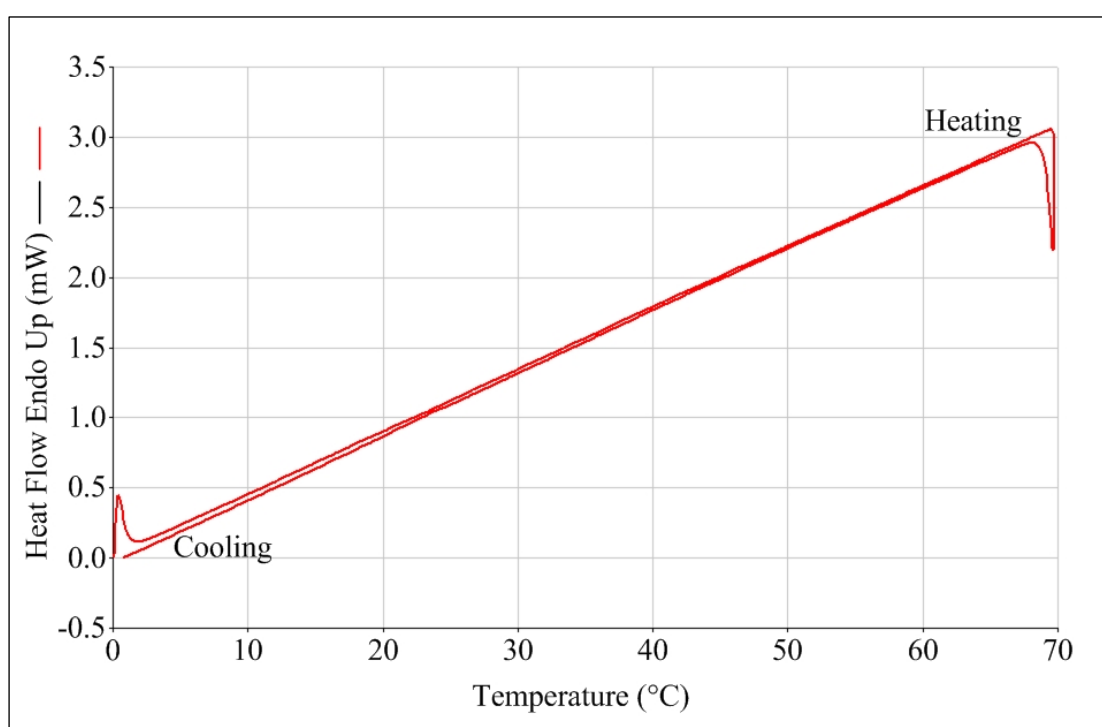


Figure 2.4 Baselines from Perkin-Elmer PYRIS Diamond DSC.

2.5.2. Calibration Curve of the DSC Analysis

Heating curve obtained when indium was used as the standard sample is shown in Fig. 2.5. The experimental results for melting temperature and enthalpy of fusion measured from the DSC are 159.35°C and 29.388 J·g⁻¹, respectively. Both values are in good agreement with the reported values (Groenewoud et al., 2001).

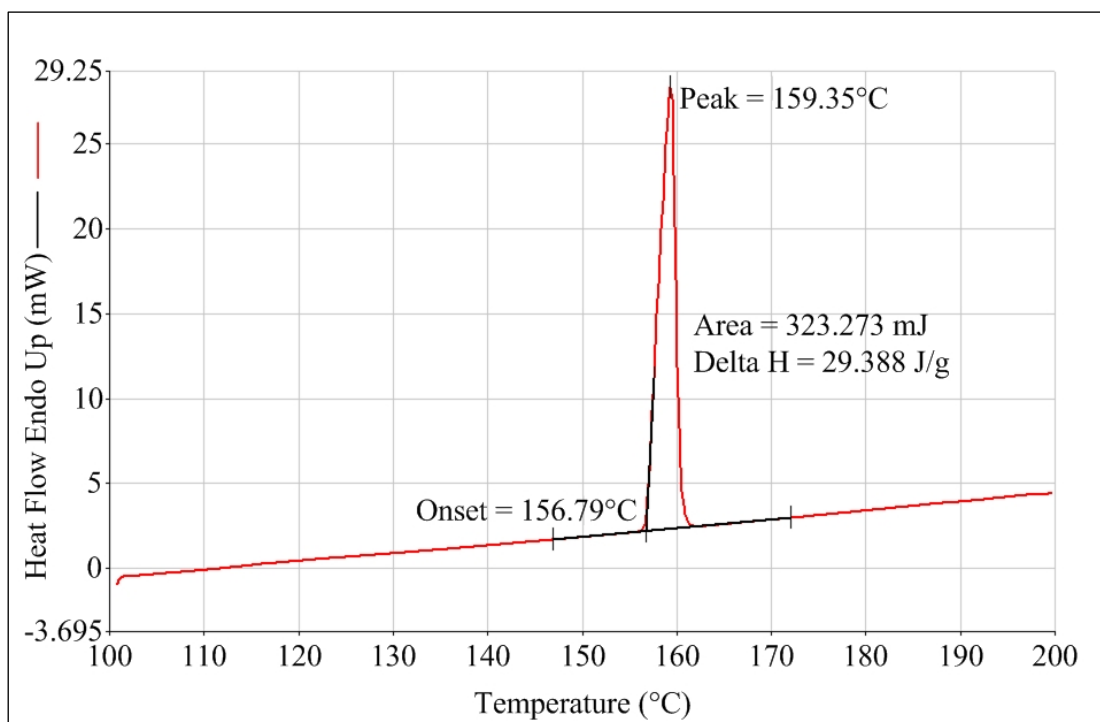


Figure 2.5 Calibration curve of the DSC using indium as the standard sample.

2.5.3. DSC Analysis for Pure Palmitic Acid

DSC analysis for pure palmitic acid is shown in Fig. 2.6. Solid–liquid phase transition is observed on the heating curve with the onset and melting temperatures of 59.90°C and 62.03°C, respectively. The enthalpy of fusion is found to be 208.019 J·g⁻¹. The experimental results for melting temperature and enthalpy of fusion are in good agreement with the value previously reported in the literatures as shown in Table 2.3. Liquid–solid phase transition is observed on the cooling curve with the onset and peak temperatures for solidification of 58.67°C and 57.15°C, respectively. The enthalpy of solidification is found to be -206.292 J·g⁻¹.

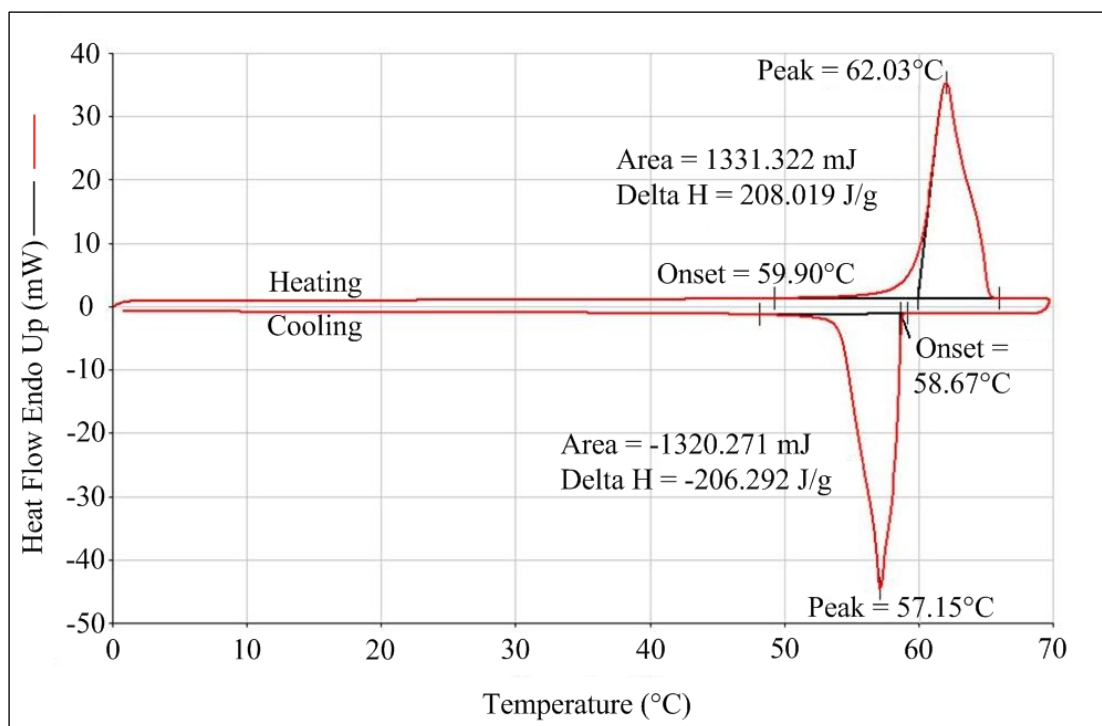


Figure 2.6 The DSC analysis for pure palmitic acid.

Table 2.3 Thermal properties for phase transition of pure palmitic acid.

Melting temperature T_m (K)	%diff.*	Enthalpy of fusion ΔH_f ($J \cdot g^{-1}$)	%diff.	Reference
335.2	–	208.02	–	This work
337.5	-0.7	208.20	-0.09	Cedeño et al., 2001
336.1	-0.3	211.85	-1.81	Formo et al., 1979
335.0	-0.1	163.95	26.88	Acree, 1991
336.2	-0.3	163.93	26.90	Weast, 1988
336.1	-0.3	210.14	-1.01	Gunstone et al., 1986
335.7	-0.2	209.46	-0.69	Domalski et al., 1984
336.1	-0.3	212.15	-1.95	Pryde, 1979

Remark: * %diff. is the percentage of difference between the values obtained in this work and from the references relative to the values from the corresponding references.

According to phase transition can be plotted the DSC curve for specific heat capacity of pure palmitic acid in melting process as shown in Fig. 2.7. Table 2.4 shows the experimental specific heat capacities for the solid and liquid phase of pure palmitic acid. Results of \bar{C}_p value for the solid phase are slowly increased in a temperature range of 1.03–50.06°C. For the liquid phase, \bar{C}_p have similar values in a temperature range of 66.05–69.07°C. It is found that liquid specific heat capacities from the DSC measurement are in good agreement with the estimated values obtained from the Rowlinson–Bodi equation (Eq. 2.6) with the %diff. values less than $\pm 5\%$.

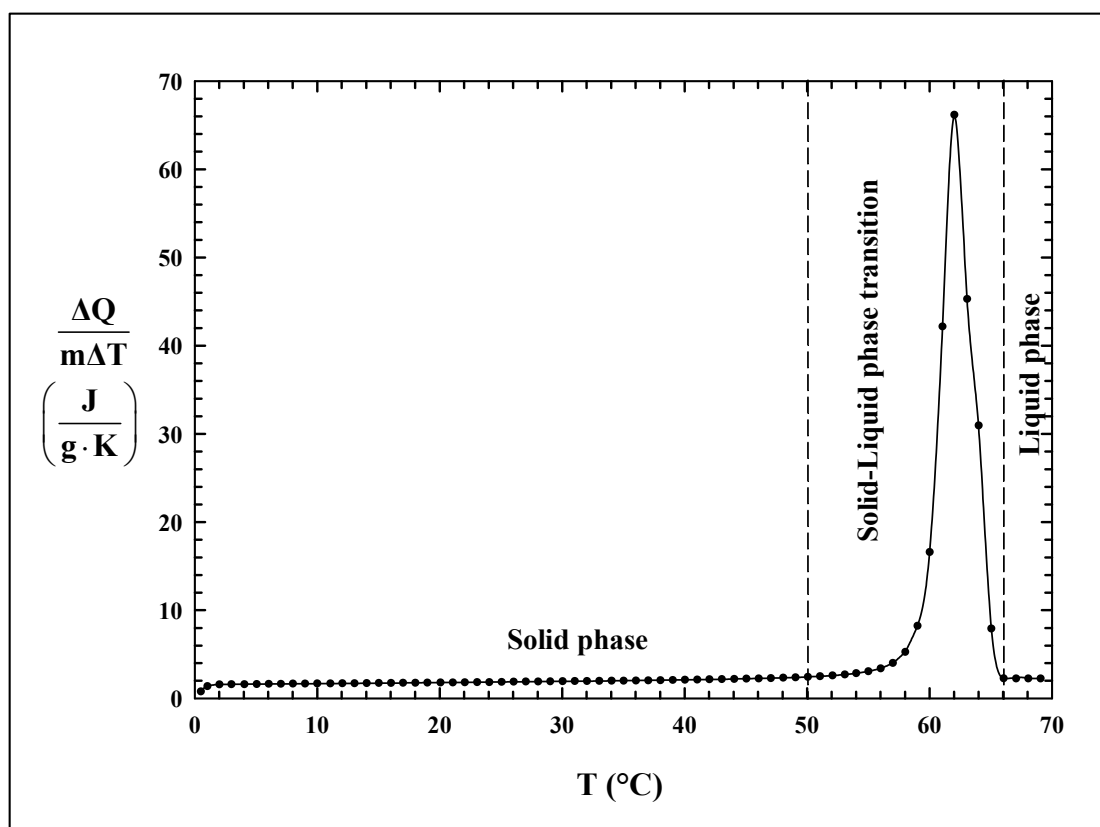


Figure 2.7 The DSC curve for specific heat capacity of pure palmitic acid in melting process.

Table 2.4 Specific heat capacities for the solid and liquid phase of pure palmitic acid.

In Solid Phase			
T, °C	\bar{C}_p (DSC), J/g·K		
1.03	1.400		
2.01	1.581		
5.05	1.630		
10.00	1.682		
15.03	1.739		
20.07	1.798		
25.05	1.871		
30.03	1.947		
40.02	2.112		
50.06	2.447		
In Liquid Phase			
T, °C	\bar{C}_p (DSC), J/g·K	\bar{C}_p (est.), J/g·K	% diff.
66.05	2.283	2.222	-2.745
67.06	2.264	2.225	-1.762
68.06	2.260	2.228	-1.454
69.07	2.262	2.231	-1.412

2.5.4. DSC Analysis for Pure Oleic Acid

DSC analysis of oleic acid with a 1°C/min is shown in Fig. 2.8 (experimental results for the heating and cooling rate of 3, 5, 7, 9 and 10°C/min are shown in Appendix D). Two endothermic peaks present on the heating curve at around 0.04°C and 12.58°C. These results should be a reversible solid–solid phase transition from γ to α phase at 0.04°C, the α phase melts at 12.58°C by continued

heating. One exothermic peak presents at 3.78°C is observed on the cooling curve with the enthalpy value of $-6.398 \text{ J}\cdot\text{g}^{-1}$.

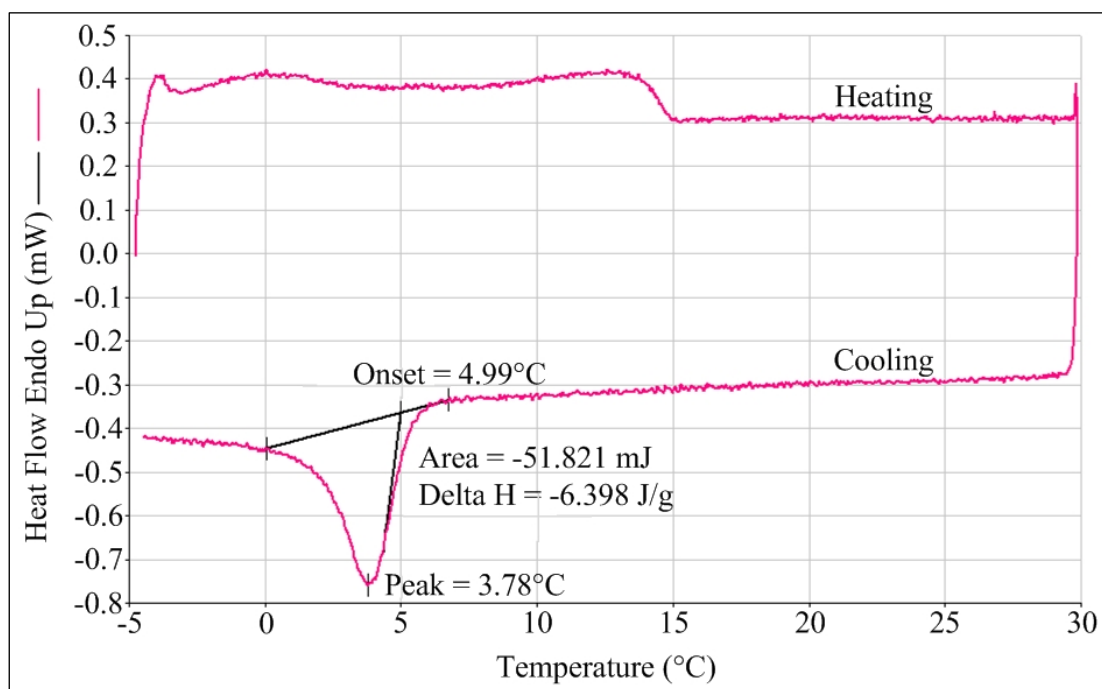


Figure 2.8 DSC analysis for pure oleic acid.

Thermal behavior of oleic acid corresponds to a study of polymorphism in oleic acid by Suzuki et al. (1985). As shown in Fig. 2.9, in melting and cooling processes are measured using the DSC method at the temperature range of -20 – 30°C with a $2^\circ\text{C}/\text{min}$ for the heating and cooling rate. On the heating curve, a reversible solid–solid phase transition from γ to α phase occurs at -2.2°C , continued heating causes the α phase melts at 13.3°C . Two exothermic peaks are appeared on the cooling curve at 4.7°C and -3.6°C . Performance of the DSC used in this work is not suitable to study thermal properties for pure oleic acid. Therefore, it cannot determine clearly for the phase transition temperature.

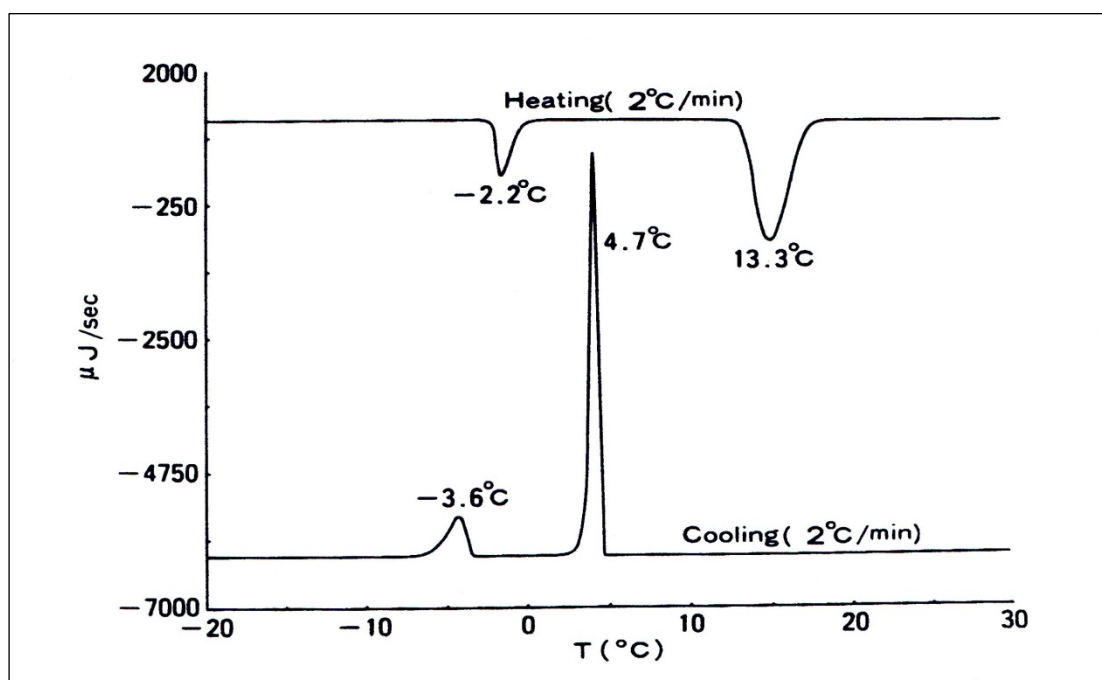


Figure 2.9 A study of polymorphism in oleic acid (Suzuki et al., 1985).

The DSC curve for specific heat capacity of pure oleic acid in melting process with the heating rate of $1^{\circ}\text{C}/\text{min}$ is shown in Fig. 2.10. For the liquid phase, \bar{C}_p values of pure oleic acid were observed in a temperature range of $15.00\text{--}29.76^{\circ}\text{C}$. The experimental results of \bar{C}_p values for the liquid phase are shown in Table 2.5. It is found that liquid specific heat capacities obtained from the DSC analysis are in good agreement with estimated values from the Rowlinson–Bodi equation (Eq. 2.6).

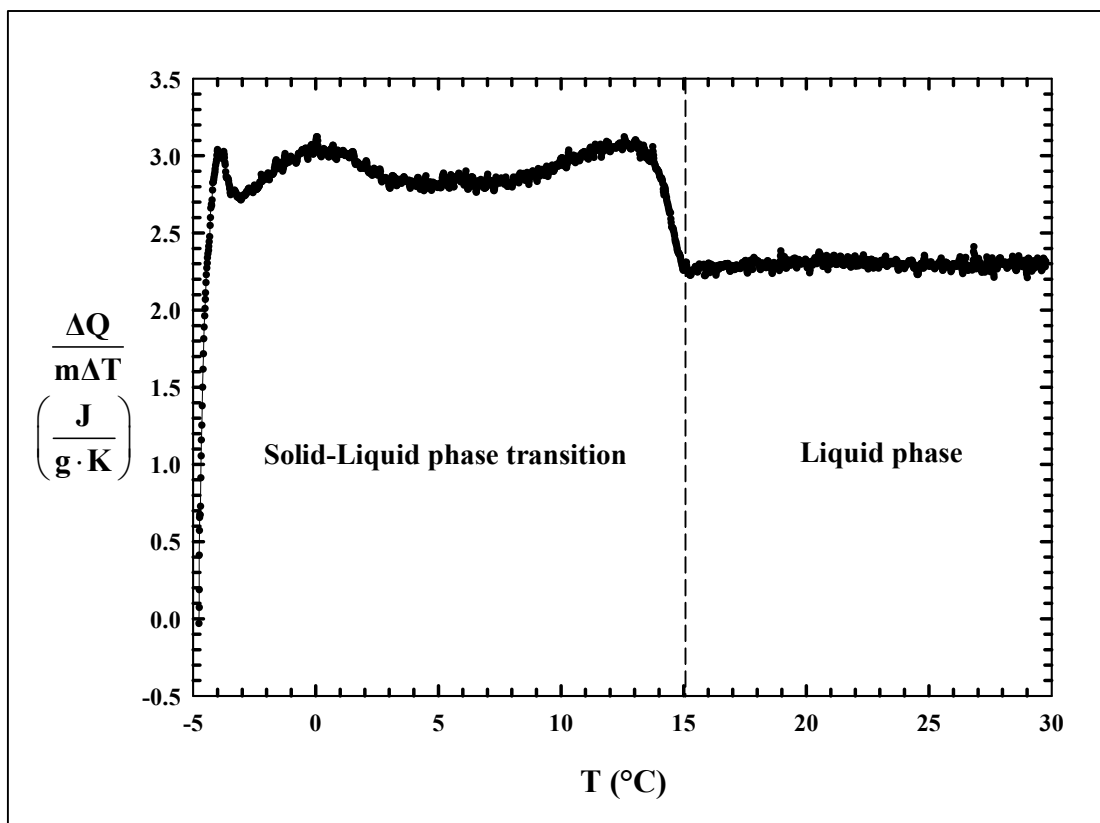


Figure 2.10 The DSC curve for specific heat capacity of pure oleic acid in melting process.

Table 2.5 Specific heat capacities for the liquid phase of pure oleic acid.

T, °C	\bar{C}_p (DSC), J/g·K	\bar{C}_p (est.), J/g·K	% diff.
15.00	2.259	2.261	0.088
17.00	2.278	2.265	-0.574
19.00	2.327	2.269	-2.556
21.00	2.312	2.273	-1.716
23.00	2.308	2.277	-1.361
25.01	2.291	2.281	-0.438
27.00	2.323	2.286	-1.619
29.76	2.315	2.291	-1.048

2.5.5. DSC Analysis of n-Decane – Palmitic Acid – Oleic Acid Mixture with Mass Ratio (D:P:O) of 1:1:1

Results from the DSC analysis for ternary mixture with mass ratio (D:P:O) of 1:1:1 is shown in Fig. 2.11. It appears a single peak on the heating and cooling curve. On the heating curve presents solid–liquid phase transition with the onset and melting temperature of 28.75°C and 41.41°C, respectively. The enthalpy of melting is found to be 62.456 J·g⁻¹. On the cooling curve presents liquid–solid phase transition with the onset and peak temperatures for solidification of 36.28°C and 34.48°C. The enthalpy of solidification is found to be -62.986 J·g⁻¹.

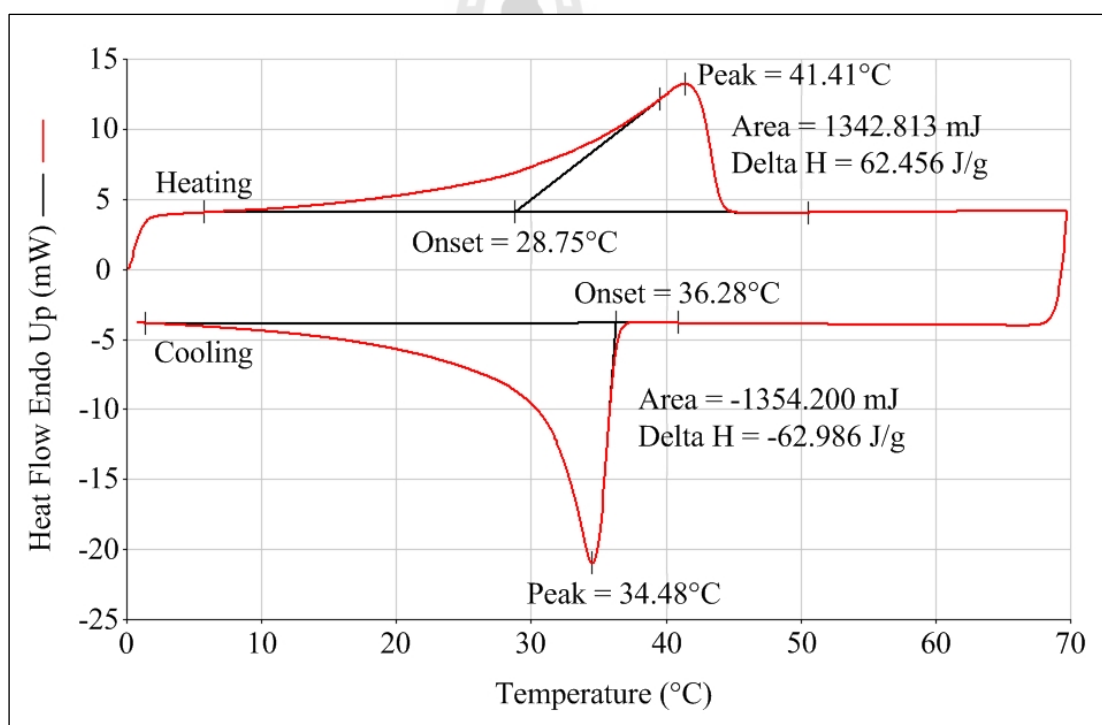


Figure 2.11 DSC analysis for ternary mixture with n-decane :
palmitic acid : oleic acid mass ratio of 1:1:1.

Fig. 2.12 shows the DSC curve for specific heat capacity with mass ratio of 1:1:1 in melting process. Specific heat capacity for the liquid phase is observed in a temperature range of 46.05–69.48°C at which the \bar{C}_p values as a function of the temperature. The experimental results of the \bar{C}_p values for the liquid phase are shown in Table 2.6. It is found that the experimental specific heat capacities are in good agreement with the estimated values obtained from Teja equation (Eq. 2.9). The correlation equation according to mass ratio of 1:1:1 in a temperature range of 46.05–69.48°C is $\bar{C}_p (\text{J/g} \cdot \text{K}) = 2.0379 + 0.0042T/^\circ\text{C}$ with $r^2 = 0.9987$.

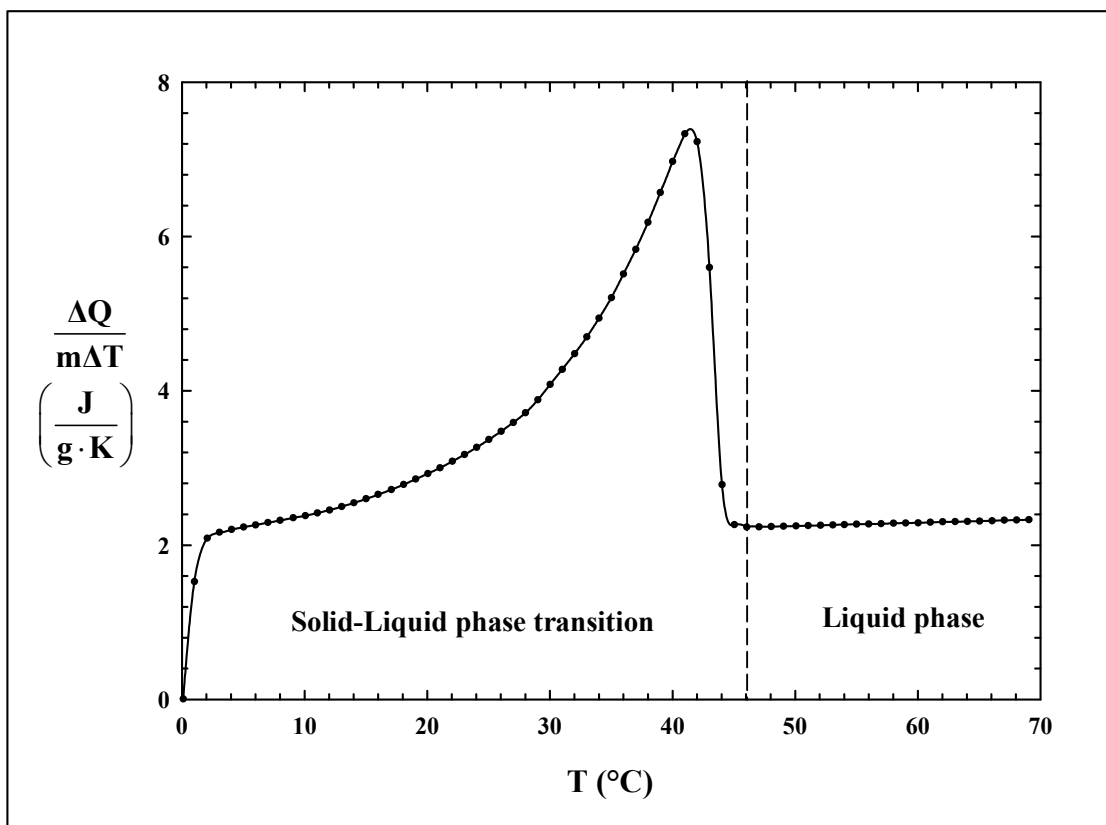


Figure 2.12 Specific heat capacity for ternary mixture with mass ratio of 1:1:1 in melting process.

Table 2.6 Specific heat capacities for the liquid phase of the ternary mixture with mass ratio (D:P:O) of 1:1:1.

In Liquid Phase			
T, °C	\bar{C}_p (DSC), J/g·K	\bar{C}_p (est.), J/g·K	% diff.
46.05	2.234	2.201	-1.487
48.05	2.240	2.208	-1.471
51.06	2.253	2.217	-1.622
54.00	2.267	2.226	-1.827
57.01	2.277	2.236	-1.838
60.02	2.289	2.246	-1.933
63.04	2.304	2.255	-2.157
66.05	2.316	2.265	-2.244
69.48	2.331	2.276	-2.395

2.5.6. DSC Analysis of n-Decane – Palmitic Acid – Oleic Acid Mixture with Mass Ratio (D:P:O) of 1:0.5:1

Fig. 2.13 shows the DSC analysis of ternary mixture with mass ratio of 1:0.5:1. It is appear a single peak on the heating and cooling curve. Solid–liquid phase transition is detected on the heating curve shows the onset and melting temperatures of 21.77°C and 33.67°C, respectively. The enthalpy of melting is found to be 35.727 J·g⁻¹. Liquid–solid phase transition is detected on the cooling curve shows the onset and peak temperatures for solidification of 26.99°C and 25.10°C, respectively. The enthalpy of solidification is found to be -35.016 J·g⁻¹.

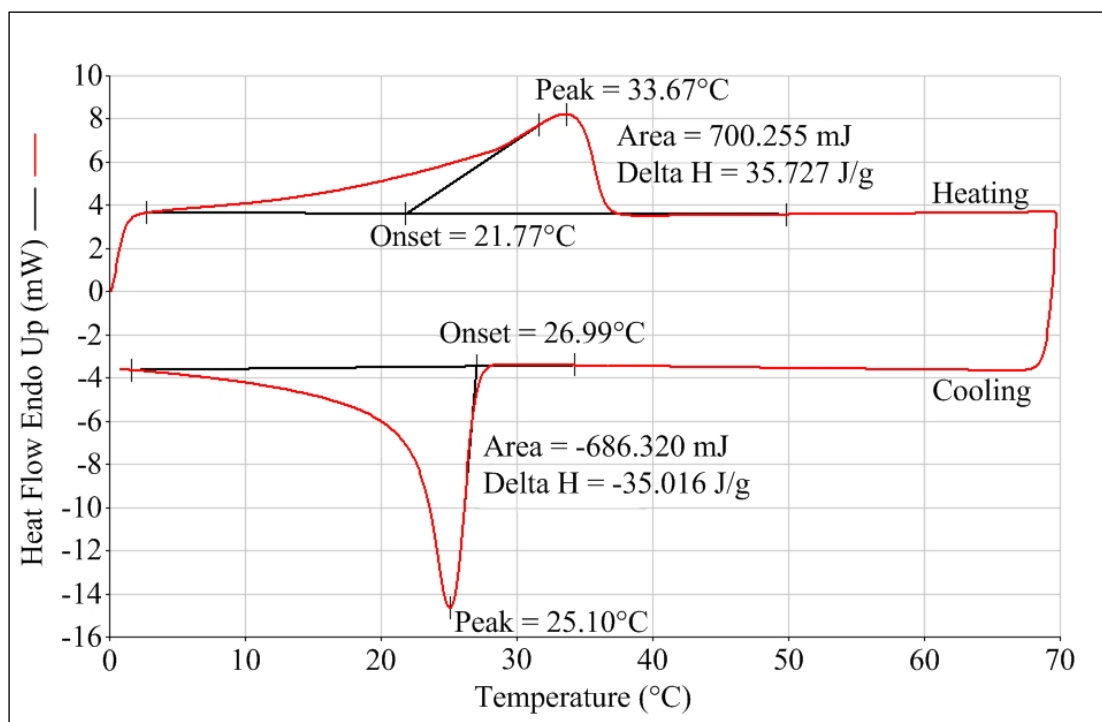


Figure 2.13 DSC analysis for ternary mixture with n-decane :
palmitic acid : oleic acid mass ratio of 1:0.5:1.

Fig. 2.14 presents the DSC curve for specific heating capacity with mass ratio of 1:0.5:1 in melting process. The liquid specific heat capacities are observed in a temperature range of 39.02–69.48°C at which the \bar{C}_p values as a function of the temperature. Table 2.7 shows the experimental specific heat capacities for the liquid phase. It is found that the experimental \bar{C}_p values are in good agreement with the estimated values. The correlation equation according to specific heat capacity for the liquid phase with mass ratio of 1:0.5:1 in a temperature range of 39.02–69.48°C is $\bar{C}_p (\text{J/g} \cdot \text{K}) = 2.0008 + 0.0037T/^\circ\text{C}$ with $r^2 = 0.9988$.

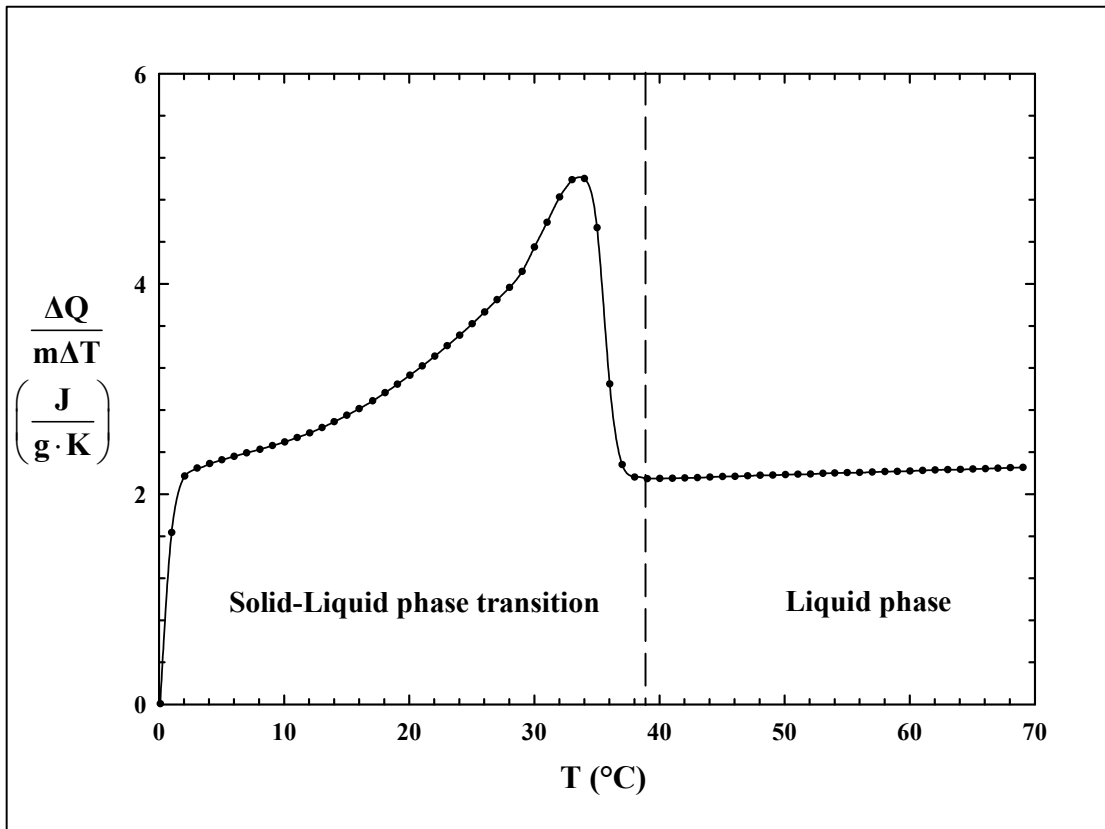


Figure 2.14 Specific heat capacity for ternary mixture with mass ratio of 1:0.5:1 in melting process.

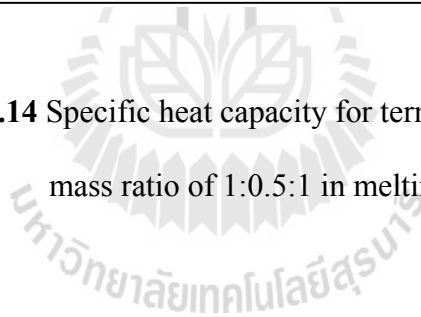


Table 2.7 Specific heat capacities for the liquid phase of the ternary mixture with mass ratio (D:P:O) of 1:0.5:1.

In Liquid Phase			
T, °C	\bar{C}_p (DSC), J/g·K	\bar{C}_p (est.), J/g·K	% diff.
39.02	2.146	2.185	1.779
42.03	2.154	2.194	1.833
45.04	2.167	2.204	1.666
48.05	2.178	2.213	1.591
51.06	2.189	2.223	1.524
54.00	2.201	2.232	1.402
57.01	2.209	2.242	1.475
60.02	2.220	2.252	1.419
63.04	2.233	2.262	1.277
66.05	2.242	2.272	1.317
69.48	2.255	2.283	1.246

2.5.7. DSC Analysis of n-Decane – Palmitic Acid – Oleic Acid Mixture with Mass Ratio (D:P:O) of 1:0.3:1

Results of the DSC analysis for ternary mixture with mass ratio of 1:0.3:1 are shown in Fig. 2.15. It is appear a single peak on the heating and cooling curve. Solid–liquid phase transition is observed on the heating curve with the onset and melting temperatures of 12.10°C and 28.84°C, respectively. The enthalpy of melting is found to be 24.130 J·g⁻¹. Liquid–solid phase transition is observed on the cooling curve with the onset and peak temperatures for solidification of 20.82°C and 18.06°C, respectively. The enthalpy of solidification is found to be -23.961 J·g⁻¹.

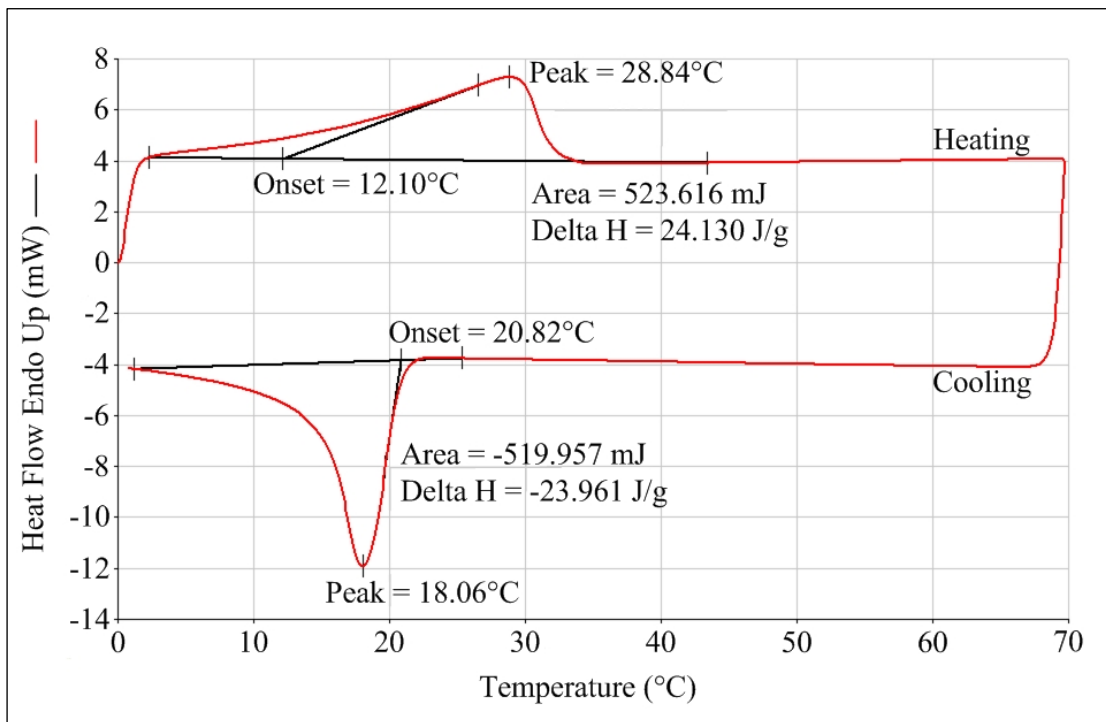


Figure 2.15 DSC analysis for ternary mixture with n-decane :
palmitic acid : oleic acid mass ratio of 1:0.3:1.

The DSC curve for specific heat capacity with mass ratio of 1:0.3:1 in melting process is shown in Fig. 2.16. For the liquid phase, the \bar{C}_p values are observed in a temperature range of 36.02–69.48°C at which the \bar{C}_p values as a function of the temperature. The \bar{C}_p values for the liquid phase measured by the DSC method are listed in Table 2.8. It is found that the experimental liquid specific heat capacities are in good agreement with the estimated values. The correlation equation according to specific heat capacity for the liquid phase with mass ratio of 1:0.3:1 in a temperature range of 36.02–69.48°C is $\bar{C}_p \text{ (J/g} \cdot \text{K)} = 2.0137 + 0.0035T/^\circ\text{C}$ with $r^2 = 0.9988$.

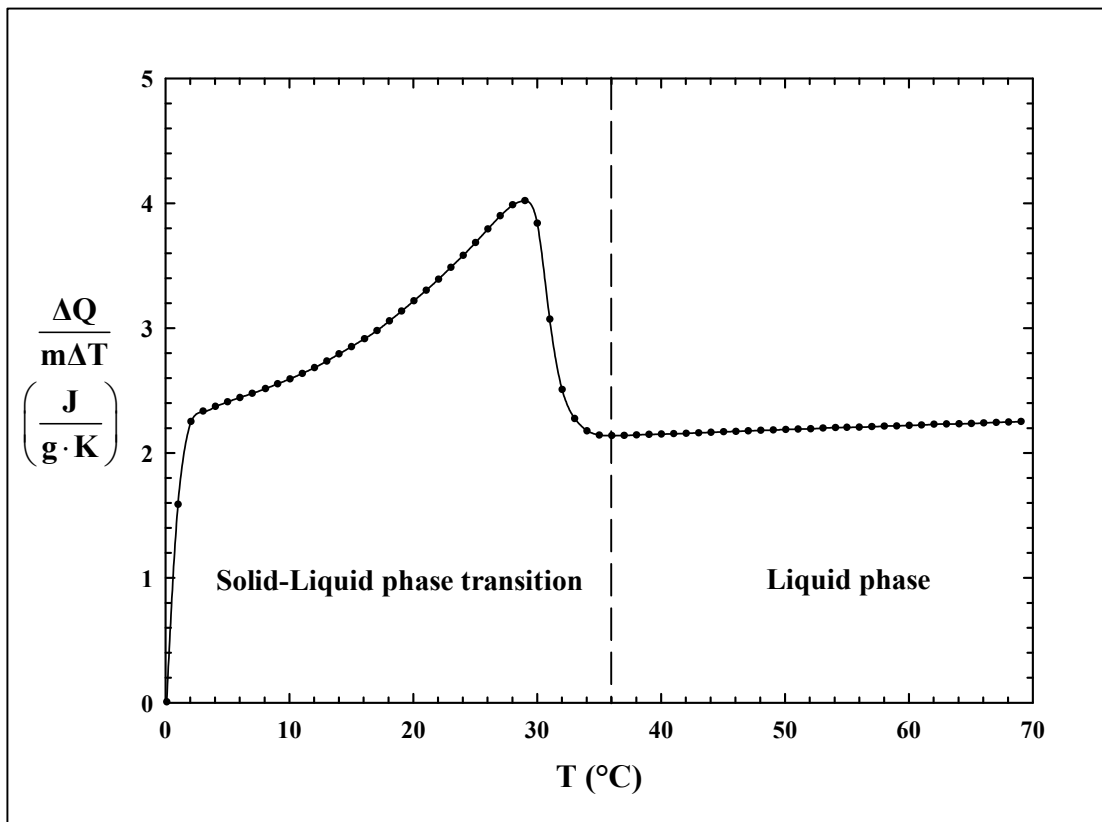


Figure 2.16 Specific heat capacity for ternary mixture with mass ratio of 1:0.3:1 in melting process.

Table 2.8 Specific heat capacities for the liquid phase of the ternary mixture with mass ratio (D:P:O) of 1:0.3:1.

In Liquid Phase			
T, °C	\bar{C}_p (DSC), J/g·K	\bar{C}_p (est.), J/g·K	% diff.
36.02	2.139	2.178	1.775
39.02	2.148	2.187	1.783
42.03	2.157	2.196	1.794
45.04	2.170	2.206	1.630
48.05	2.181	2.216	1.558
51.06	2.191	2.225	1.539
54.08	2.203	2.235	1.432
57.00	2.210	2.245	1.543
60.02	2.221	2.255	1.488
63.04	2.232	2.265	1.437
66.04	2.240	2.275	1.524
69.48	2.253	2.286	1.456

2.5.8. DSC Analysis of n-Decane – Palmitic Acid – Oleic Acid Mixture with Mass Ratio (D:P:O) of 1:0.2:1

DSC analysis of ternary mixture with mass ratio of 1:0.2:1 is shown in Fig. 2.17. The behavior observed on the heating curve for this system is different from mass ratios of 1:1:1, 1:0.5:1 and 1:0.3:1. Solid–liquid phase transition presents two peaks at around 15.91°C and 24.03°C, respectively. Two moments of the release of heat for this system; these release heats are different in magnitude and are functions of the composition of mass ratio. When the concentration of oleic acid in the mixture is increased, appearance of an endothermic peak for solid–liquid phase transition is also observed (F.O. Cedeño et al., 2001). The onset and peak temperature detected in

melting process are 13.59°C and 24.03°C , respectively. The enthalpy of melting is found to be $13.698\text{ J}\cdot\text{g}^{-1}$. Liquid–solid phase transition observed on the cooling curve presents a single peak with the onset and peak temperatures for solidification of 13.44°C and 10.24°C , respectively. The enthalpy of solidification is found to be $-13.878\text{ J}\cdot\text{g}^{-1}$.

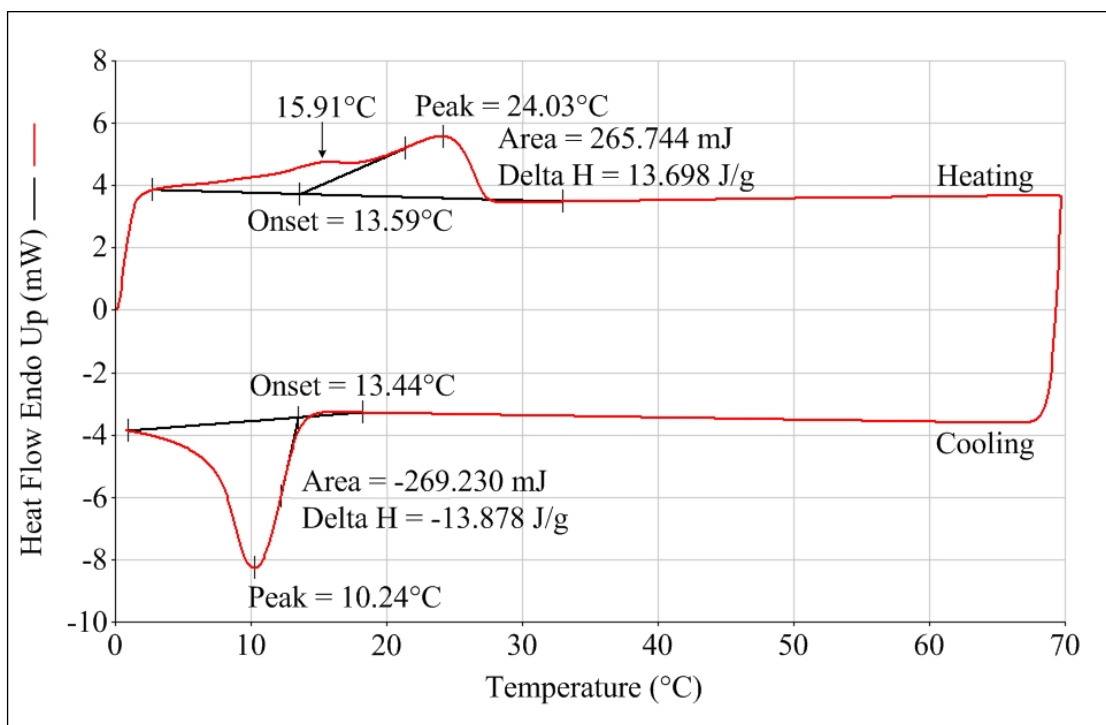


Figure 2.17 DSC analysis for ternary mixture with n-decane :
palmitic acid : oleic acid mass ratio of 1:0.2:1.

Fig. 2.18 shows the DSC curve for specific heat capacity with mass ratio of 1:0.2:1 in melting process. In a temperature range of $29.27\text{--}69.48^{\circ}\text{C}$ is observed the \bar{C}_p values for the liquid phase, which as a function of the temperature. Table 2.9 shows the comparison of specific heat capacity for the liquid phase between the experimental and estimated values. It is found that the experimental specific heat

capacities are in good agreement with the estimated values. The correlation equation according to specific heat capacity for the liquid phase with mass ratio of 1:0.2:1 in a temperature range of 29.27–69.48°C is $\bar{C}_p (\text{J/g} \cdot \text{K}) = 2.0323 + 0.0036T/^\circ\text{C}$ with $r^2 = 0.9968$.

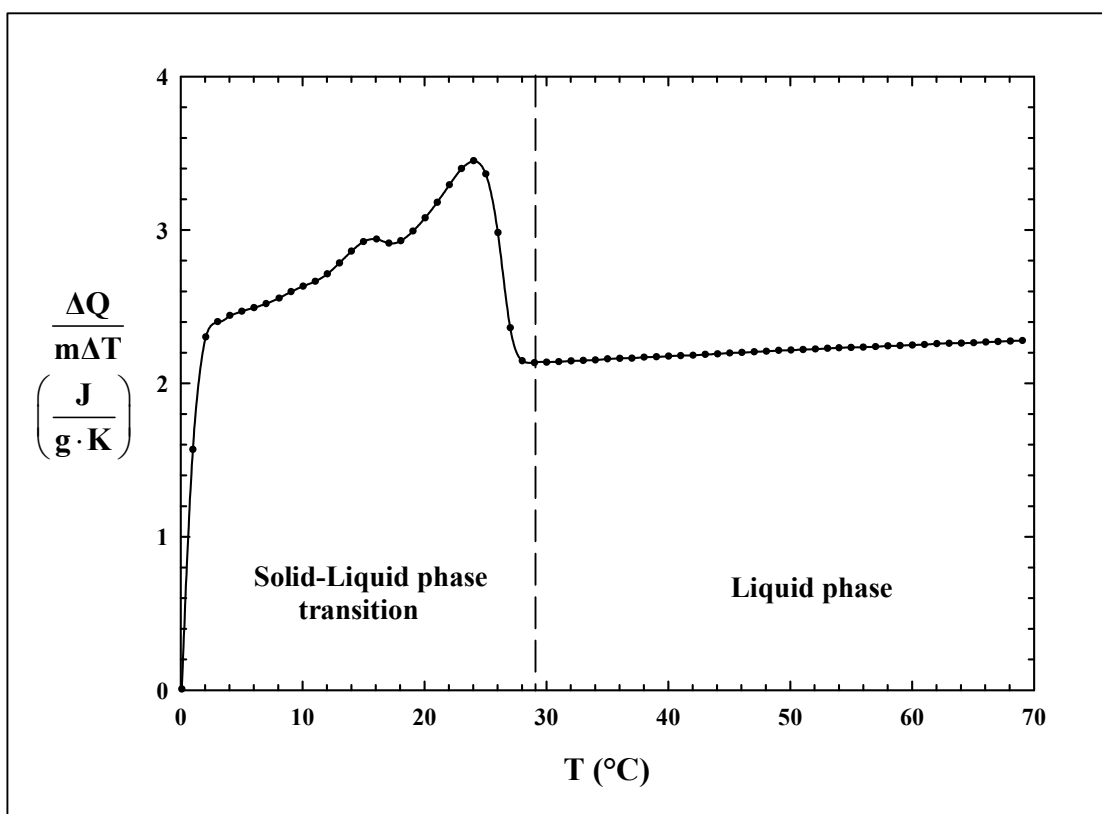


Figure 2.18 Specific heat capacity for ternary mixture with mass ratio of 1:0.2:1 in melting process.

Table 2.9 Specific heat capacities for the liquid phase of the ternary mixture with mass ratio (D:P:O) of 1:0.2:1.

In Liquid Phase			
T, °C	\bar{C}_p (DSC), J/g·K	\bar{C}_p (est.), J/g·K	% diff.
29.27	2.135	2.159	1.102
30.02	2.138	2.161	1.067
33.02	2.149	2.170	0.978
36.02	2.163	2.179	0.757
39.02	2.173	2.189	0.725
42.02	2.183	2.198	0.697
45.04	2.198	2.208	0.450
48.05	2.209	2.218	0.385
51.06	2.220	2.227	0.330
54.00	2.232	2.237	0.218
57.01	2.239	2.247	0.347
60.02	2.250	2.257	0.302
63.04	2.261	2.267	0.259
66.05	2.269	2.277	0.355
69.48	2.279	2.289	0.428

2.5.9. DSC Analysis of n-Decane – Palmitic Acid – Oleic Acid Mixture with Mass Ratio (D:P:O) of 1:0.1:1

The DSC analysis of ternary mixture with mass ratio of 1:0.1:1 is shown in Fig. 2.19. At the studied temperature range, it is not clearly shown for phase transition in melting and cooling processes. On the heating curve presents solid–liquid phase transition in a temperature range of 1.56–20.96°C. On the cooling curve presents liquid–solid phase transition is lower than 0°C.

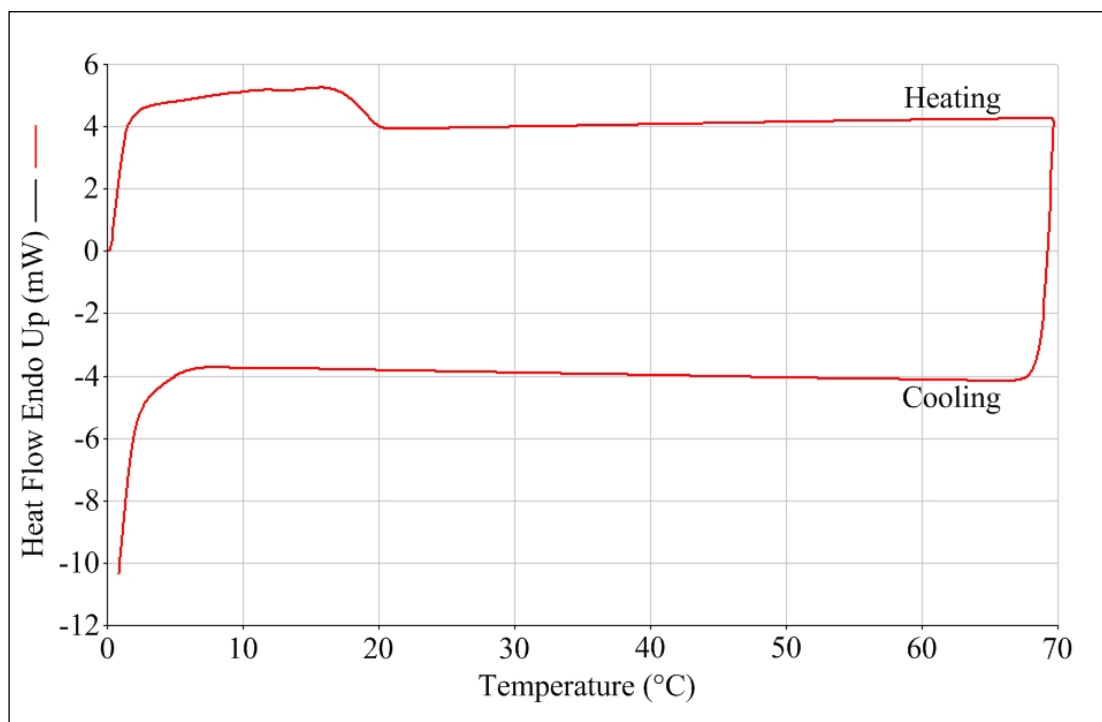


Figure 2.19 DSC analysis for ternary mixture with n-decane :
palmitic acid : oleic acid mass ratio of 1:0.1:1.

Thermal properties for phase transition of pure palmitic acid and ternary n-decane – palmitic acid – oleic acid mixtures obtained from the DSC analysis are summarized in Table 2.10. It is found that the decreasing quantity of palmitic acid affects the phase transition with the lower temperature, due to the quantity of oleic acid is increased in the mixtures. The concentration of n-decane in the mixture does not affect the phase transition, since melting temperature of n-decane is very low (Appendix B).

Table 2.10 Thermal properties for phase transition of pure palmitic acid and ternary n-decane – palmitic acid – oleic acid mixtures obtained from the DSC analysis.

Mass ratio D:P:O	Solid–Liquid Transition			Liquid–Solid Transition		
	T _{im} (°C)	T _m (°C)	ΔH _f (J·g ⁻¹)	T _{i,cryst} (°C)	T _{cryst} (°C)	ΔH _{cryst} (J·g ⁻¹)
Pure palmitic acid	59.90	62.03	208.019	58.67	57.15	-206.292
1:1:1	28.75	41.41	62.456	36.28	34.48	-62.986
1:0.5:1	21.77	33.67	35.727	26.99	25.10	-35.016
1:0.3:1	12.10	28.84	24.130	20.82	18.06	-23.961
1:0.2:1	13.59	24.03	13.698	13.44	10.24	-13.878

The DSC curve for specific heat capacity with mass ratio of 1:0.1:1 in melting process is shown in Fig. 2.20. Specific heat capacity for the liquid phase is observed in a temperature of 21.04–69.47°C at which the \bar{C}_p values as a function the temperature. The \bar{C}_p values for the liquid phase obtained from the DSC measurement are presented in Table 2.11. It is found that the \bar{C}_p values from the DSC measurement are in good agreement with the estimated values. The correlation equation of the \bar{C}_p values for the liquid phase with mass ratio of 1:0.1:1 in a temperature range of 21.04–69.47°C is \bar{C}_p (J/g·K) = 2.0094 + 0.0039T/°C with $r^2 = 0.9968$.

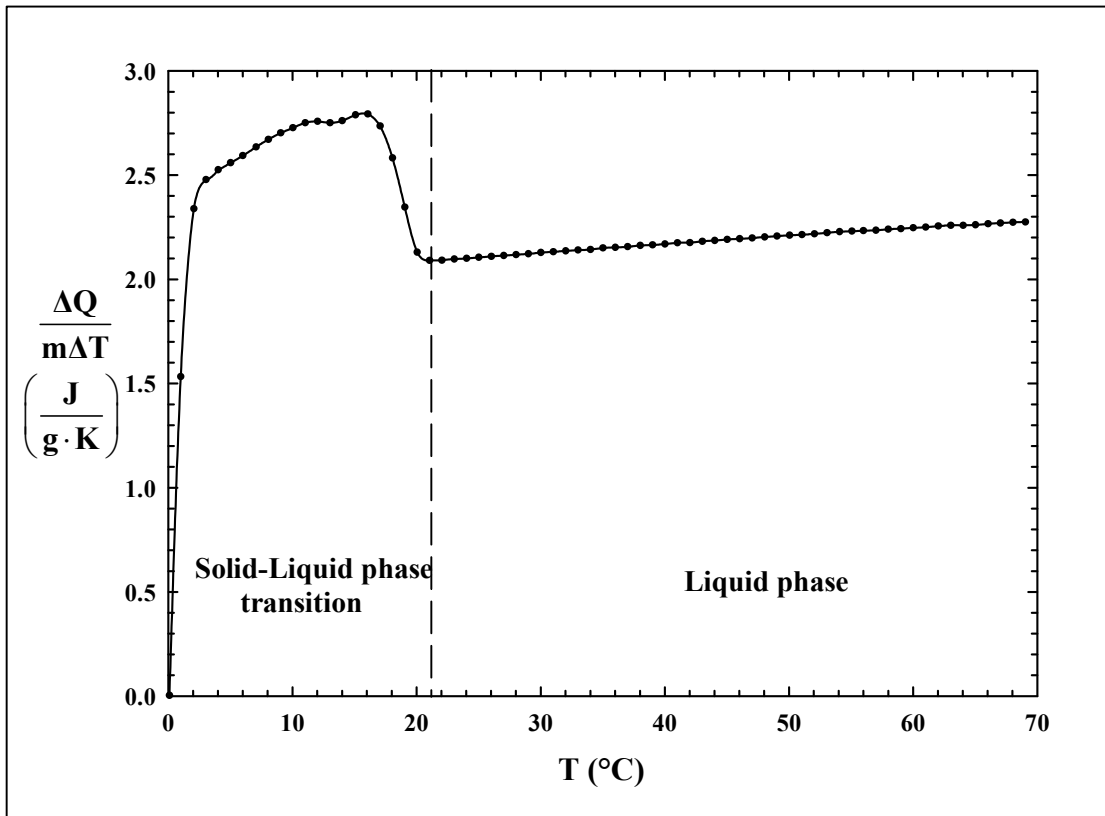


Figure 2.20 Specific heat capacity for ternary mixture with mass ratio of 1:0.1:1 in melting process.

Table 2.11 Specific heat capacities for the liquid phase of the ternary mixture with mass ratio (D:P:O) of 1:0.1:1.

In Liquid Phase			
T, °C	\bar{C}_p (DSC), J/g·K	\bar{C}_p (est.), J/g·K	% diff.
21.04	2.090	2.135	2.129
24.03	2.100	2.144	2.070
27.02	2.114	2.153	1.828
30.01	2.128	2.162	1.592
33.01	2.140	2.172	1.459
36.01	2.153	2.181	1.283
39.01	2.165	2.190	1.160
42.01	2.176	2.200	1.083
45.03	2.191	2.209	0.837
48.04	2.203	2.219	0.728
51.05	2.214	2.229	0.671
54.07	2.228	2.239	0.486
57.00	2.235	2.249	0.605
60.01	2.247	2.259	0.515
63.03	2.259	2.269	0.431
66.04	2.266	2.279	0.572
69.47	2.277	2.291	0.601

2.6 Conclusion

Solid–liquid and liquid–solid phase transitions of pure fatty acids and its mixtures with n-decane were thermally analyzed by means of differential scanning calorimetry (DSC). Melting temperature and enthalpy of melting obtained for pure palmitic acid are in good agreement with the values previously reported in the literatures. Solid–liquid phase transition for pure oleic acid presents two endothermic peaks, which related to a reversible solid–solid phase transition from γ to α phase. Thermal properties obtained from the solid–liquid and liquid–solid phase transitions for five ternary mixtures have different behaviors. Mass ratios of 1:1:1, 1:0.5:1, and 1:0.3:1 appear a single peak on the heating and cooling curve. In contrast to this, the presence of two peaks for mass ratio of 1:0.2:1 on the heating curve. Due to the quantity of oleic acid in the mixture increased, the appearance of an endothermic peak of oleic acid is observed. Mass ratio of 1:0.1:1 is not clearly shown for the phase transition in the studied temperature range. These behaviors result from the compositions in the mixture, especially palmitic acid and oleic acid while n-decane remains as a liquid state at the studied temperature range. The measurements of specific heat capacity for the liquid phase for pure fatty acids and ternary mixtures are in good agreement with the estimated values with the error values are within $\pm 5\%$. Liquid specific heat capacity for ternary mixtures shows linear behavior in the studied temperature range.

2.7 References

- Mang, T., and Dresel, W. (2007). **Lubricants and Lubrication**. Weinheim, Germany: Wiley.
- Johnson, R.W., and Fritz, E. (1989). **Fatty Acids in Industry: Processes, Properties, Derivatives, Applications**. New York: Marcel Dekker.
- Hatakeyama, T., and Quinn, F.X. (1999). **Thermal Analysis: Fundamentals and Applications to Polymer Science**. Chichester, New York: Wiley.
- Hatakeyama, T., and Liu, Z. (1998). **Handbook of Thermal Analysis**. Chichester, New York: Wiley.
- Huang, D., Simon, S.L., and McKenna, G.B. (2005). Chain length dependence of the thermodynamic properties of linear and cyclic alkanes and polymers. **The Journal of Chemical Physics**. 122(8), Art. No. 084907.
- Cedeño, F.O., Prieto, M.M., and Xiberta, J. (2000). Measurements and estimate of heat capacity for some pure fatty acids and their binary and ternary mixtures. **Journal of Chemical and Engineering Data**. 45(1): 64-69.
- Reid, R.C., Prausnitz, J.M., and Poling, B.E. (1987). **The Properties of Gases & Liquids**. New York: McGraw-Hill.
- Rihani, D.N., and Doraiswamy, L.K. (1965). Estimation of heat capacity of organic compounds from group contributions. **Industrial & Engineering Chemistry Fundamentals**. 4(1): 17-21.
- Teja, A. (1983). Simple method for the calculation of heat capacities of liquid mixtures. **Journal of Chemical and Engineering Data**. 28: 83-85.
- Morad, N.A., Mustafa Kamal, A.A., and Yew, T.W. (2000). Liquid specific heat capacity estimation for fatty acids, triacylglycerols, and vegetable oils based

- on their fatty acid composition. **Journal of the American Oil Chemists' Society.** 77(9): 1001-1005.
- Groenewoud, W.M., (2001). **Characterisation of Polymers by Thermal Analysis.** Amsterdam, New York: Elsevier.
- Cedeño, F.O., Prieto, M.M., Espina, A., and García, J.R. (2001). Measurements of temperature and melting heat of some pure fatty acids and their binary and ternary mixtures by differential scanning calorimetry. **Thermochimica Acta.** 369(1-2): 39–50.
- Formo, M.W., Jungermann, E., Norris, F.A., and Sonntag, N.O.V. (1979). **Bailey's Industrial Oil and Fat Products.** New York: Wiley.
- Acree, W.E. (1991). Thermodynamic properties of organic compounds: enthalpy of fusion and melting point temperature compilation. **Thermochimica Acta.** 189(1): 37–56.
- Weast, R.C. (1988). **Handbook of Chemistry and Physics.** Boca Raton, Florida: CRC Press.
- Gunstone, F.D., Harwood, J.L., and Padley, F.B. (1986). **The Lipids Handbook.** New York: Chapman & Hall.
- Domalski, E.S., Evans, W.H., and Hearing, E.D. (1984). **Heat Capacities and Entropies of Organic Compounds in the Condensed Phase.** New York: American Chemical Society.
- Pryde, E.H. (1979). **Fatty Acids.** New York: American Oil Society.
- Kim, Y., Strauss, H.L., and Snyder, R.G. (1988). Raman evidence for premelting in the α and β phases of oleic acid. **The Journal of Physical Chemistry.** 92(18): 5080-5082.

- Suzuki, M., Ogaki, T., and Sato, K. (1985). Crystallization and transformation mechanisms of α , β - and γ -polymorphs of ultra-pure oleic acid. **Journal of the American Oil Chemists' Society**. 62(11): 1600-1604.
- Garti, N., and Sato, K. (1988). **Crystallization and Polymorphism of Fats and Fatty Acids**. New York: Marcel Dekker.



CHAPTER III

STUDY OF SOLID–LIQUID EQUILIBRIA OF TERNARY

N-DECANE + PALMITIC ACID + OLEIC ACID

MIXTURES

3.1 Abstract

Solid–liquid equilibria of mixtures containing n-decane, palmitic acid and oleic acid were investigated in the temperature range of 305.15 to 323.15 K. The co-existing solid and liquid phases were found to contain substantial difference in compositions. Palmitic acid was the major component in the solid phase in all systems. Activity coefficient of palmitic acid in n-decane–oleic acid shows positive deviations from ideal-solution behavior. It is indicated that the solubilities of palmitic acid in these mixtures were lower than the calculated values for an ideal solubility. The experimental solubility data of palmitic acid in n-decane–oleic acid were correlated with the NRTL and UNIQUAC models. The best description was obtained using UNIQUAC with the root mean square deviation of temperature was lower than the NRTL model. The results obtained in this study could be an explanation of the solid deposit formation in a process involving fluids containing linear hydrocarbon and fatty acids.

3.2 Introduction

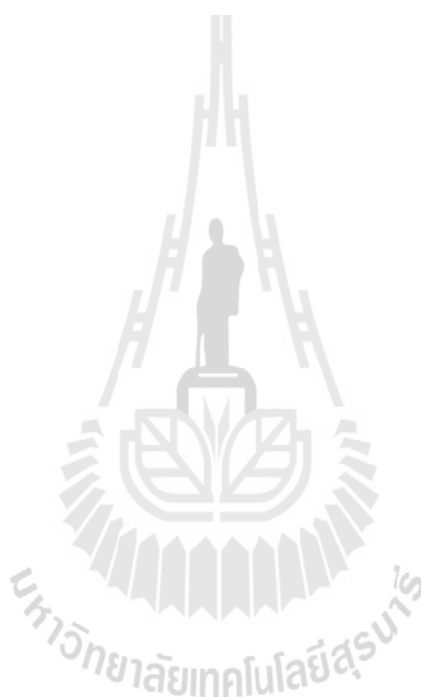
Metal working fluids or cutting fluids are extensively used in machining operations where the primary functions of a cutting fluid are lubrication and cooling. The characteristics of machining processes are the most parameter in the selection of cutting fluids. They are grouped into four major classes, which compose of straight oil or neat oil, soluble oil, semi-synthetic oil, and synthetic oil.

Straight oil can be used for applications in heavy machining process. The general components of straight oil are mineral oil and other additives. Fatty acids are widely used as additive to reduce friction between metal surfaces by the physical adsorption (Davey, 1950), which called the adsorption layer forming friction modifiers (Mang et al., 2007).

One manufacturer of spindle motor uses straight cutting oil for lubrication and cooling during the cutting and machining processes. It consists of mineral oil and mixed fatty acids. Straight oil was washed out using cleaning solvent with n-decane is a major component. The solid contaminant was observed on a product surface, it is a major problem encountered. Analysis of the contaminant revealed that the most component is aliphatic hydrocarbon. This result can be considered that the solubility between fatty acids absorbed on metal surface and hydrocarbon solvent may be the cause of the solid contaminant on a product surface.

Description of solid–liquid equilibrium (SLE) between fatty acids and hydrocarbon mixtures is needed in order to understand the phase behavior of fatty acids–hydrocarbon solvent mixture and to predict the mechanism of surface contamination encountered in the previously mentioned process. This research uses ternary mixtures of n-decane, palmitic acid, and oleic acid at various mass ratios for

determination of solid–liquid equilibrium between fatty acids and hydrocarbon. Equilibrium composition and temperature of each mass ratio was obtained. The experimental results was calculated the activity coefficients and correlated with the NRTL and UNIQUAC models. Interaction parameters corresponding to the system of n-decane–palmitic acid–oleic acid mixture were obtained.



3.3 Theory

3.3.1 Solid–Liquid Equilibria

For the binary two-phase system at temperature T , one phase is a liquid and the other is a solid. Let component 1 is the liquid solvent and component 2 is the solid solute. The equation of equilibrium is

$$f_2^S = f_2^L \quad (3.1)$$

where f_2^S is the fugacity of the solid solute in the solid phase and

f_2^L is the fugacity of the solid solute in the liquid phase.

An important simplifying assumption is considering that the solid phase consists only of component 2; that is, there is no solubility of component 1 in the solid phase. Eq. (3.1) may then be rewritten

$$\gamma_2 x_2 = \frac{f_2^S}{f_2^L} \quad (3.2)$$

where γ_2 is the liquid phase-activity coefficient of component 2 and

x_2 is the solubility of component 2 in the liquid phase.

The product $\gamma_2 x_2$ is the liquid phase activity (a_2) of component 2. The standard state fugacity for this activity is the fugacity of pure liquid 2 at system temperature. However, since system temperature is lower than the melting temperature of pure liquid 2, pure liquid 2 cannot exist (at equilibrium) at T . Pure liquid 2 at T is a subcooled liquid (Rousseau et al., 1987).

These two fugacities (f_2^S and f_2^L) depend only on the solid solute (component 2); they are independent of the nature of the liquid solvent (component 1). The ratio of these two fugacities can be calculated by the thermodynamic cycle indicated in Fig. 3.1 (Prausnitz et al., 1999).

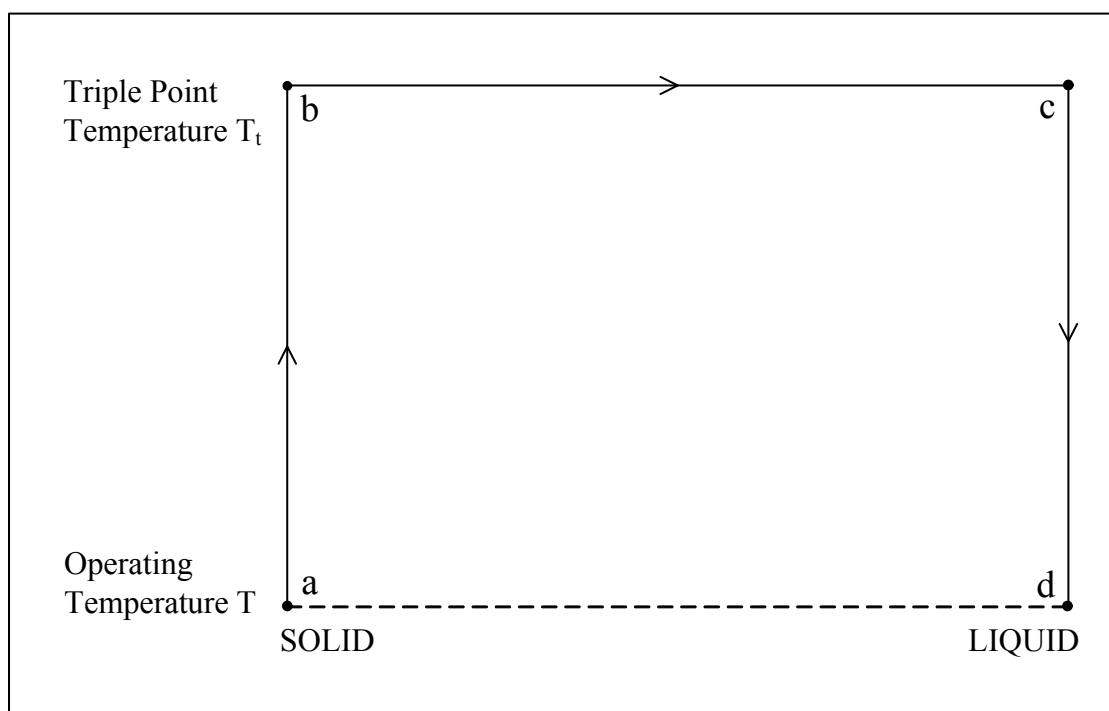


Figure 3.1 Thermodynamic cycle for calculating the fugacity of pure subcooled liquid.

The molar Gibbs energy change for component 2 in going from a to d is related to the fugacities of solid and subcooled liquid by

$$\Delta g_{a \rightarrow d} = RT \ln \frac{f^L}{f^S} \quad (3.3)$$

where, for simplicity, subscript 2 has been omitted. The Gibbs energy change is also related to the corresponding enthalpy and entropy changes by

$$\Delta g_{a \rightarrow d} = \Delta h_{a \rightarrow d} - T \Delta s_{a \rightarrow d} \quad (3.4)$$

The thermodynamic cycle in Fig. 3.1 provides a method to evaluate the enthalpy and entropy changes given in Eq. (3.4). For the enthalpy change from a to d :

$$\Delta h_{a \rightarrow d} = \Delta h_{a \rightarrow b} + \Delta h_{b \rightarrow c} + \Delta h_{c \rightarrow d} \quad (3.5)$$

Equation (3.5) can be rewritten in terms of heat capacity C_p and enthalpy of fusion ΔH_f :

$$\Delta h_{a \rightarrow d} = (\Delta H_f)_{\text{at } T_t} + \int_{T_t}^T \Delta C_p dT \quad (3.6)$$

where $\Delta C_p \equiv C_{p(\text{liquid})} - C_{p(\text{solid})}$ and T_t is the triple-point temperature. Similarly, for the entropy change from a to d ,

$$\Delta s_{a \rightarrow d} = \Delta s_{a \rightarrow b} + \Delta s_{b \rightarrow c} + \Delta s_{c \rightarrow d} \quad (3.7)$$

which becomes

$$\Delta s_{a \rightarrow d} = (\Delta s_f)_{\text{at } T_t} + \int_{T_t}^T \frac{\Delta C_p}{T} dT \quad (3.8)$$

At the triple point, the entropy of fusion is

$$\Delta s_f = \frac{\Delta H_f}{T_t} \quad (3.9)$$

Substituting Eqs. (3.4), (3.6), (3.8), and (3.9) into Eq. (3.3), and assuming that ΔC_p is constant over the temperature range $T \rightarrow T_t$, obtains

$$\ln(x_i \gamma_i) = -\frac{\Delta H_{f,i}}{RT_{t,i}} \left(\frac{T_{t,i}}{T} - 1 \right) + \frac{\Delta C_{p,i}}{R} \left(\frac{T_{t,i}}{T} - 1 \right) - \frac{\Delta C_{p,i}}{R} \ln \frac{T_{t,i}}{T} \quad (3.10)$$

where x_i = mole fraction of component i in liquid phase,

γ_i = activity coefficients of component i in liquid phase,

$\Delta H_{f,i}$ = enthalpy of fusion of component i ,

$\Delta C_{p,i}$ = difference between the heat capacity of the liquid and solid phases,

$T_{t,i}$ = triple-point temperature of component i ,

T = equilibrium temperature, and

R = universal gas constant

An assumption is applied to Eq. (3.10) is considering that the triple-point temperature is close to the normal melting temperature, so triple-point temperature (T_t) in Eq. (3.10) can be substituted by normal melting temperature (T_f).

The equation of solid–liquid equilibrium becomes

$$\ln(x_i \gamma_i) = -\frac{\Delta H_{f,i}}{RT_{f,i}} \left(\frac{T_{f,i}}{T} - 1 \right) + \frac{\Delta C_{p,i}}{R} \left(\frac{T_{f,i}}{T} - 1 \right) - \frac{\Delta C_{p,i}}{R} \ln \frac{T_{f,i}}{T} \quad (3.11)$$

The thermophysical properties of pure component ($\Delta H_{f,i}$, $T_{f,i}$, and $\Delta C_{p,i}$) are obtained from the DSC analysis. The activity coefficients (γ_i) calculated from Eq. (3.11) are correlated with the thermodynamic models.

3.3.2 Thermodynamic Models

3.3.2.1 The Non-Random Two-Liquid (NRTL) Model

The non-random two-liquid or NRTL equation has been proposed for the relation between activity coefficient (γ_i) and mole fraction (x_i) in liquid phase concerned. The NRTL equation was published by Henri Renon and John M. Prausnitz (1968) as local compositions in thermodynamic excess functions for liquid mixtures. It is applicable to partially miscible as well as completely miscible systems. The excess Gibb energy of the NRTL equation for multicomponent mixtures is

$$\frac{g^E}{RT} = \sum_{i=1}^m x_i \frac{\sum_{j=i}^m \tau_{ji} G_{ji} x_j}{\sum_{l=1}^m G_{li} x_l} \quad (3.12)$$

where $\tau_{ji} = \frac{g_{ji} - g_{ii}}{RT}$

$$G_{ji} = \exp(-\alpha_{ji} \tau_{ji}) \quad (\alpha_{ji} = \alpha_{ij})$$

The significance of g_{ij} is an energy parameter characteristic of the $i-j$ interaction. Parameter α_{ij} is related to the nonrandomness in the mixture. The value of α_{ij} are often be set arbitrarily and normally varies from about 0.20 to

0.47. A typical choice is $\alpha_{ij} = 0.30$. The activity coefficient for any component i is given by

$$\ln \gamma_i = \frac{\sum_{j=1}^m \tau_{ji} G_{ji} x_j}{\sum_{l=1}^m G_{li} x_l} + \sum_{j=1}^m \frac{x_j G_{ij}}{\sum_{l=1}^m G_{lj} x_l} \left(\tau_{ij} - \frac{\sum_{r=1}^m x_r \tau_{rj} G_{rj}}{\sum_{l=1}^m G_{lj} x_l} \right) \quad (3.13)$$

The NRTL parameters can be determined by fitting the activity coefficients that have been derived from the experimental solid–liquid phase equilibrium.

3.3.2.2 The UNiVersal QUasi-Chemical (UNIQUAC) Model

In universal quasi-chemical model or, in short, UNIQUAC equation, the activity coefficient has two parts: combinatorial and residual. The combinatorial part describes the dominant entropic contribution, and the residual part is due to intermolecular forces that are responsible for the enthalpy of mixing. The excess Gibbs energy (g^E) for multicomponent mixtures for UNIQUAC equation is

$$\frac{g_{(\text{combinatorial})}^E}{RT} = \sum_{i=1}^m x_i \ln \frac{\Phi_i^*}{x_i} + \frac{z}{2} \sum_{i=1}^m q_i x_i \ln \frac{\theta_i}{\Phi_i^*} \quad (3.14)$$

And

$$\frac{g_{(\text{residual})}^E}{RT} = - \sum_{i=1}^m q'_i x_i \ln \left(\sum_{j=1}^m \theta'_j \tau_{ji} \right) \quad (3.15)$$

where the coordination number z is set equal to 10. Segment fraction, Φ^* , and area fractions, θ and θ' , are given by

$$\Phi_i^* = \frac{r_i x_i}{\sum_{j=1}^m r_j x_j} \quad \theta_i = \frac{q_i x_i}{\sum_{j=1}^m q_j x_j} \quad \theta'_i = \frac{q'_i x_i}{\sum_{j=1}^m q'_j x_j}$$

And

$$\tau_{ij} = \exp\left(-\frac{a_{ij}}{T}\right) \quad \text{and} \quad \tau_{ji} = \exp\left(-\frac{a_{ji}}{T}\right)$$

Parameters r , q , and q' are pure-component molecular-structure constants depending on molecular size and external surface areas. In the original formulations, $q = q'$. The values of the parameters r and q used in this research are shown in Table 3.1. For any component i , the activity coefficient is given by

$$\begin{aligned} \ln \gamma_i = & \ln \frac{\Phi_i^*}{x_i} + \frac{z}{2} q_i \ln \frac{\theta_i}{\Phi_i^*} + l_i - \frac{\Phi_i^*}{x_i} \sum_{j=1}^m x_j l_j \\ & - q'_i \ln \left(\sum_{j=1}^m \theta'_j \tau_{ji} \right) + q'_i - q'_i \sum_{j=1}^m \frac{\theta'_j \tau_{ij}}{\sum_{k=1}^m \theta'_k \tau_{kj}} \end{aligned} \quad (3.16)$$

where

$$l_j = \frac{z}{2} (r_j - q_j) - (r_j - 1) \quad (3.17)$$

The UNIQUAC equation is applicable to a wide variety of nonelectrolyte liquid mixtures containing nonpolar or polar fluids such as hydrocarbons, alcohols, nitriles, ketones, aldehydes, organic acids, etc. and water, including partially miscible mixtures. The UNIQUAC parameters (τ_{ij} and τ_{ji}) are the empirical parameter between components that describes the intermolecular behavior.

Table 3.1 Structure parameters for UNIQUAC equation (Abrams et al., 1975).

Component	r	q
n-Decane	7.1971	6.0160
Palmitic acid	11.6289	9.6320
Oleic acid	12.7456	10.4960

3.3.3 Broyden's Method

Broyden's method approximates Jacobian matrix rather than calculating them directly (Wang et al., 1993). This method called quasi-Newton method, which replace the Jacobian matrix in Newton's method with an approximation matrix that is updated at each iteration (Burden et al, 2005). The resulting scheme not only reduces the number of scalar function evaluations required each iteration, but also dramatically decreases the operation count associated with computing the update vector ($x^{(k)} - x^{(k-1)}$) (Bradie, 2006).

The first iteration of Broyden's method is almost identical to that of Newton's method. Using the initial vectors $x^{(0)}$, $F(x^{(0)})$ and $J(x^{(0)})$ are evaluated. For

later convenience will denote the Jacobian $J(x^{(0)})$ by J_0 . Next, compute J_0^{-1} into $F(x^{(0)})$ to form $(x^{(k)} - x^{(k-1)})$. Finally, update $x^{(0)}$ to $x^{(1)}$ (Bradie, 2006).

For all subsequent iterations, Broyden's method forgoes the calculation of the Jacobian. Rather, a matrix J_k is sought which approximates $J(x^{(k)})$ in the sense that

$$A_k (x^{(k)} - x^{(k-1)}) = F(x^{(k)}) - F(x^{(k-1)})$$

if $s_k = x_k - x_{k-1}$;

$$A_k s_k = F(x^{(k)}) - F(x^{(k-1)}). \quad (3.18)$$

For the case $n = 1$, Eq. (3.18) does not uniquely determine the matrix A_k , it provides only n equations for the n^2 elements of A_k . The best additional constraints lead to the requirement

$$A_k u = A_{k-1} u \text{ for all vectors } u \text{ such that } (x^{(k)} - x^{(k-1)})^T u = 0.$$

Combining these conditions with Eq. (3.18) uniquely determines

$$A_k = A_{k-1} + \frac{(y_k - A_{k-1} s_k) s_k^T}{s_k^T s_k}, \quad (3.19)$$

where $y_k = F(x^{(k)}) - F(x^{(k-1)})$. In fact, Broyden's update is the minimum change to A_k subject to quasi-Newton condition, called *least change secant approximation* to Jacobian. This leads to the following iteration method of Broyden:

Given $x_0 \in R^n$ and $A_0 \in R^{n \times n}$, for $k = 0, 1, \dots$

Solve $A_k s_k = -F(x_k)$ for s_k .

Then $x_k = x_{k-1} + s_k$, $y_k = F(x_k) - F(x_{k-1})$.

Set $A_k = A_{k-1} + \frac{(y_k - A_{k-1}s_k)s_k^T}{s_k^T s_k}$.

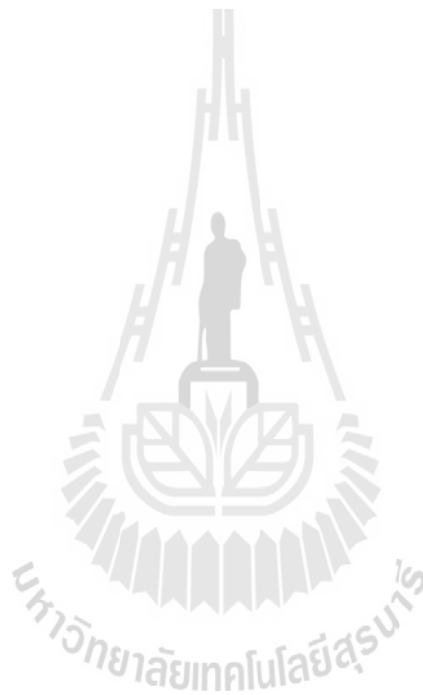
A more significant reduction in computational effort is achieved by making use of the Sherman–Morrison formula. If M is a nonsingular matrix and \mathbf{u} and \mathbf{v} are vectors, then $M + \mathbf{u}\mathbf{v}^T$ is nonsingular, provided that $\mathbf{v}^T M^{-1}\mathbf{u} \neq -1$, and

$$(M + \mathbf{u}\mathbf{v}^T)^{-1} = M^{-1} - \frac{M^{-1}\mathbf{u}\mathbf{v}^T M^{-1}}{1 + \mathbf{v}^T M^{-1}\mathbf{u}}. \quad (3.20)$$

Identifying the matrix A_{k-1} with M , the vector $(y_k - A_{k-1}s_k)/(s_k^T s_k)$ with \mathbf{u} and the vector s_k with \mathbf{v} , Eq. (3.19) and (3.20) imply

$$\begin{aligned} A_k^{-1} &= \left(A_{k-1} + \frac{(y_k - A_{k-1}s_k)s_k^T}{s_k^T s_k} \right)^{-1} \\ &= A_{k-1}^{-1} - \frac{A_{k-1}^{-1} \left(\frac{(y_k - A_{k-1}s_k)s_k^T}{s_k^T s_k} \right) A_{k-1}^{-1}}{1 + s_k^T A_{k-1}^{-1} \left(\frac{y_k - A_{k-1}s_k}{s_k^T s_k} \right)} \\ &= A_{k-1}^{-1} + \frac{(s_k - A_{k-1}^{-1}y_k)s_k^T A_{k-1}^{-1}}{s_k^T A_{k-1}^{-1}y_k}. \end{aligned} \quad (3.21)$$

The computation of Eq. (3.21) involves only matrix-vector multiplication at each step and therefore provides a procedure for calculating A_k^{-1} directly from A_{k-1}^{-1} in only $O(n^2)$ algebraic operations. With A_k^{-1} known, the need to solve a linear system at each iteration to compute the update vector $(x^{(k)} - x^{(k-1)})$ is eliminated; instead, $(x^{(k)} - x^{(k-1)})$ is determined by forming the matrix-vector product $A_k^{-1}F(x^{(k)})$.



3.4 Experimental Procedures

3.4.1 Chemicals

n-Decane (99+% purity) and palmitic acid (98% purity) were purchased from ACROS. Pure oleic acid and dichloromethane (99.5% purity) were obtained from CARLO ERBA. All the chemicals were used as received without further purification.

3.4.2 Preparation of Ternary Mixtures

Ternary mixtures were prepared on an analytical balance (Sartorius BP 221 model) with a ± 0.0001 g precision. The compositions for ternary mixtures were prepared with six different mass ratios. Mass ratio of n-decane (D) : palmitic acid (P) : oleic acid (O) studied in this work were 1:1:1, 1:0.5:1, 1:0.3:1, 3:1:1, 0.2:1:1 and 1:1:0.5. Weighed quantities of the mixture components were charged into a 50 ml laboratory glass bottle (SCHOTT DURAN), which was then capped tightly and immersed in a water bath (NESLAB GP-400) at 60°C and left for thermal equilibration for 1 hour. After that, the mixtures were manually shaken to ensure complete dissolution of all components. The solutions were kept at room temperature until later use.

3.4.3 Solid–liquid Equilibria

Ternary mixtures prepared as previously described were immersed in the water bath at equilibrium temperature of each mass ratio (was obtained by the DSC data in the previous chapter) for 24 hours for a fully separation of the mixture into liquid (top layer) and solid (bottom layer) phase. Approximately 30 to 50 mg for liquid phase was collected into a 2.0 ml vial (Agilent Technologies) using micropipette (BIO-RAD). Sample for solid phase can be collected by filtering. All liquid and solid

phases in a 50 ml laboratory glass bottle were filtered through a 0.45 μm cellulose acetate membrane filter using 47 mm filter holder (Millipore Swinnex). The filtered solid and liquid phase was weighed on an analytical balance (Sartorius BP 221 model) to calculate total weight of liquid and solid phase obtained from the solid–liquid phase separation.

3.4.4 Analysis of the Compositions

The compositions (n-decane, palmitic acid and oleic acid) of both phases were analyzed by a Shimadzu GC-14B, equipped with flame ionization detector (FID) using a DB-1HT capillary column, (30 m length, 0.25 mm internal diameter and 0.10 μm film thickness). Table 3.2 shows temperature program used in this work and Fig. 3.2 was a corresponding chart with a temperature program. The injector and detector temperatures were set at 300°C and 350°C, respectively. Helium was used as a carrier gas. All samples were diluted with dichloromethane before being analyzed in order to reduce the concentration of the samples to be in the range of the area of calibration standard curve for n-decane, palmitic acid, and oleic acid. In addition to dissolve the solid sample for the component analysis in the solid phase. Dilution ratio was considered with mass ratio of sample : dichloromethane as shown in Appendix E. The quantity of dichloromethane used will be recorded to calculate the real concentration after dilution. Approximately 1.0 μl of sample was injected using a micro syringe (Hamilton Microliter Syringe 801RN, 10 μl) into the GC analysis.

3.4.5 Determination of Components in Liquid and Solid Phases

Determination of n-decane, palmitic acid and oleic acid in liquid and solid phases is shown in Appendix E. It is the component analysis of solid–liquid equilibrium for mass ratio of 1:1:1 at equilibrium temperature of 43.0°C. For other

mass ratios can be determined as same as mass ratio of 1:1:1. The obtained total mass in liquid and solid phase was compared with the initial mass ratio of each system where the error percentage should be less than $\pm 10\%$.

Table 3.2 Temperature program for the analysis.

Rate ($^{\circ}\text{C} \cdot \text{min}^{-1}$)	Temperature ($^{\circ}\text{C}$)	Hold (min)
-	40.0	3.0
20.0	140.0	-
8.0	220.0	3.0
10.0	340.0	5.0
	Total	38.0

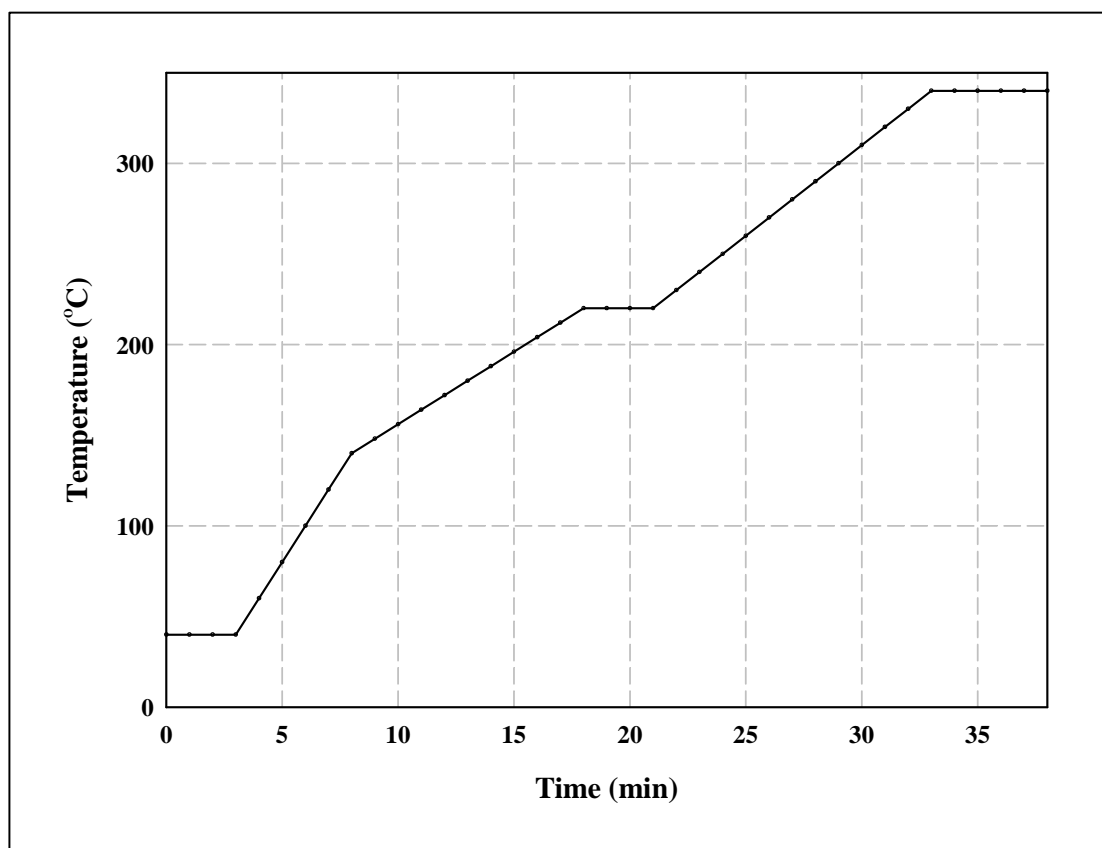


Figure 3.2 Illustration of temperature program.

3.5 Results and Discussion

3.5.1 Solid–Liquid Equilibria

Equilibrium temperatures and compositions of the ternary mixtures obtained from solid–liquid equilibrium experiments are listed in Table 3.3. Solubility of each component in the ternary mixture is represented by their mole fractions in the liquid and solid phases. It is observed that mole fraction of each component in liquid phase to be resemblance to the mole fraction in the starting mixtures.

The ternary mixtures for six mass ratios studied in solid–liquid equilibrium experiments could be classified into 3 groups which correspond to their mass ratios. The first group is the group of mixtures with mass ratio of 1:0.3:1, 1:0.5:1 and 1:1:1, which is based on the quantity of palmitic acid. This group, the relationship between the measured mole fraction of palmitic acid in liquid phase versus equilibrium temperature is shown in Fig. 3.3. It can be seen that equilibrium temperature increases with increasing mole fraction of palmitic acid. While tendency for mole fraction of n-decane and oleic acid are decrease values since the incremental quantity of palmitic acid. It is shown that influence of palmitic acid in mixture increases whereas n-decane and oleic acid decreases. Therefore, equilibrium temperature for this group is proportional to palmitic acid only.

The second group is the group of mixtures with mass ratio of 0.2:1:1, 1:1:1 and 3:1:1, which is based on the quantity of n-decane. Fig. 3.4 shows ternary phase diagram of n-decane + palmitic acid + oleic acid in liquid phase for this group. It is found that equilibrium temperature decreases with increasing mole fraction of n-decane. While mole fraction of palmitic acid and oleic acid is continuously decrease values. Thus, the component in the mixtures that affected the equilibrium temperature

is n-decane only. Low melting point of n-decane is the cause of the decrease of the solid–liquid equilibrium temperature.

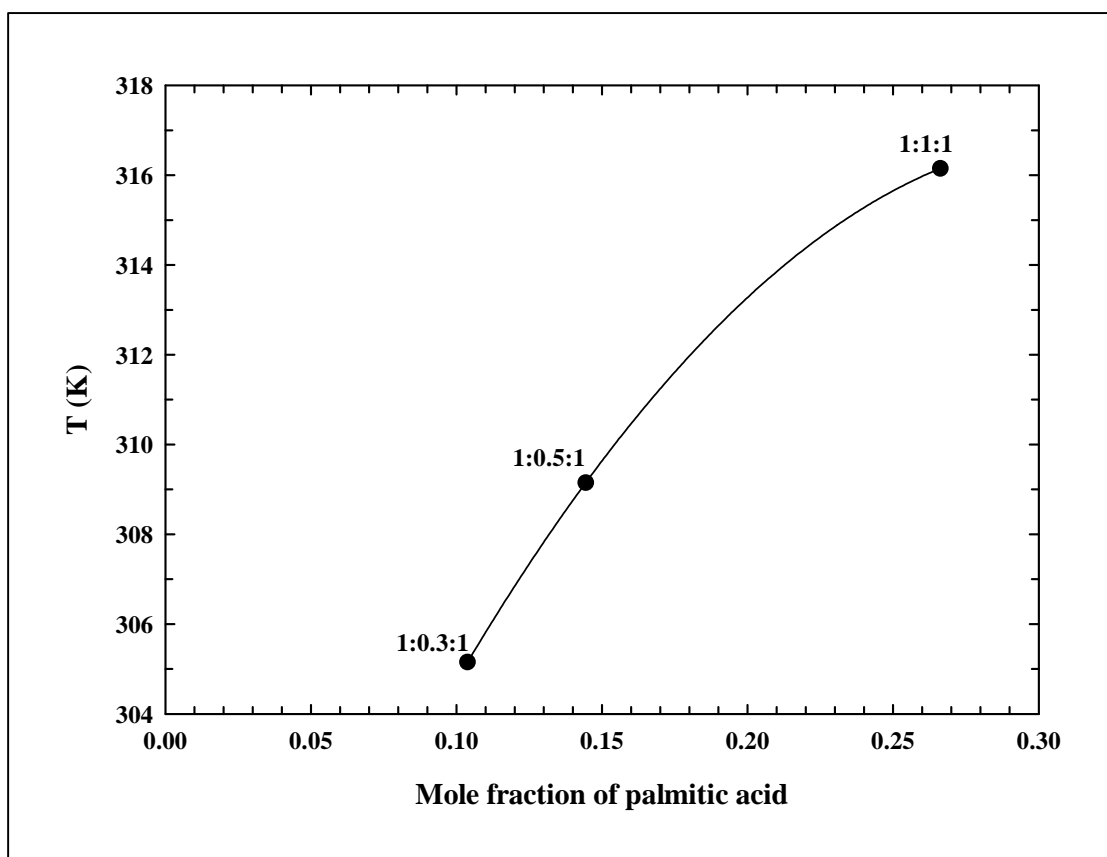


Figure 3.3 Mole fraction of palmitic acid in liquid phase with mass ratios (D:P:O) of 1:0.3:1, 1:0.5:1 and 1:1:1.

The last group is the group of mixtures with mass ratio of 1:1:0.5 and 1:1:1, which is based on the quantity of oleic acid. Tendency for this group, equilibrium temperature decreases with increasing mole fraction of oleic acid, is observed from Table 3.3. Oleic acid in the mixtures affects the decreases of equilibrium temperature in this group. It is related to the melting point of oleic acid results in the solid–liquid equilibrium temperature decreases.

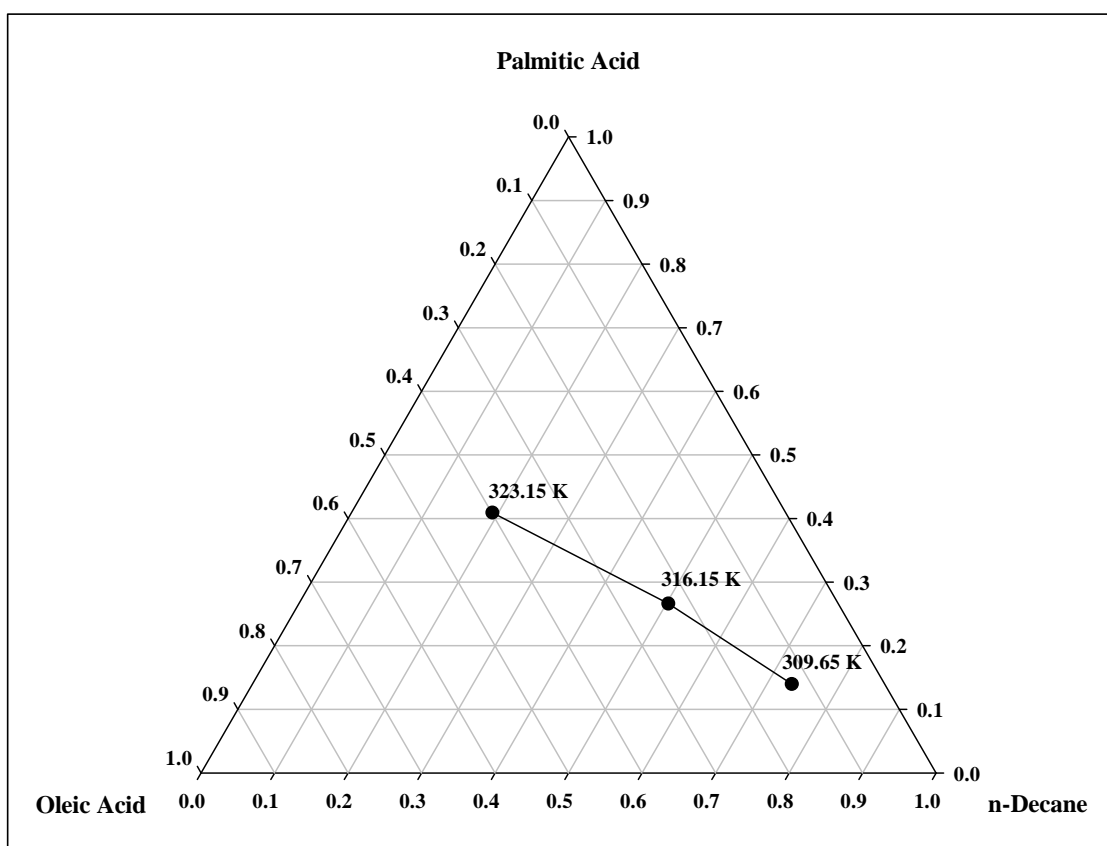


Figure 3.4 Ternary phase diagram of n-decane + palmitic acid + oleic acid

in liquid phase with mass ratios of 0.2:1:1, 1:1:1 and 3:1:1.

Equilibrium mole fractions of n-decane, palmitic acid and oleic acid in solid phase in all mass mixtures, palmitic acid is the major component in solid phase as listed in Table 3.3. This result supports the fact that the melting point of palmitic acid is higher than melting point of n-decane and oleic acid. Furthermore, the temperature range used in this study is higher than melting point of n-decane and oleic acid, but lower than the melting point of palmitic acid. It is expected that both these components are not appear in solid phase; n-decane and oleic acid are exist in liquid phase and palmitic acid is a pure solid in solid phase. However, the experimental results of the component analysis in solid phase observed in Table 3.3 are not pure as

expected. It appears quantities of n-decane and oleic acid in solid phase, may be due to solid samples obtained from the filtering are not dry completely. Some quantities of n-decane and oleic acid in liquid phase contaminate in solid samples.

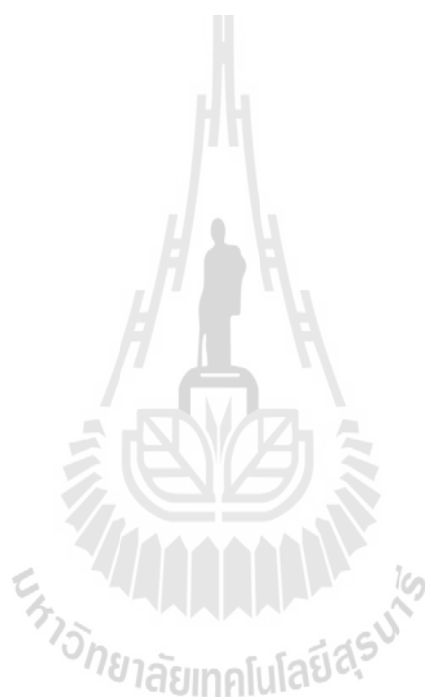


Table 3.3 Equilibrium temperature and composition of ternary n-decane (1) + palmitic acid (2) + oleic acid (3) mixtures.

Initial mass ratio (D:P:O)	Starting mixtures			Liquid phase (Top layer)			Solid phase (Bottom layer)			T (K)
	x_1	x_2	x_3	x_1	x_2	x_3	x_1	x_2	x_3	
1:0.3:1	0.5921	0.1096	0.2983	0.6009	0.1038	0.2953	0.2198	0.6711	0.1091	305.15
1:0.5:1	0.5613	0.1558	0.2829	0.6202	0.1444	0.2354	0.2168	0.5753	0.2079	309.15
1:1:1	0.4859	0.2695	0.2446	0.5025	0.2662	0.2313	0.2662	0.5490	0.1848	316.15
0.2:1:1	0.1592	0.4406	0.4002	0.1919	0.4092	0.3989	0.1527	0.5239	0.3234	323.15
1:1:1	0.4859	0.2695	0.2446	0.5025	0.2662	0.2313	0.2662	0.5490	0.1848	316.15
3:1:1	0.7390	0.1367	0.1243	0.7338	0.1397	0.1265	0.1977	0.7008	0.1015	309.65
1:1:0.5	0.5534	0.3072	0.1394	0.6043	0.2617	0.1340	0.2694	0.6233	0.1073	319.15
1:1:1	0.4859	0.2695	0.2446	0.5025	0.2662	0.2313	0.2662	0.5490	0.1848	316.15

3.5.2 Solid–Liquid Equilibrium Models

In order to consistent with the experimental results, solid–liquid equilibrium of palmitic acid in two-component solvents (n-decane–oleic acid) was taken into consideration. Activity coefficient of palmitic acid in n-decane–oleic acid can be calculated from Eq. (3.11) by considering that palmitic acid is pure solid in solid phase. Thermal properties for pure palmitic acid obtained from the DSC analysis contain $\Delta H_f = 208.019 \text{ J}\cdot\text{g}^{-1}$ and $T_f = 62.03^\circ\text{C}$. The ΔC_p for pure palmitic acid has minor value, it can be neglected the two terms from Eq. (3.11) becomes

$$\ln(x_i\gamma_i) = -\frac{\Delta H_{f,i}}{RT_{f,i}} \left(\frac{T_{f,i}}{T} - 1 \right) \quad (3.22)$$

Solubilities and activity coefficients of palmitic acid in n-decane–oleic acid at six equilibrium temperatures are shown in Table 3.4. The solubilities of palmitic acid appeared to increase with increasing temperature, which is expected and is similar to the results observed in the case of palmitic acid in various pure solvents such as ethanol, 2-propanol, hexane, heptane, acetone, trichloroethylene and their mixtures (Calvo et al., 2009).

The activity coefficient of palmitic acid in the n-decane–oleic acid mixtures show positive deviations ($\gamma_2 > 1$) from the ideality behavior as presented in Fig. 3.5. It is indicated that the solubility of this acid in these mixtures are lower than the ideal values.

Table 3.4 Solubility and activity coefficient of palmitic acid in n-decane – oleic acid.

Equilibrium temperature (K)	x_2	γ_2
305.15	0.1038	1.4646
309.15	0.1444	1.3820
309.65	0.1397	1.4771
316.15	0.2662	1.1868
319.15	0.2617	1.4611
323.15	0.4092	1.1984

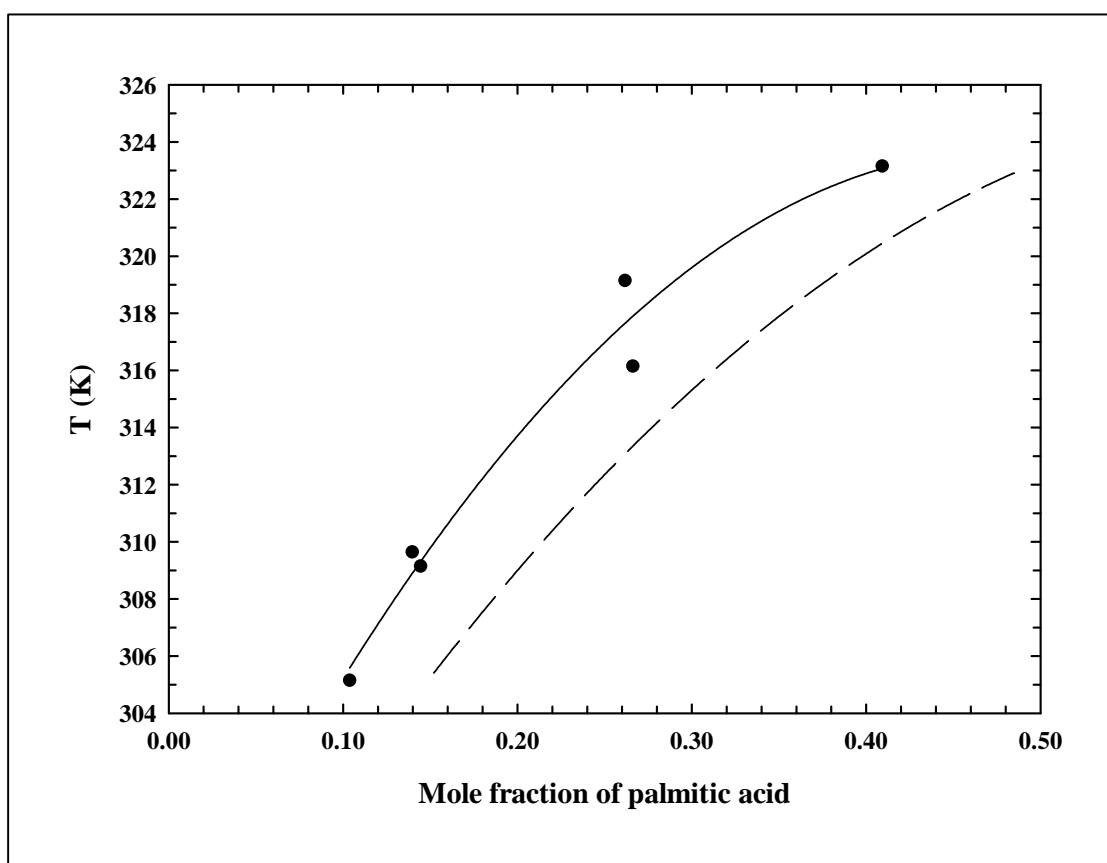


Figure 3.5 Solubility of palmitic acid in n-decane – oleic acid: (—) is experiment and (- -) is ideal solution ($\gamma_2 = 1$) calculated from Eq. (3.22).

This could be due to the difference in natures of all the components in the mixtures. n-Decane is a linear hydrocarbon with low polarity, while oleic acid and palmitic acid possess a carboxylic polar portion. Palmitic acid is one of the most common saturated fatty acids found in animal and plants (Gunstone, 1996). Oleic acid is a monounsaturated fatty acid with one double bond in the molecule. The dissimilarity in molecular nature could rather lead to the attraction between molecules of the same type and result in low solubility of the components in the mixture. In addition, palmitic acid is a carboxylic acid which is self-associate by hydrogen bonding in case of acid dissolved in linear hydrocarbon.

The solubility of palmitic acid in ternary mixtures that was lower than the ideal value could also be due to the influence of hydrogen bonding interaction on the solubility of palmitic acid in n-decane which exists as dimeric structures in the liquid and solid states (Brown, 1997). The existence of palmitic acid dimers in n-decane–oleic acid should be improved for the enthalpy of fusion (ΔH_f) and for mole fraction of palmitic acid (x_2), but in oleic acid probably is a monomer due to dimerization of solvent. Type of solvents was reported to have profound effect on temperature dependency of palmitic acid activity coefficients. In some pure solvents such as acetone, ethanol, heptanes, hexane and 2-propanol, value of palmitic acid coefficients were decreased with increasing temperature, while in others, for example trichloroethylene, the values were increased with increasing temperature (Calvo et al., 2009). Activity coefficient of palmitic acid was found to depend on temperature, which was clearly shown in the mixtures with the same mole fractions of palmitic acid ($x_2 \approx 0.26$), the activity coefficient was larger at higher equilibrium temperature.

NRTL and UNIQUAC models are used for correlation of the activity coefficient of palmitic acid in n-decane – oleic acid. The activity coefficient for NRTL model is calculated with the nonrandomness parameter $\alpha = 0.3$, which corresponds to the study of solubility of palmitic acid in pure solvents and its mixtures (Calvo et al., 2009).

The root mean square deviation of temperature, σ between experimental and calculated values is defined by the following equation (Domańska., 1987, Cepeda et al., 2009, Calvo et al., 2009)

$$\sigma = \left[\frac{\sum_{i=1}^n (T_i^{\text{cal}} - T_i^{\text{exp}})^2}{n-1} \right]^{1/2} \quad (3.23)$$

where n is the number of experimental data,

T_i^{cal} is the equilibrium temperature calculated from Eq. (3.22) with the γ_i^{cal} values, and

T_i^{exp} is the experimental equilibrium temperature.

The interaction energy parameters of the NRTL and UNIQUAC models are listed in Table 3.5 and 3.6, respectively. The parameters for both models are dependent on temperature.

The best description of solid–liquid equilibrium was given by the UNIQUAC model with the root mean square deviation of temperature $\sigma_U = 1.94$ K. While the NRTL model presents $\sigma_N = 2.36$ K.

Table 3.5 Energy parameters of NRTL model for the palmitic acid in n-decane – oleic acid system.

Mass ratio	T (K)	Energy Parameters (A_{ij} , $\text{J}\cdot\text{mol}^{-1}$)					
		A_{12}	A_{21}	A_{13}	A_{31}	A_{23}	A_{32}
1:0.3:1	305.15	1872.32	-211.08	-347.57	-465.29	2108.77	-2292.70
1:0.5:1	309.15	1896.86	-213.85	-352.13	-471.39	2136.41	-2322.76
3:1:1	309.65	1899.93	-214.19	-352.70	-472.15	2139.87	-2326.51
1:1:1	316.15	1939.81	-218.69	-360.10	-482.06	2184.79	-2375.35
1:1:0.5	319.15	1958.22	-220.76	-363.52	-486.64	2205.52	-2397.89
0.2:1:1	323.15	1982.76	-223.53	-368.07	-492.74	2233.16	-2427.94

$A_{ij} = g_{ij} - g_{jj}$; g_{ij} ($\text{J}\cdot\text{mol}^{-1}$) is an energy parameter characteristic of the i - j interaction.

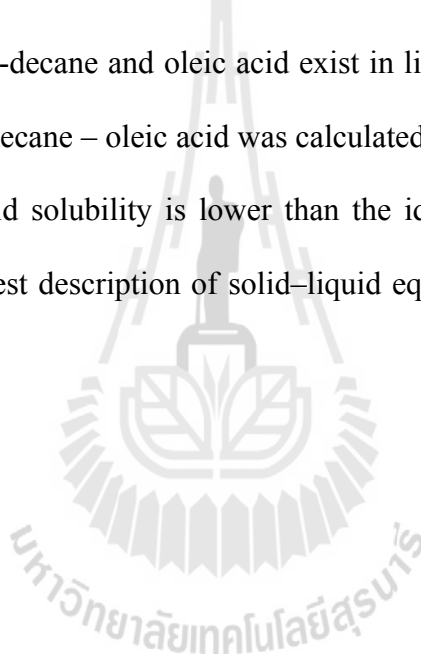
Table 3.6 Energy parameters of UNIQUAC model for the palmitic acid in n-decane – oleic acid system.

Mass ratio	T (K)	Energy Parameters (a_{ij} , K)					
		a_{12}	a_{21}	a_{13}	a_{31}	a_{23}	a_{32}
1:0.3:1	305.15	-112.03	166.43	149.79	-194.90	739.22	-312.81
1:0.5:1	309.15	-113.50	168.62	151.75	-197.45	748.91	-316.91
3:1:1	309.65	-113.68	168.89	151.99	-197.77	750.13	-317.43
1:1:1	316.15	-116.07	172.43	155.19	-201.92	765.87	-324.09
1:1:0.5	319.15	-117.17	174.07	156.66	-203.84	773.14	-327.16
0.2:1:1	323.15	-118.64	176.25	158.62	-206.39	782.83	-331.26

$a_{ij} = (u_{ij} - u_{jj})/R$; u_{ij} ($\text{J}\cdot\text{mol}^{-1}$) is an energy parameter characteristic of the i - j interaction.

3.6 Conclusion

Solid–liquid equilibria of the n-decane + palmitic acid + oleic acid mixtures were studied in this work. Equilibrium mole fractions obtained in liquid phase are similar values with the starting mixtures. Equilibrium temperature depends on the component containing the most quantity in the mixtures. Equilibrium mole fraction in solid phase contains palmitic acid as the major component in all mixtures. The occurrences of n-decane and oleic acid have the less quantity than palmitic acid. The mostly quantities of n-decane and oleic acid exist in liquid phase. Activity coefficient of palmitic acid in n-decane – oleic acid was calculated by the solid–liquid equilibrium equation. Palmitic acid solubility is lower than the ideal solubility. The UNIQUAC equation shows the best description of solid–liquid equilibrium of palmitic acid in n-decane – oleic acid.



3.7 References

- Davey, W. (1950). Boundary lubrication of steel blends of acids, esters, and soaps in mineral oil. **Industrial and Engineering Chemistry**. 42(9): 1837-1841.
- Mand, T., and Dresel, W. (2007). **Lubricants and Lubrication**. Weinheim, Germany: Wiley-VCH.
- Rousseau, R.W. (1987). **Handbook of Separation Process Technology**. Canada: John Wiley & Sons.
- Prausnitz, J.M., Lichtenthaler, R.N., and de Azevedo, E.G. (1999). **Molecular Thermodynamics of Fluid-Phase Equilibrium**. New Jersey: Prentice-Hall.
- Abrams, D.S., and Prausnitz, J.M. (1975). Statistical thermodynamics of liquid mixtures: A new expression for the excess Gibbs energy of partly or completely miscible systems. **AIChE Journal**. 21(1): 116-128.
- Calvo, B., and Cepeda, E.A. (2008). Solubilities of stearic acid in organic solvents and in azeotropic solvent mixtures. **Journal of Chemical & Engineering Data**. 53(3): 628-633.
- Cepeda, E.A., Bravo, R., and Calvo, B. (2009). Solubilities of lauric acid in n-hexane, acetone, propanol, 2-propanol, 1-bromopropane, and trichloroethylene from (279.0 to 315.3) K. **Journal of Chemical & Engineering Data**. 54(4): 1371-1374.
- Calvo, B., Collado, I., and Cepeda, E.A. (2009). Solubilities of palmitic acid in pure solvents and its mixtures. **Journal of Chemical & Engineering Data**. 54: 64-68.
- Bradie, B. (2006). **A Friendly Introduction to Numerical Analysis**. Upper Saddle River, New Jersey: Prentice Hall.

- Burden, R.L., and Faires, J.D. (2005). **Numerical Analysis**. Belmont, CA: Thomson Brooks/Cole.
- Wang, H., and Tewarson, R.P. (1993). A quasi-gauss-newton method for solving non-linear algebraic equations. **Computers & Mathematics with Applications**. 25(1): 53-63.
- Gunstone, F.D. (1996). **Fatty Acid and Lipid Chemistry**. London, New York: Blackie Academic & Professional.
- Brown, W.H. (1997). **Introduction to Organic Chemistry**. Fort Worth: Saunders College Publishing.
- Domańska, U. (1987). Solid-liquid phase relations of some normal long-chain fatty acids in selected organic one- and two-component solvents. **Industrial & Engineering Chemistry Research**. 26(6): 1153-1162.



CHAPTER IV

CONCLUSIONS AND RECOMMENDATIONS

4.1 Conclusions

The solid hydrocarbon of aliphatic structure contaminated on surface of the spindle motor is a major problem encountered in manufacturing of the hard disk drive components. In the production line, there are two possible fluids that may be the cause of this problem: cutting fluid and cleaning solvent used in machining and cleaning step.

The cutting fluid analyzed in this study consists of mineral oil and mixed fatty acids with palmitic acid and oleic acid as the main components. The cleaning solvent was found to mainly consist of linear hydrocarbons with n-decane as a major component. Result of a study on miscibility of cutting fluid and cleaning solvent used in this particular manufacturer at the temperature range of 5–50°C using spectrophotometer revealed that fatty acids in cutting fluid cannot dissolve in cleaning solvent in some temperature ranges. It is therefore hypothesized that partial miscibility between fatty acids and linear hydrocarbon is the cause of the solid contamination of the spindle motor.

Thermal behaviors of pure palmitic acid and oleic acid and ternary mixtures (n-decane + palmitic acid + oleic acid) were analyzed using the differential scanning calorimetry (DSC) in order to understand the phase transition which would be useful when working with the fatty acids containing linear hydrocarbon solution. For pure palmitic

acid, melting temperature and enthalpy of melting are in good agreement with the values previously reported in the literatures. There are two endothermic peaks appeared in DSC thermogram of pure oleic acid, which indicate to a reversible solid–solid phase transition. The specific heat capacity for pure liquid palmitic acid and oleic acid obtained from the DSC analysis are in good agreement with the estimated values calculated by the Rowlinson–Bodi method.

For the ternary mixtures, it is observed that the thermal properties (peak temperature and enthalpy values) in solid–liquid and liquid–solid phase transitions are decrease with decreasing palmitic acid. Behaviors of solid–liquid phase transition were found to alter with the starting mass ratio of the mixtures.

One endothermic peak was observed for mixtures with mass ratios of 1:1:1, 1:0.5:1 and 1:0.3:1. Palmitic acid is a main component for phase transition of these mass ratios, since temperature of phase transition lower than melting temperature of pure palmitic acid but higher than melting temperature of pure n-decane and oleic acid. Therefore, mass ratios of 1:1:1, 1:0.5:1 and 1:0.3:1 are trend as the solid at room temperature.

Mass ratio of 1:0.2:1 appears two noticeable peaks and not clearly shown for mass ratio of 1:0.1:1, were observed at low temperature (less than 25°C). It is shown that oleic acid in mixture affects temperature of phase transition. Natural of pure oleic acid, it is a liquid at room temperature, which corresponds to the behaviors of both mass ratios. For n-decane does not affect the phase transition, since melting temperature of n-decane lower than the measured temperature range. The measurements of specific heat capacity in liquid phase for ternary mixtures are in good agreement with the estimated values obtained from equation of Teja with the

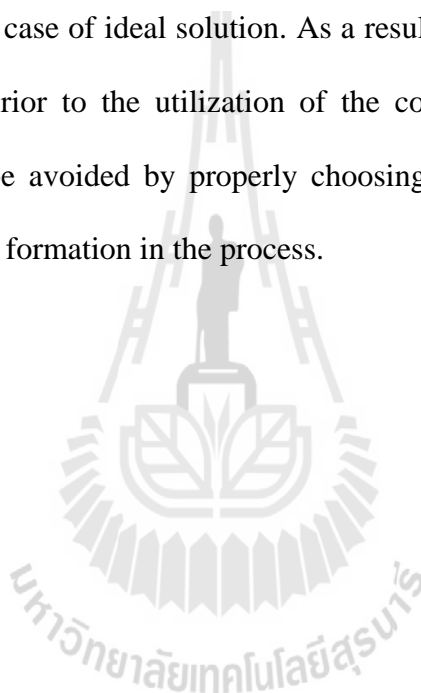
error values are less than $\pm 5\%$. Liquid specific heat capacity for ternary mixtures shows linear behavior in the measured temperature range.

A study of thermal behavior for pure fatty acids and ternary mixtures indicated that solid–liquid phase transition can be occurred for the mixture between fatty acids and linear hydrocarbon. The solid–liquid equilibria of mixtures containing n-decane, palmitic acid and oleic acid mixtures are investigated in the temperature range of 305.15 to 323.15 K in order to understand the phase behavior of fatty acids–linear hydrocarbon mixture and to predict the mechanism of the solid contamination encountered in the previous mentioned process. Solubility of each component in the ternary mixtures is represented by their mole fractions in the liquid and solid phases. It is observed that equilibrium mole fraction of each component in liquid phase to be resemblance to the mole fraction in the starting mixtures. Equilibrium temperature depends on the component containing the most quantity in the mixtures. The major component in solid phase for all mass ratios is palmitic acid where the occurrences of n-decane and oleic acid have the less quantity than palmitic acid. The mostly quantities of n-decane and oleic acid exist in liquid phase.

Activity coefficient of palmitic acid in n-decane – oleic acid was considered by calculating with the equation of solid–liquid equilibrium. It is indicated that the solubility of palmitic acid is lower than the ideal values. The NRTL and UNIQUAC equations were used for the correlation of the activity coefficient. The UNIQUAC equation shows the best description of solid–liquid equilibrium of palmitic acid in n-decane – oleic acid. The description on solubility of palmitic acid in n-decane – oleic acid in this research does not improve the dimers existence.

4.2 Recommendations

Co-existence of solid and liquid phase in the temperature range studied here could be a reason for the aforementioned surface contamination of spindle motor components and other products that utilized hydrocarbons and fatty acids containing fluids. Likely, the observed phenomenon could be resulted from positive deviation behavior that led to lower solubility of ternary mixture, specifically palmitic acid, than the value predicted in case of ideal solution. As a result, optimum working conditions should be obtained prior to the utilization of the concerned fluid. If possible, the problem could also be avoided by properly choosing the fluid formula in order to minimize the biphasic formation in the process.





APPENDIX A

**COMPONENT ANALYSIS OF CUTTING FLUID AND
CLEANING SOLVENT SAMPLES**

มหาวิทยาลัยเทคโนโลยีสุรนารี

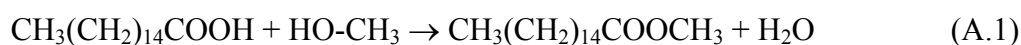
Fatty acid content of cutting fluid and hydrocarbon composition in mineral oil and in cleaning solvent sample was analyzed with gas chromatography (CP-3800)–mass spectrometer (1200L). Quantities of fatty acids in the cutting fluid were reported in term of mg of fatty acid methyl esters (FAME), which is the product of the reaction.

Table A.1 Component analysis of fatty acid methyl ester in 1 g of cutting fluid.

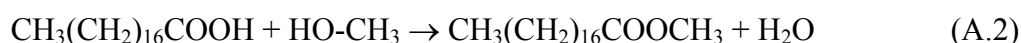
FAMES	Average (mg)	Standard Deviation, σ
Hexadecanoic acid methyl ester	23.100	0.130
Octadecanoic acid methyl ester	3.811	0.016
9-Octadecenoic acid methyl ester	19.210	0.010
9,12-Octadecadienoic acid methyl ester	6.110	0.060

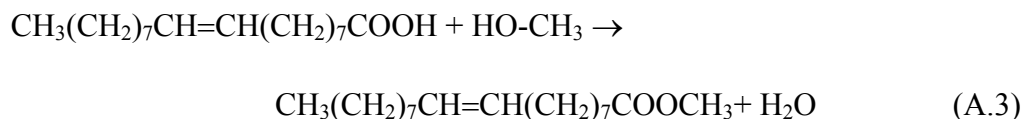
The FAME is a reaction between fatty acid (R-COOH) and methanol (CH₃OH). Equations of (A.1)–(A.4) show the reaction of four FAMES obtained from the GC–MS analysis.

Hexadecanoic acid methyl ester:



Octadecanoic acid methyl ester:



9-Octadecenoic acid methyl ester:**9,12-Octadecadienoic acid methyl ester:**

It can be seen that the molar ratio of fatty acid and fatty acid methyl ester was equal to 1:1 in all the reactions. Thus, 1 mole of fatty acid methyl ester is equal to 1 mole of fatty acid. The quantities of fatty acids in cutting fluid were thus obtained by the following calculation,

$$\text{Hexadecanoic acid methyl ester} = 23.10 \times 10^{-3} \text{ g} \times \frac{\text{mol}}{270.45 \text{ g}} = 8.54 \times 10^{-5} \text{ mol}$$

$$\therefore \text{Hexadecanoic acid (Palmitic acid)} = 8.54 \times 10^{-5} \text{ mol}$$

$$\text{Octadecanoic acid methyl ester} = 3.811 \times 10^{-3} \text{ g} \times \frac{\text{mol}}{298.51 \text{ g}} = 1.277 \times 10^{-5} \text{ mol}$$

$$\therefore \text{Octadecanoic acid (Stearic acid)} = 1.277 \times 10^{-5} \text{ mol}$$

$$\text{9-Octadecenoic acid methyl ester} = 19.21 \times 10^{-3} \text{ g} \times \frac{\text{mol}}{296.49 \text{ g}} = 6.48 \times 10^{-5} \text{ mol}$$

$$\therefore \text{9-Octadecenoic acid (Oleic acid)} = 6.48 \times 10^{-5} \text{ mol}$$

$$9,12\text{-Octadecadienoic acid methyl ester} = 6.11 \times 10^{-3} \text{ g} \times \frac{\text{mol}}{294.47 \text{ g}} = 2.07 \times 10^{-5} \text{ mol}$$

$$\therefore 9,12\text{-Octadecadienoic acid (Linoleic acid)} = 2.07 \times 10^{-5} \text{ mol}$$

Quantities of four fatty acids in 1 g of cutting fluid can be summarized in Table A.2. Total mass of four fatty acids was found to be 49.64 mg. Thus, quantity of mineral oil in cutting fluid is equal to 950.36 mg.

Table A.2 Quantities of four fatty acids (mg) in 1 g of cutting fluid.

Fatty acid	Quantity (mg)
Hexadecanoic acid (Palmitic acid, C16:0)	21.90
Octadecanoic acid (Stearic acid, C18:0)	3.63
9-Octadecenoic acid (Oleic acid, C18:1n9c)	18.30
9,12-Octadecadienoic acid (Linoleic acid, C18:2n6c)	5.81

Table A.3 shows the hydrocarbon content of mineral oil. It was aliphatic hydrocarbons with the carbon atom of C₈ to C₂₀. Average molecular weight of mineral oil can be calculated as 255.64 g/mol. Quantities of mineral oil and fatty acids in percent by mole (% by mole) were reported in Table A.4.

Results of hydrocarbon content of cleaning solvent were shown in Table A.5. The two hydrocarbons of aliphatic structure existed in cleaning solvent, compose of n-octane (C₈H₁₈) and n-decane (C₁₀H₂₂). According to percent by mole of each component, it is found that n-decane was considered as a main hydrocarbon compound of cleaning solvent.

Table A.3 Hydrocarbon content of mineral oil.

Component	Concentration	
	mg/L	mol/L
Octane (C ₈ H ₁₈)	17.69	1.55×10 ⁻⁴
Nonane (C ₉ H ₂₀)	–	–
Decane (C ₁₀ H ₂₂)	–	–
Undecane (C ₁₁ H ₂₄)	5.34	3.42×10 ⁻⁵
Dodecane (C ₁₂ H ₂₆)	19.53	1.15×10 ⁻⁴
Tridecane (C ₁₃ H ₂₈)	14.93	8.10×10 ⁻⁵
Tetradecane (C ₁₄ H ₃₀)	35.80	1.80×10 ⁻⁴
Pentadecane (C ₁₅ H ₃₂)	62.01	2.92×10 ⁻⁴
Hexadecane (C ₁₆ H ₃₄)	122.50	5.41×10 ⁻⁴
Heptadecane (C ₁₇ H ₃₆)	319.00	1.33×10 ⁻³
Octadecane (C ₁₈ H ₃₈)	597.70	2.35×10 ⁻³
Nonadecane (C ₁₉ H ₄₀)	584.50	2.18×10 ⁻³
Eicosane (C ₂₀ H ₄₂)	812.70	2.88×10 ⁻³
Total	2591.70	1013.82×10 ⁻⁵

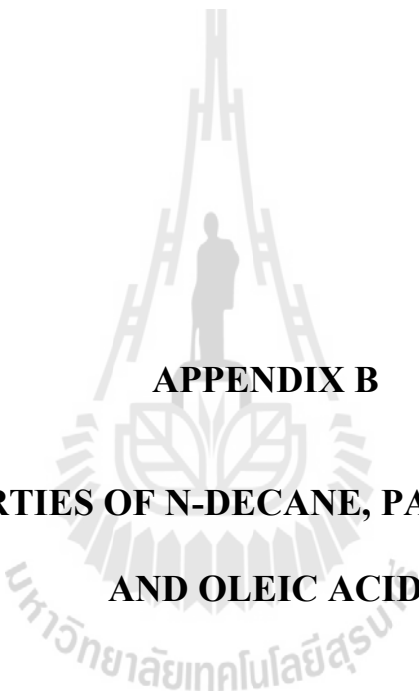
Table A.4 Percent by mole of mineral oil and four fatty acids in cutting fluid.

Component	Quantity (mg)	Molar mass (g/mol)	% by mole
Mineral oil (C ₈ –C ₂₀)	950.36	255.64	95.29
Palmitic acid (C ₁₆ :0)	21.90	256.42	2.19
Stearic acid (C ₁₈ :0)	3.63	284.48	0.33
Oleic acid (C ₁₈ :1n9c)	18.30	282.46	1.66
Linoleic acid (C ₁₈ :2n6c)	5.81	280.45	0.53

Table A.5 Hydrocarbon content of cleaning solvent.

Component	Concentration (mg/L)	% by mole
Octane (C ₈ H ₁₈)	8.550×10^3	1.18
Decane (C ₁₀ H ₂₂)	8.892×10^5	98.82





APPENDIX B
PROPERTIES OF N-DECANE, PALMITIC ACID
AND OLEIC ACID

B.1 n-Decane

n-Decane (decane or alkane C₁₀) is an aliphatic hydrocarbon with the chemical formula of CH₃(CH₂)₈CH₃. 75 isomers of decane exist, all of which are flammable liquids. Molecular structure of decane is shown in Fig. B.1, it is nonpolar and therefore will not dissolve in polar liquids such as water. Most decane is prepared from petroleum refining. Decane is one of the components of engine fuels (Carvender, 1994). Other uses include as a solvent, in organic synthesis, as a hydrocarbon standard, in jet fuel research, in the manufacturing of paraffin products, in the rubber industry, in the paper-processing industry as well as in cleaning agent (Lewis, 2002; Verscheuren, 2001; Wolkoff et al., 1998). Some chemical and physical properties of n-decane are shown in Table B.1.

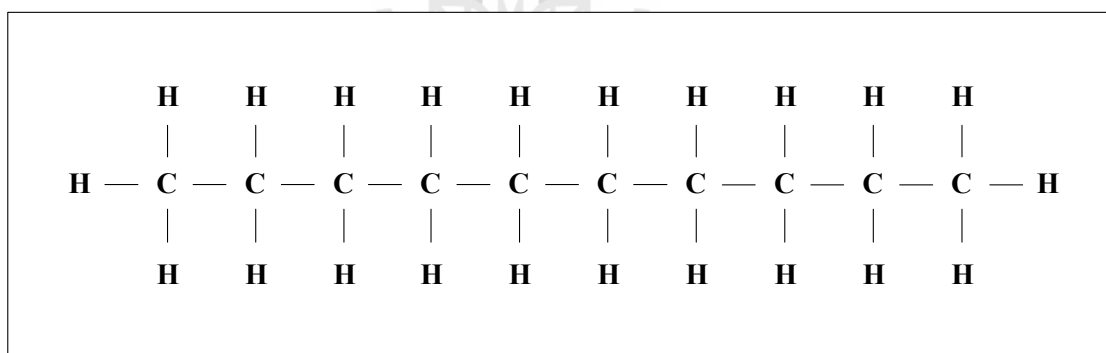


Figure B.1 Molecular structure of n-decane.

Table B.1 Chemical and physical properties of n-decane.

Chemical and physical properties	
Appearance:	Colorless liquid
Purity:	99+% from ACROS Organics
Molecular Weight:	142.28 g/mol
Melting Point:	-30°C
Boiling Point:	174°C
Flash Point:	46°C
Density:	0.735 g/ml
Solubility:	- Partially soluble in methanol, diethyl ether. - Insoluble in cold water.

B.2 Palmitic Acid

Palmitic acid ($\text{CH}_3(\text{CH}_2)_{14}\text{COOH}$ or n-hexadecanoic acid or 16:0) is one of the most widely occurring saturated acid. It is present in fish oils (10-30%), in milk and body fats of land animals (up to 30%), and in virtually all vegetable fats at a range of levels between 5 and 50% (Gunstone, 1996). Useful sources of palmitic acid obtained by the hydrolysis of triglycerides include kernel palm, palm, tallow, and coconut oil (Calvo et al., 2009). It is used in the manufacture of soaps, cosmetic formulations, lube oils, as metallic palmitates as an additive to vegetable oil that can substitute mineral oil as a base fluid in grease making (Adhvaryu et al., 2005), nondrying oil (surface coatings), and as a phase change material (PCM) for low-temperature latent heat thermal energy storage (Karaipekli et al., 2007). The basic structure of palmitic acid includes a hydrophobic hydrocarbon chain with 16 carbons and a hydrophilic polar group at one end as shown in Fig. B.2. Some chemical and physical properties of palmitic acid are reported in Table B.2.

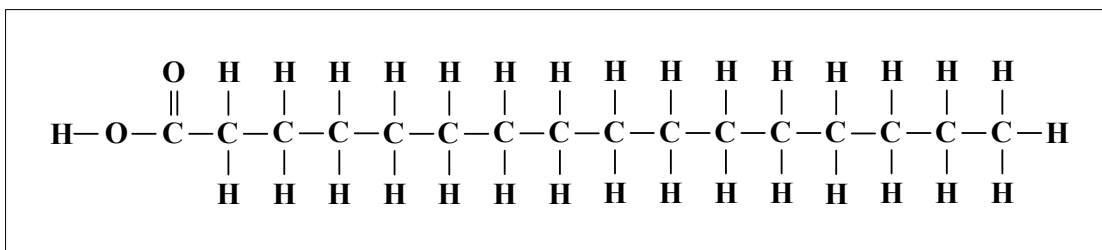


Figure B.2 Molecular structure of palmitic acid.

Table B.2 Chemical and physical properties of palmitic acid.

Chemical and physical properties	
Appearance:	White solid
Purity:	98% from ACROS Organics
Molecular Weight:	256.43 g/mol
Melting Point:	59-63°C
Boiling Point:	351.5°C (at 760 mmHg)
Flash Point:	206°C
Specific Gravity:	0.85 at 62°C
Solubility:	<ul style="list-style-type: none"> - Soluble in diethyl ether, acetone, ethanol, aromatic, chlorinated and oxygenated solvents. - Partially insoluble in cold water. - Sparingly soluble in cold alcohol or petroleum ether. - Freely soluble in hot alcohol, propyl alcohol, chloroform.

B.3 Oleic Acid

Oleic acid (cis-9-Octadecenoic acid or 18:1 cis-9) is the most widely distributed and the most extensively produced of all fatty acids. It is a mono-unsaturated fatty acid found in various animal and vegetable sources. Olive oil (60-80%) and almond oil (60-70%) are rich sources of this acid and it is also present at high levels (55-75%) in several nut oils include peanut, pecan, cashew, pistachio, and macadamia (Gunstone, 1996). It is also abundantly present in many animal fats such

as chicken fats and lard. Oleic acid has many applications of detergents, soaps, lubricants, cosmetics and emulsifying agents in food. Molecular structure of oleic acid is shown in Fig. B.3, it has 18 carbons and one double bond between carbon 9 and carbon 10, has a kink in it. Some chemical and physical properties of oleic acid are presented in Table B.3.

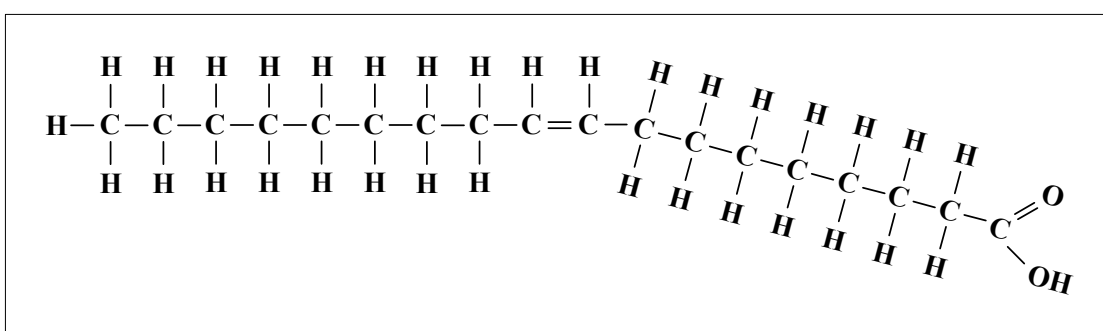


Figure B.3 Molecular structure of oleic acid.

Table B.3 Chemical and physical properties of oleic acid.

Chemical and physical properties	
Appearance:	Pale yellow or brownish yellow oily liquid with lard-like odor
Purity:	Pure from CARLO ERBA
Molecular Weight:	282.47 g/mol
Melting Point:	13.4°C
Boiling Point:	360°C
Flash Point:	189°C
Density:	0.90 g/ml at 20°C
Solubility:	- Soluble in many organic solvents such as methanol. - Insoluble in water.

B.4 References

Carvender, F. (1994). **Aliphatic Hydrocarbons**. New York: John Wiley & Sons.

Lewis, R.J. (2002). **Hawley's Condensed Chemical Dictionary**. New York: John Wiley & Sons.

Verscheuren, K. (2001). **Handbook of Environmental Data on Organic Chemicals**. New York: John Wiley & Sons.

Wolkoff, P., Schneider, T., Kildesø, J., Degerth, R., Jaroszewski, M., and Schunk, H. (1998). Risk in cleaning: chemical and physical exposure. **Science of The Total Environment**. 215: 135-156.

Gunstone, F.D. (1996). **Fatty Acids and Lipid Chemistry**. London: Blackie Academic & Professional.

Calvo, B., Collado, I., and Cepeda, E.A. (2009). Solubilities of palmitic acid in pure solvents and its mixtures. **Journal of Chemical & Engineering Data**. 54(1): 64-68.

Adhvaryu, A., Sung, C., and Erhan, S.Z. (2005). Fatty acids and antioxidant effects on grease microstructures. **Industrial Crops and Products**. 21(3): 285-291.

Karaipekli, A., and Sari, A. (2007). Capric acid and palmitic acid eutectic mixture applied in building wallboard for latent thermal energy storage. **Journal of Scientific & Industrial Research**. 66(6): 470-476.



APPENDIX C

**PRELIMINARY STUDY OF MISCIBILITY OF CUTTING FLUID
AND CLEANING SOLVENT BY SPECTROPHOTOMETER**

The absorbance measurements of miscibility of cutting fluid and cleaning solvent by spectrophotometer with the wavelength of 500 nm were studied at the temperature of 5, 10, 15, 20, 25, 30, 35, 40, 45 and 50°C. Binary mixtures of cutting fluid (1) + cleaning solvent (2) were prepared in various volume ratios. Total volume of each system is equal to 30 ml. Fig. C.1 shows the relationship between absorbance versus volume of cutting fluid from the volume of 0 ml of cutting fluid (30 ml of cleaning solvent) to 30 ml of cutting fluid (0 ml of cleaning solvent). It can be seen that at the temperature of 5 and 10°C, the absorbance value increases with volume of cutting fluid. For the temperature range of 15–50°C, the absorbance has similar values in all the volume of cutting fluid.

White solid appeared at the temperature of 5 and 10°C may be some fatty acids existed in the cutting fluid. Mineral oil does not affect the occurrence of white solid, since aliphatic hydrocarbons are the main component of mineral oil as presented in Appendix A. It can be dissolved with cleaning solvent in all temperature ranges.

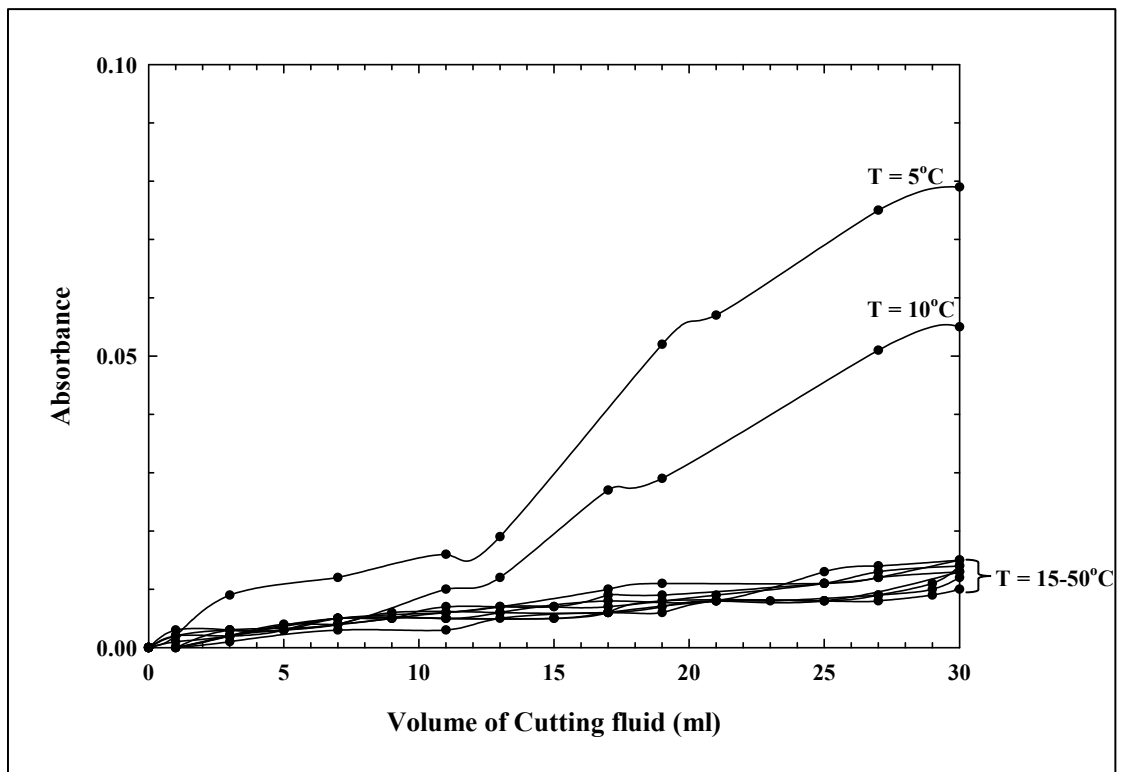


Figure C.1 The absorbance measurement at T = 5–50°C.





APPENDIX D
DSC ANALYSIS FOR PURE OLEIC ACID

The DSC analysis for pure oleic acid was analyzed in the temperature range from -5°C to 30°C with the heating and cooling rates of 1, 3, 5, 7, 9 and $10^{\circ}\text{C}/\text{min}$. A scanning rate of $1^{\circ}\text{C}/\text{min}$ was explained in the topic of Results and Discussion in Chapter 2. For the remaining experimental results can be presented in Figs D.1–D.5. In all the scanning rates, on the melting curve appear two endothermic peaks at around $0\text{--}15^{\circ}\text{C}$ which is related to the solid-state phase transition of pure oleic acid.

For the liquid–solid phase transition presents the different values of thermal properties as summarized in Table D.1. Phase transition for solidification of oleic acid at 7, 9 and $10^{\circ}\text{C}/\text{min}$ presents the incomplete curve. Because of the scanning rate is unsuitable with the analysis of pure oleic acid, including the specification of the DSC equipment.

The DSC curves for specific heat capacity of oleic acid in melting process at 3, 5, 7, 9 and $10^{\circ}\text{C}/\text{min}$ are shown in Figs D.6–D.10. The values of specific heat capacity of each scanning rate were presented in Tables D.2–D.6. It is found that the \bar{C}_p values for solid–liquid phase transition observe at around $-2\text{--}16^{\circ}\text{C}$. In the liquid phase, the difference of the \bar{C}_p values between the experimental values and the evaluated values are less than $\pm 5\%$ for only the scanning rate of 3, 7 and $9^{\circ}\text{C}/\text{min}$. While the %diff. values for the scanning rate of 5 and $10^{\circ}\text{C}/\text{min}$ are not satisfy, may be due to the obtaining DSC curve is not respond with the baselines.

Table D.1 Thermal properties for liquid–solid phase transition of pure oleic acid at 3, 5, 7, 9 and 10°C/min.

Scanning rate (°C/min)	Liquid–Solid Phase Transition		
	Onset (°C)	T _{cryst} (°C)	ΔH _{cryst} (J·g ⁻¹)
3	3.41	0.95	-8.347
5	3.22	0.49	-7.521
7	2.82	0.01	-7.304
9	2.33	-0.37	-6.289
10	2.23	0.03	-5.492

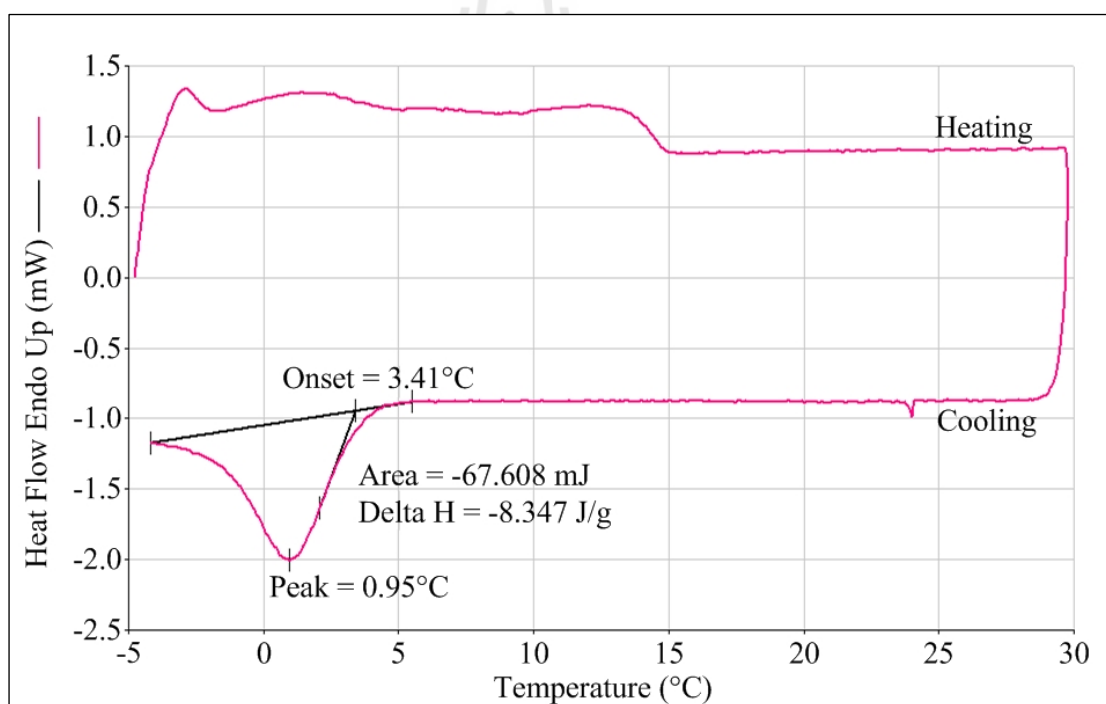


Figure D.1 DSC analysis for pure oleic acid with the scanning rate of 3°C/min.

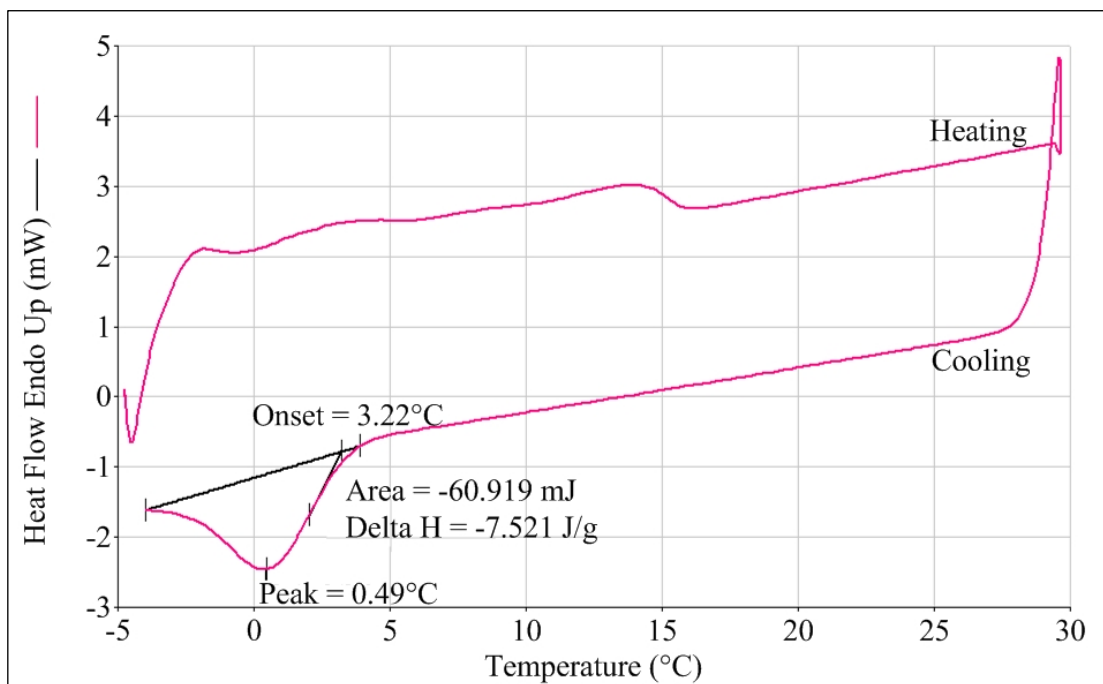


Figure D.2 DSC analysis for pure oleic acid with the scanning rate of 5°C/min.

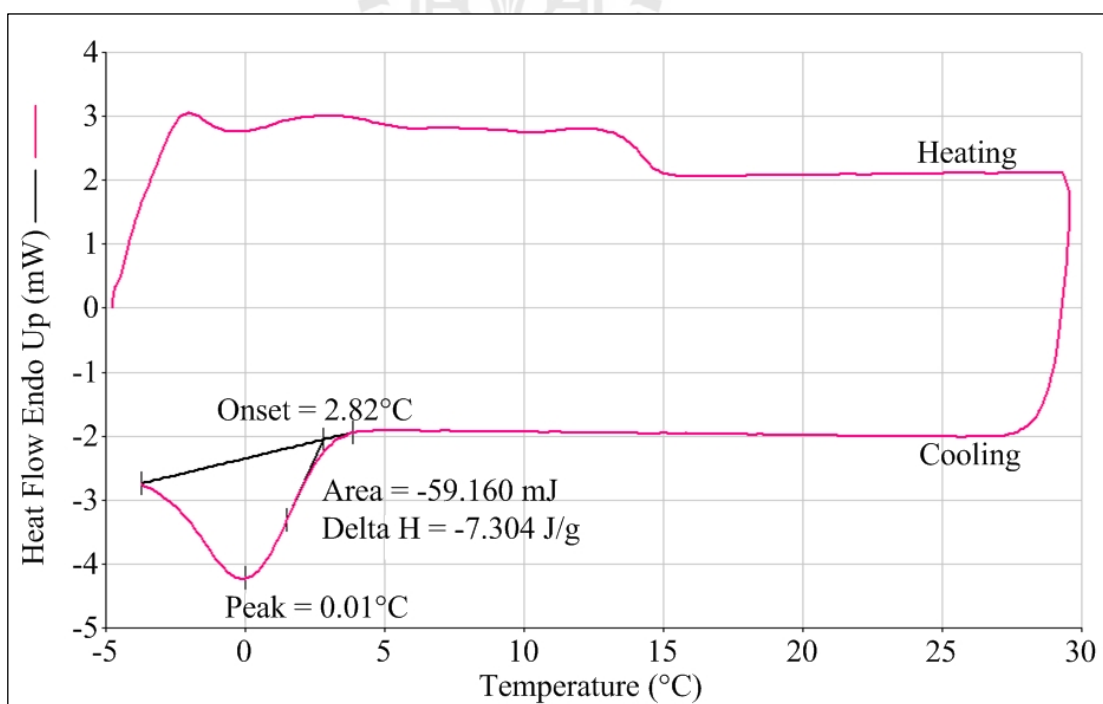


Figure D.3 DSC analysis for pure oleic acid with the scanning rate of 7°C/min.

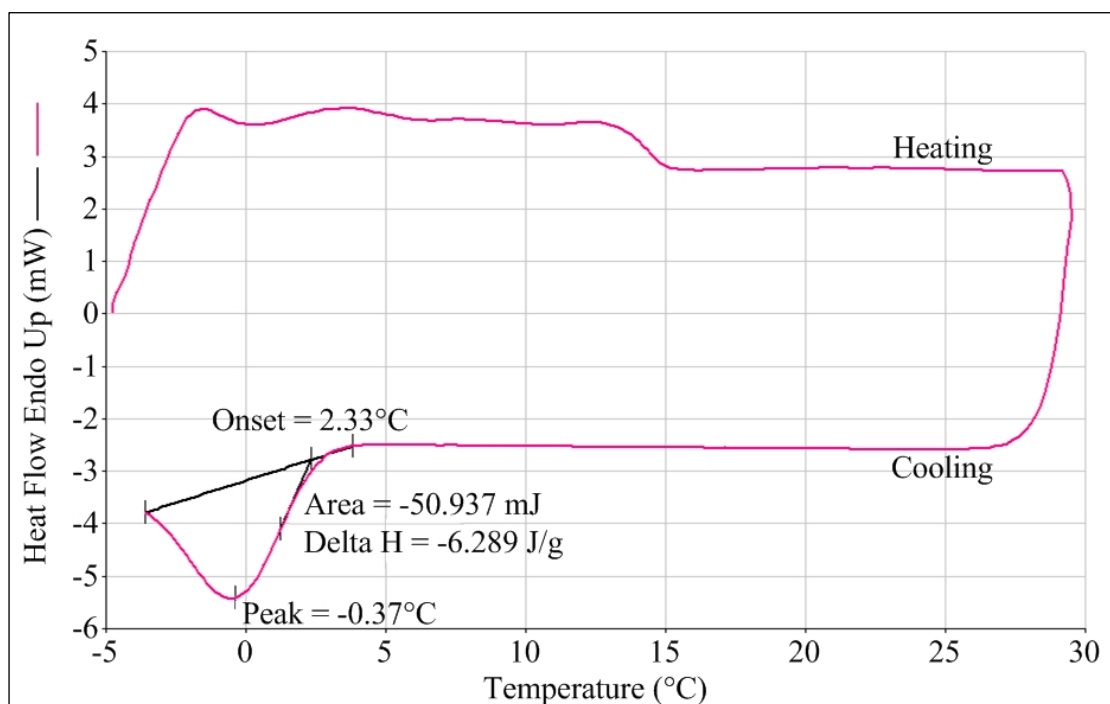


Figure D.4 DSC analysis for pure oleic acid with the scanning rate of 9°C/min.

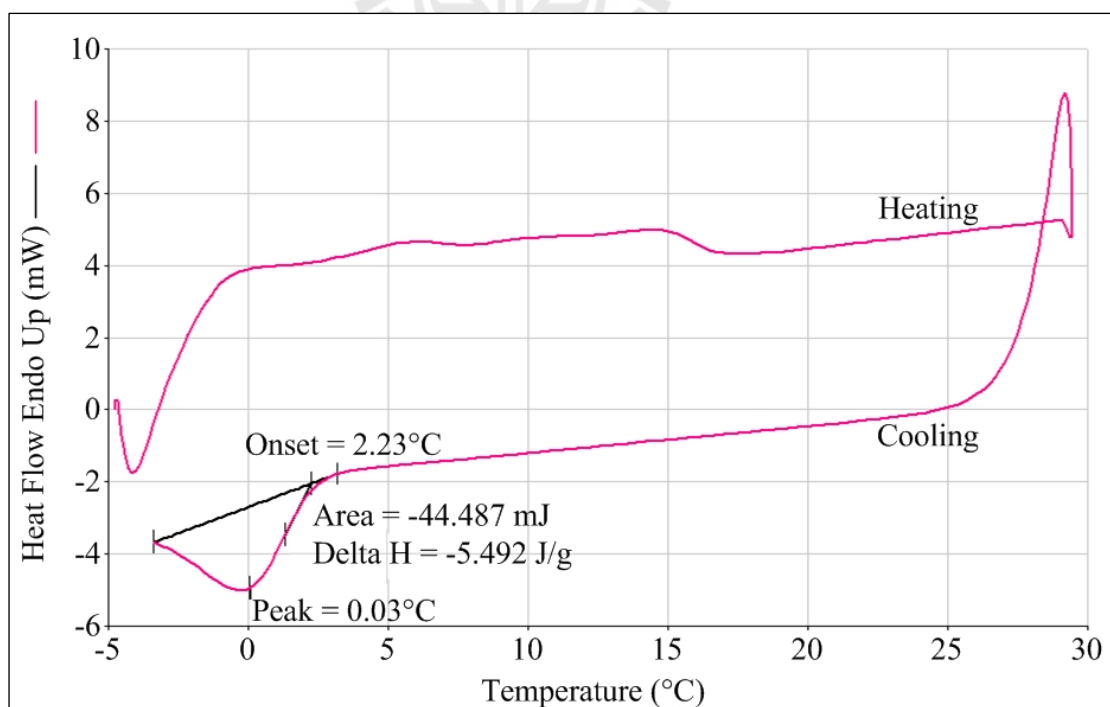


Figure D.5 DSC analysis for pure oleic acid with the scanning rate of 10°C/min.

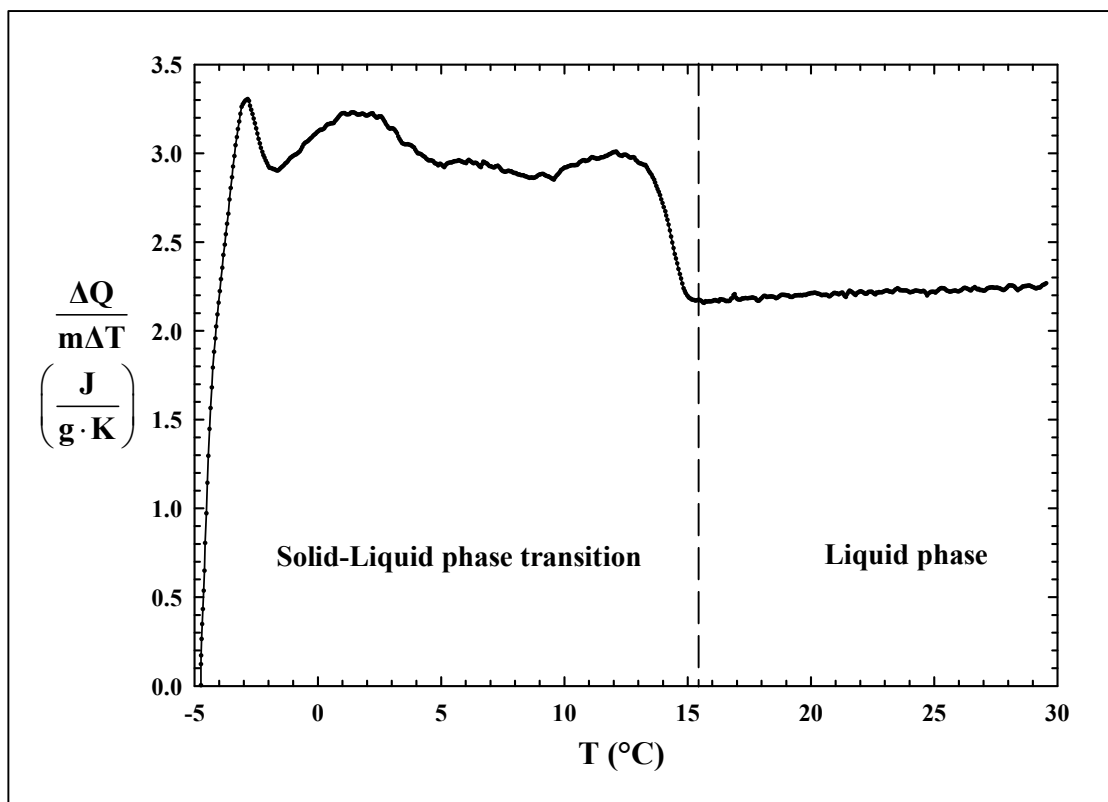


Figure D.6 The DSC curve for specific heat capacity of oleic acid in melting process with the heating rate of 3°C/min.

Table D.2 Specific heat capacity of oleic acid for the liquid phase with the scanning rate of 3°C/min.

T, °C	\bar{C}_p (DSC), J/g·K	\bar{C}_p (est.), J/g·K	% diff.
16.02	2.168	2.263	4.198
20.03	2.212	2.271	2.598
23.02	2.225	2.277	2.284
26.00	2.222	2.283	2.672
29.04	2.244	2.290	2.009

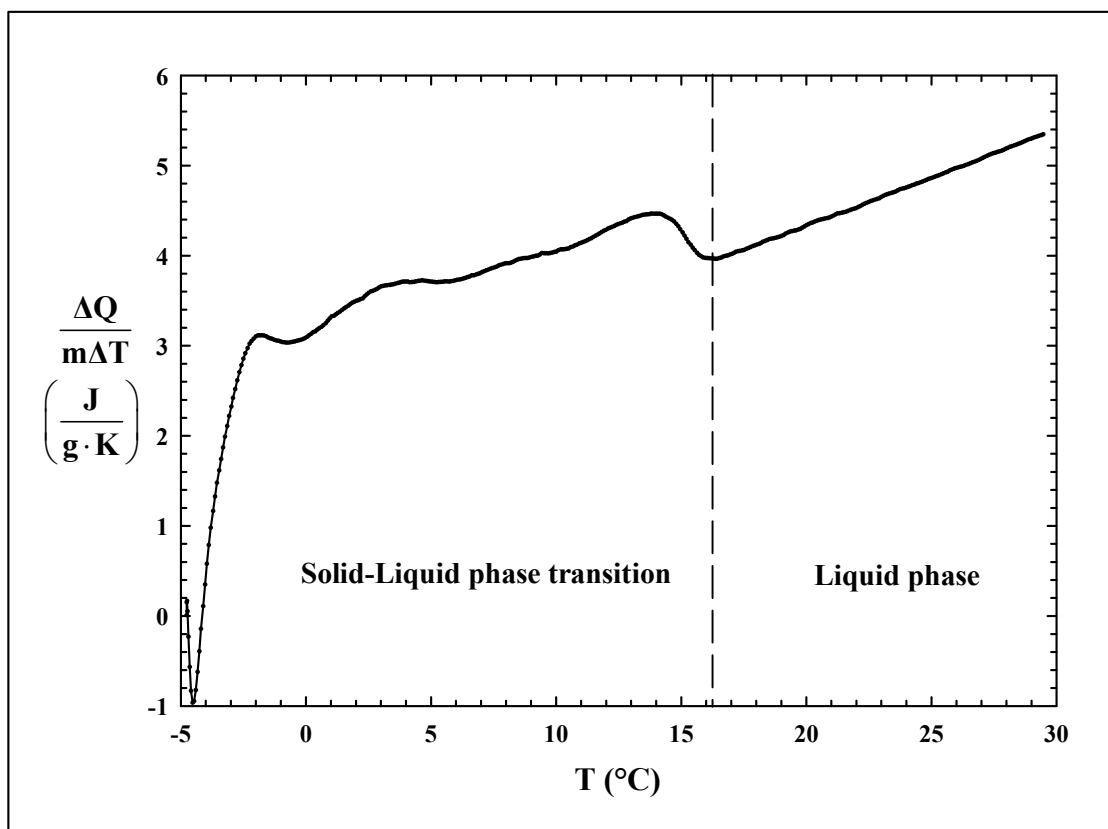


Figure D.7 The DSC curve for specific heat capacity of oleic acid in melting process with the heating rate of 5°C/min.

Table D.3 Specific heat capacity of oleic acid for the liquid phase with the scanning rate of 5°C/min.

T, °C	\bar{C}_p (DSC), J/g·K	\bar{C}_p (est.), J/g·K	% diff.
16.04	3.972	2.263	-75.519
20.01	4.337	2.271	-90.973
23.07	4.662	2.277	-104.743
26.06	4.978	2.284	-117.951
29.05	5.305	2.290	-131.659

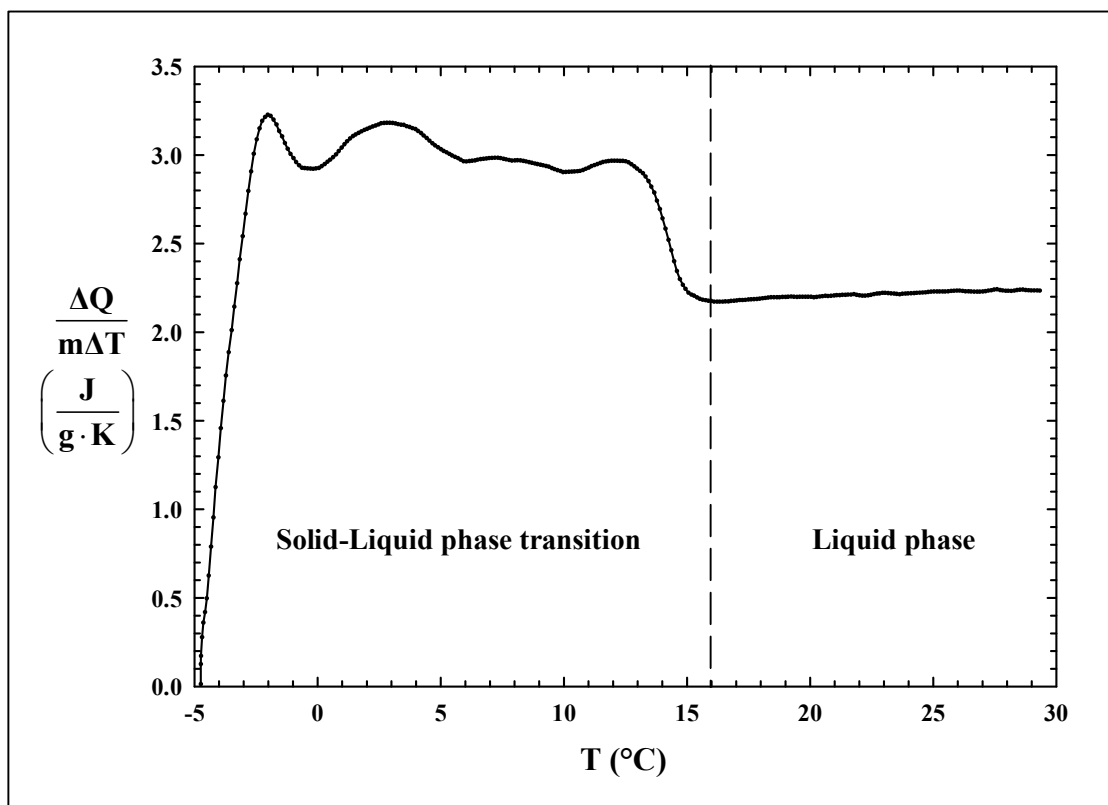


Figure D.8 The DSC curve for specific heat capacity of oleic acid in melting process with the heating rate of 7°C/min.

Table D.4 Specific heat capacity of oleic acid for the liquid phase with the scanning rate of 7°C/min.

T, °C	\bar{C}_p (DSC), J/g·K	\bar{C}_p (est.), J/g·K	% diff.
16.10	2.172	2.264	4.064
20.04	2.199	2.271	3.170
23.05	2.221	2.277	2.459
26.07	2.234	2.284	2.189
29.10	2.235	2.290	2.402

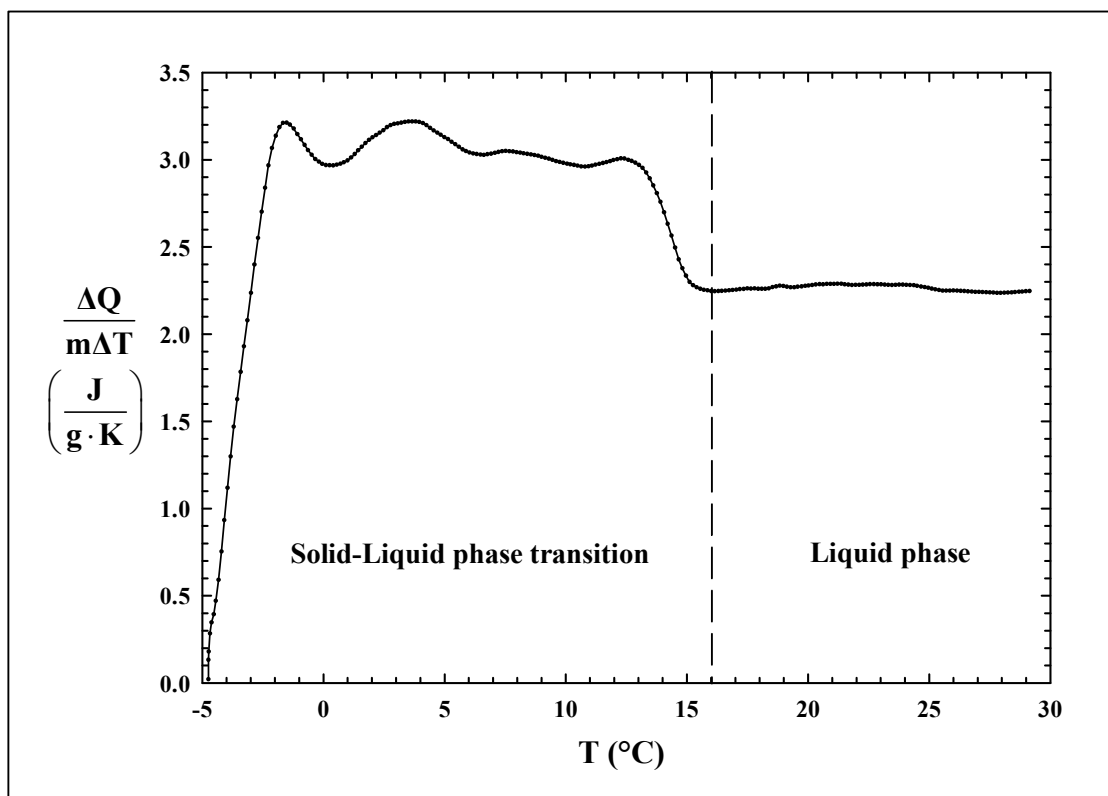


Figure D.9 The DSC curve for specific heat capacity of oleic acid in melting process with the heating rate of 9°C/min.

Table D.5 Specific heat capacity of oleic acid for the liquid phase with the scanning rate of 9°C/min.

T, °C	\bar{C}_p (DSC), J/g·K	\bar{C}_p (est.), J/g·K	% diff.
16.00	2.247	2.263	0.707
20.02	2.279	2.271	-0.352
23.01	2.285	2.277	-0.351
26.00	2.250	2.283	1.445
29.14	2.247	2.290	1.878

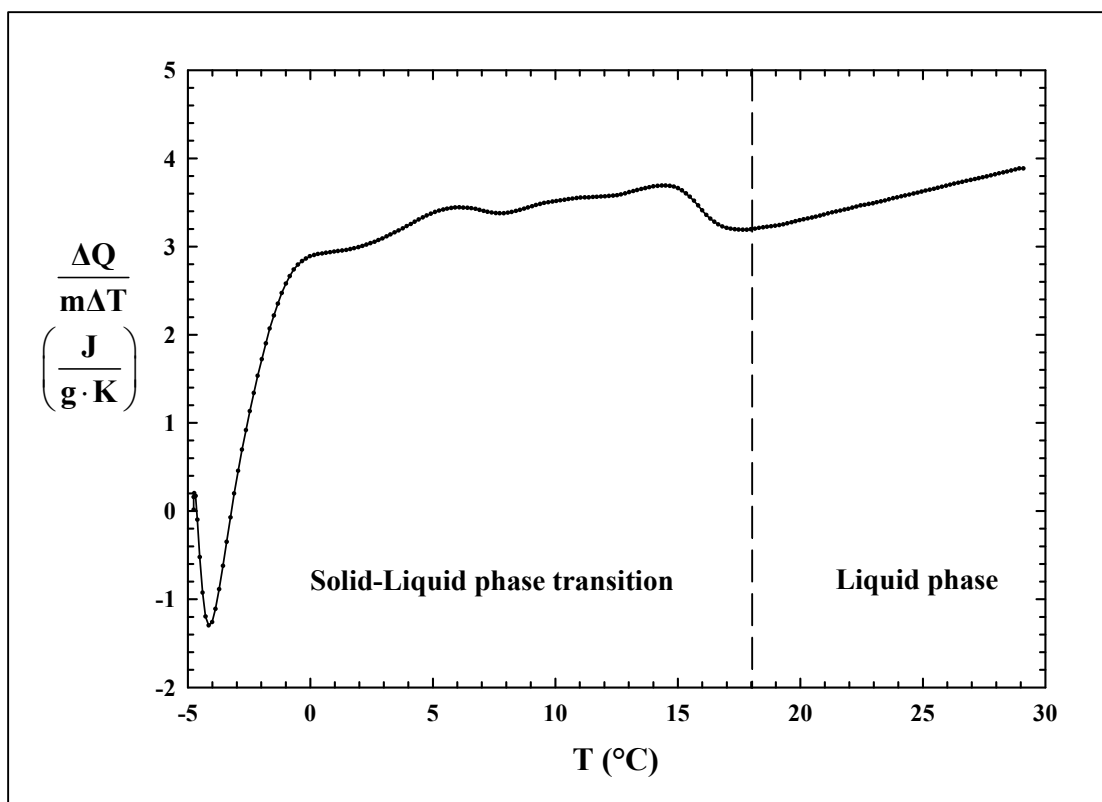


Figure D.10 The DSC curve for specific heat capacity of oleic acid in melting process with the heating rate of 10°C/min.

Table D.6 Specific heat capacity of oleic acid for the liquid phase with the scanning rate of 10°C/min.

T, °C	\bar{C}_p (DSC), J/g·K	\bar{C}_p (est.), J/g·K	% diff.
18.97	3.234	2.269	-42.530
20.13	3.308	2.272	-45.599
23.12	3.501	2.278	-53.687
25.11	3.633	2.282	-59.202
29.11	3.885	2.290	-69.651



APPENDIX E

**EXAMPLE OF COMPONENT ANALYSIS OF
N-DECANE + PALMITIC ACID + OLEIC ACID MIXTURE**

Procedures of component analysis consist of 1.) Preparation of n-Decane, Palmitic Acid, and Oleic Acid. 2.) Solid–Liquid Phase Separation. 3.) Component Analysis of n-Decane, Palmitic Acid and Oleic Acid in Liquid Phase. 4.) Component Analysis of n-Decane, Palmitic Acid and Oleic Acid in Solid Phase. 5.) Mass Balance. Mass ratio of 1:1:1 was used as an example of component analysis of solid–liquid equilibrium as this below:

E.1 Preparation of n-Decane, Palmitic Acid, and Oleic Acid

n-Decane (D), palmitic acid (P), and oleic acid (O) were carefully prepared on an analytical balance with the weight corresponding to the given mass ratio. In this case, mass ratio (D:P:O) of 1:1:1, all components were prepared with the equal quantity as below:

$$\begin{array}{l}
 \text{Weight of palmitic acid} = 7.0014 \text{ g} \\
 \text{Weight of n-decane} = 7.0056 \text{ g} \\
 \text{Weight of oleic acid} = 7.0005 \text{ g}
 \end{array}
 \left. \vphantom{\begin{array}{l} \text{Weight of palmitic acid} \\ \text{Weight of n-decane} \\ \text{Weight of oleic acid} \end{array}} \right\} \text{Total weight of three components} = 21.0075 \text{ g}$$

According to the topic of experimental procedures in Chapter 3, mass ratio D:P:O of 1:1:1 occurs the solid–liquid equilibrium at temperature of 43.0°C.

E.2 Solid–Liquid Phase Separation

The obtaining results for the solid–liquid phase separation for mass ratio of 1:1:1 was shown as below:

Separation time = 18 second

Weight of liquid phase = 19.5038 g

Weight of solid phase = 1.2427 g

Total weight of liquid + solid phase = 20.7465 g

$$\text{Percent error} = \frac{21.0075 - 20.7465}{21.0075} \times 100 = 1.2424\%$$

The quantity of n-decane, palmitic acid, and oleic acid existed in solid and liquid phases can be determined from the GC analysis.

E.3 Component Analysis of n-Decane, Palmitic Acid and Oleic Acid in Liquid Phase

Weight of liquid phase = 0.0415 g

Weight of liquid phase + CH₂Cl₂ = 0.9326 g

1st dilution: Weight of solution = 0.0640 g

Weight of CH₂Cl₂ = 1.2290 g

Total weight = 0.0640 + 1.2290 = 1.2930 g

$$\therefore \text{Weight of liquid phase in 1}^{\text{st}} \text{ dilution} = \frac{0.0415 \text{ g}}{0.9326 \text{ g}} \times 0.0640 \text{ g} = 2.8480 \times 10^{-3} \text{ g}$$

Injection 1 μl ≈ 1.2940 × 10⁻³ g :

$$\therefore \text{Weight of liquid phase} = \frac{2.8480 \times 10^{-3} \text{ g}}{1.2930 \text{ g}} \times 1.2940 \times 10^{-3} \text{ g} = 2.8502 \times 10^{-6} \text{ g}$$

So, weight of liquid phase in 1 mg:

$$= \frac{2.8502 \times 10^{-6} \text{ g}}{1.2940 \times 10^{-3} \text{ g}} \times 10^{-3} \text{ g} = 2.2026 \times 10^{-6} \text{ g} = 2.2026 \text{ } \mu\text{g}$$

Component analysis in 2.2026 μg of the liquid phase is shown in Fig. E.1. The area of n-decane, palmitic acid, and oleic acid will be taken to calculate the quantity from the calibration curve of each component. It is found that in 2.2026 μg of the liquid phase comprises of n-decane = 0.7582 μg ,

palmitic acid = 0.7240 μg and

oleic acid = 0.6927 μg

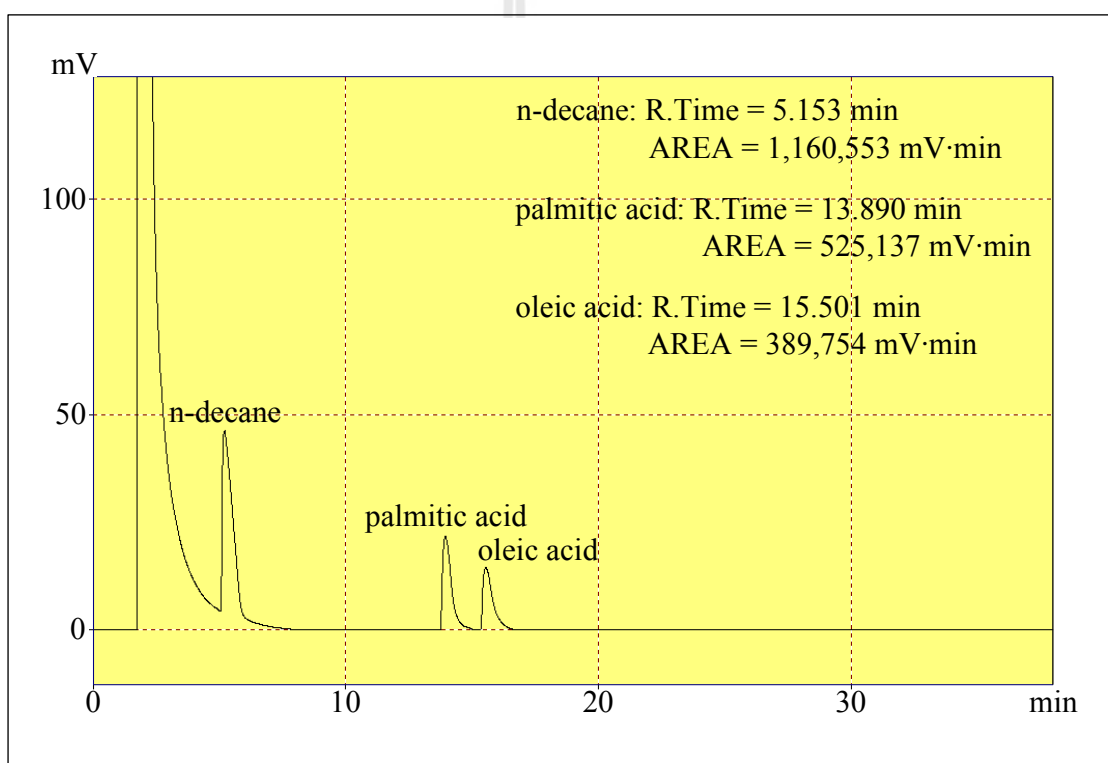


Figure E.1 Component analysis in liquid phase.

In total weight of liquid phase (19.5038 g):

$$\left. \begin{aligned} \text{n-decane} &= \frac{0.7582}{2.2026} \times 19.5038 = 6.7138 \text{ g} \\ \text{palmitic acid} &= \frac{0.7240}{2.2026} \times 19.5038 = 6.4109 \text{ g} \\ \text{oleic acid} &= \frac{0.6927}{2.2026} \times 19.5038 = 6.1338 \text{ g} \end{aligned} \right\} \text{Total weight} = 19.2585 \text{ g}$$

$$\text{Percent error} = \frac{19.5038 - 19.2585}{19.5038} \times 100 = 1.2577\%$$

$$\begin{aligned} \text{Mass ratio of n-decane : palmitic acid : oleic acid} &= 0.3486 : 0.3329 : 0.3185 \\ &= 1.0945 : 1.0452 : 1.0000 \end{aligned}$$

E.4 Component Analysis of n-Decane, Palmitic Acid and Oleic Acid in Solid Phase

$$\text{Weight of solid phase} = 0.0153 \text{ g}$$

$$\text{Weight of solid phase} + \text{CH}_2\text{Cl}_2 = 0.9168 \text{ g}$$

$$1^{\text{st}} \text{ dilution: Weight of solution} = 0.1293 \text{ g}$$

$$\text{Weight of CH}_2\text{Cl}_2 = 1.0688 \text{ g}$$

$$\text{Total weight} = 0.1293 + 1.0688 = 1.1981 \text{ g}$$

$$\therefore \text{Weight of solid phase in } 1^{\text{st}} \text{ dilution} = \frac{0.0153 \text{ g}}{0.9168 \text{ g}} \times 0.1293 \text{ g} = 2.1578 \times 10^{-3} \text{ g}$$

Injection $1 \mu\text{l} \approx 1.2675 \times 10^{-3} \text{ g}$:

$$\therefore \text{Weight of solid phase} = \frac{2.1578 \times 10^{-3} \text{ g}}{1.1981 \text{ g}} \times 1.2675 \times 10^{-3} \text{ g} = 2.2828 \times 10^{-6} \text{ g}$$

So, weight of solid phase in 1 mg:

$$= \frac{2.2828 \times 10^{-6} \text{ g}}{1.2675 \times 10^{-3} \text{ g}} \times 10^{-3} \text{ g} = 1.8010 \times 10^{-6} \text{ g} = 1.8010 \text{ } \mu\text{g}$$

Component analysis in 1.8010 μg of the solid phase is shown in Fig. E.2. The area of n-decane, palmitic acid, and oleic acid will be taken to calculate the quantity from the calibration curve of each component. It is found that in 1.8010 μg of the solid phase comprises of n-decane = 0.2836 μg ,

palmitic acid = 1.0542 μg and

oleic acid = 0.3909 μg

In total weight of solid phase (1.2427 g):

$$\text{n-decane} = \frac{0.2836}{1.8010} \times 1.2427 = 0.1957 \text{ g}$$

$$\text{palmitic acid} = \frac{1.0542}{1.8010} \times 1.2427 = 0.7274 \text{ g}$$

$$\text{oleic acid} = \frac{0.3909}{1.8010} \times 1.2427 = 0.2697 \text{ g}$$

Total mass = 1.1928 g

$$\text{Percent error} = \frac{1.2427 - 1.1928}{1.2427} \times 100 = 4.0155\%$$

Mass ratio of n-decane : palmitic acid : oleic acid = 0.1641 : 0.6098 : 0.2261
 = 0.7258 : 2.6970 : 1.0000

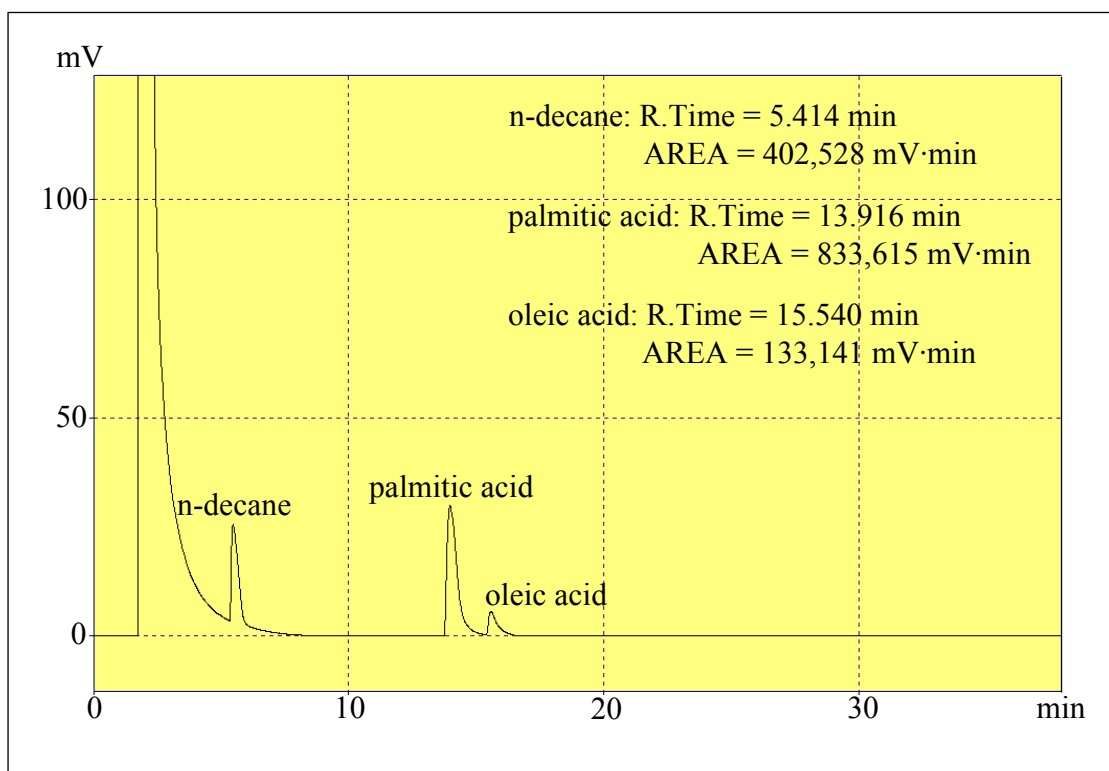


Figure E.2 Component analysis in solid phase.

Table E.1 shows the comparison of mass ratio of n-decane, palmitic acid, and oleic acid between initial preparation, in the liquid phase, and in the solid phase, respectively.

Table E.1 Mass ratio of n-decane, palmitic acid and oleic acid in ternary mixture.

Mass ratio	n-decane	palmitic acid	oleic acid
Initial preparation	1.0007	1.0001	1.0000
liquid phase	1.0945	1.0452	1.0000
solid phase	0.7258	2.6970	1.0000

E.5 Mass Balance

Total mass of n-decane, palmitic acid, and oleic acid in the liquid and the solid phases shows that the percent error of each component is less than $\pm 10\%$:

$$\text{n-decane} = 6.7138 + 0.1957 = 6.9095 \text{ g}$$

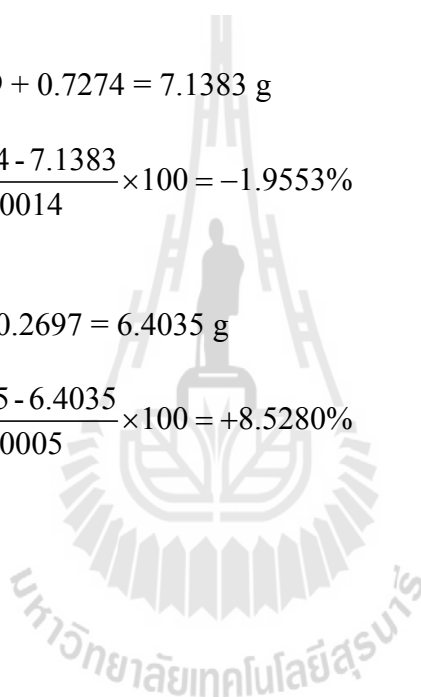
$$\text{Percent error} = \frac{7.0056 - 6.9095}{7.0056} \times 100 = +1.3718\%$$

$$\text{palmitic acid} = 6.4109 + 0.7274 = 7.1383 \text{ g}$$

$$\text{Percent error} = \frac{7.0014 - 7.1383}{7.0014} \times 100 = -1.9553\%$$

$$\text{oleic acid} = 6.1338 + 0.2697 = 6.4035 \text{ g}$$

$$\text{Percent error} = \frac{7.0005 - 6.4035}{7.0005} \times 100 = +8.5280\%$$





APPENDIX F

**ESTIMATION OF LIQUID SPECIFIC HEAT CAPACITY OF
PURE FATTY ACIDS AND TERNARY MIXTURES**

F.1 Palmitic Acid, $\text{CH}_3(\text{CH}_2)_{14}\text{COOH}$

The liquid specific heat capacity of pure palmitic acid can be estimated using the method of Rowlinson-Bodi with $T_c = 799.74$ and $\omega = 0.728$ as presented in the topic of theory in Chapter 2.

$$\begin{aligned} \frac{\bar{C}_p - C_p^\circ}{8.31451} = & 1.45 + 0.45 \left(1 - \frac{T}{799.74}\right)^{-1} \\ & + 0.25(0.728) \left[17.11 + 25.2 \left(1 - \frac{T}{799.74}\right)^{1/3} \left(\frac{T}{799.74}\right)^{-1} + 1.742 \left(1 - \frac{T}{799.74}\right)^{-1} \right] \end{aligned} \quad (\text{F.1})$$

where $T = 66.64^\circ\text{C} = 66.64 + 273.15 = 339.79 \text{ K}$

Calculation of C_p° from Eq. (2.8):

$$\begin{aligned} C_p^\circ = & [0.6087 + (0.3945 \times 14) + 1.4055] \\ & + [2.1433 + (2.1363 \times 14) + 3.4632] \times 10^{-2} \times T \\ & + [(-0.0852) + (-0.1197 \times 14) + (-0.2557)] \times 10^{-4} \times T^2 \\ & + [0.001135 + (0.002596 \times 14) + 0.006886] \times 10^{-6} \times T^3 \end{aligned}$$

$$\begin{aligned} C_p^\circ(T = 339.79 \text{ K}) = & 7.5372 + (35.5147 \times 10^{-2} \times T) - (2.0167 \times 10^{-4} \times T^2) \\ & + (0.044365 \times 10^{-6} \times T^3) \\ = & 106.6688 \times 4.187 \\ = & 446.6223 \text{ J/mol} \cdot \text{K} \end{aligned}$$

Calculation of \bar{C}_p from Eq. (F.1):

$$\begin{aligned} \bar{C}_p(T = 339.79 \text{ K}) = & (14.8745 \times 8.31451) + 446.6223 \\ = & 570.2964 \text{ J/mol} \cdot \text{K} \end{aligned}$$

Molecular weight of palmitic acid, MW = 256.42 g/mol

$$\therefore \bar{C}_p(T = 339.79 \text{ K}) = \frac{570.2964}{256.42} = 2.224 \text{ J/g} \cdot \text{K}$$

F.2 Oleic Acid, $\text{CH}_3(\text{CH}_2)_7\text{CH}=\text{CH}(\text{CH}_2)_7\text{COOH}$

Like as the pure palmitic acid, specific heat capacity in liquid phase for pure oleic acid can be calculated by method of Rowlinson-Bodi with $T_c = 819.14 \text{ K}$ and $\omega = 1.185$ as shown in Eq. (F.2).

$$\begin{aligned} \frac{\bar{C}_p - C_p^o}{8.31451} = & 1.45 + 0.45 \left(1 - \frac{T}{819.14} \right)^{-1} \\ & + 0.25(1.185) \left[17.11 + 25.2 \left(1 - \frac{T}{819.14} \right)^{1/3} \left(\frac{T}{819.14} \right)^{-1} + 1.742 \left(1 - \frac{T}{819.14} \right)^{-1} \right] \end{aligned} \quad (\text{F.2})$$

where $T = 16.00^\circ\text{C} = 16.00 + 273.15 = 289.15 \text{ K}$

Calculation of C_p^o from Eq. (2.8):

$$\begin{aligned} C_p^o = & [0.6087 + (0.3945 \times 7) + (-3.121) + (0.3945 \times 7) + 1.4055] \\ & + [2.1433 + (2.1363 \times 7) + 3.806 + (2.1363 \times 7) + 3.4632] \times 10^{-2} \times T \\ & + [(-0.0852) + (-0.1197 \times 7) + (-0.2359) + (-0.1197 \times 7) + (-0.2557)] \times 10^{-4} \times T^2 \\ & + [0.001135 + (0.002596 \times 7) + 0.005504 + (0.002596 \times 7) + 0.006886] \times 10^{-6} \times T^3 \end{aligned}$$

$$\begin{aligned} C_p^o(T = 289.15 \text{ K}) = & 4.4162 + (39.3207 \times 10^{-2} \times T) - (2.2526 \times 10^{-4} \times T^2) \\ & + (0.049869 \times 10^{-6} \times T^3) \\ = & 100.4841 \times 4.187 \\ = & 420.7269 \text{ J/mol} \cdot \text{K} \end{aligned}$$

Calculation of \bar{C}_p from Eq. (F.2):

$$\begin{aligned}\bar{C}_p(T = 289.15 \text{ K}) &= (26.3041 \times 8.31451) + 420.7269 \\ &= 639.4326 \text{ J/mol} \cdot \text{K}\end{aligned}$$

Molecular weight of palmitic acid, $MW = 282.47 \text{ g/mol}$

$$\therefore \bar{C}_p(T = 289.15 \text{ K}) = \frac{639.4326}{282.47} = 2.264 \text{ J/g} \cdot \text{K}$$

F.3 Ternary Mixture with Mass Ratio (D:P:O) of 1:1:1

Molar fractions for n-decane (D), palmitic acid (P), and oleic acid (O) in ternary mixture with mass ratio (D:P:O) of 1:1:1 are $x_D = 0.4857$, $x_P = 0.2695$, and $x_O = 0.2447$. The liquid specific heat capacity for ternary mixture can be estimated from Eq. (2.9):

$$\bar{C}_{pm} = 0.4857 \times \bar{C}_{p,n\text{-decane}} + 0.2695 \times \bar{C}_{p,palmitic\ acid} + 0.2447 \times \bar{C}_{p,oleic\ acid} \quad (\text{F.3})$$

where $T = 69.06^\circ\text{C} = 66.64 + 273.15 = 342.21 \text{ K}$


n-Decane (Eq. 2.5): $\bar{C}_p = 2.3563 \text{ J/g} \cdot \text{K}$

Palmitic acid: $\bar{C}_p = 2.2305 \text{ J/g} \cdot \text{K}$

Oleic acid: $\bar{C}_p = 2.1630 \text{ J/g} \cdot \text{K}$

Calculation of \bar{C}_{pm} from Eq. (F.3):

$$\therefore \bar{C}_{pm} = 2.275 \text{ J/g} \cdot \text{K}$$



APPENDIX G

SOLID-LIQUID EQUILIBRIUM BY

NRTL AND UNIQUAC MODELS

มหาวิทยาลัยเทคโนโลยีสุรนารี

NRTL and UNIQUAC equations are used for correlation of the activity coefficient of solid–liquid equilibrium of palmitic acid in n-decane – oleic acid. Both equations are application to partially miscible as well as completely miscible systems.

The MATLAB routine for Broyden’s method is used to determine parameters in nonlinear system of NRTL and UNIQUAC equations. This method, unlike Newton’s method, is not necessary to compute the exact value of the Jacobian at each iteration. Broyden’s method provides a way of updating an estimate of the Jacobian.

Ternary mixture of n-decane (1) + palmitic acid (2) + oleic acid (3) contains six interaction parameters, which consist of τ_{12} , τ_{13} , τ_{21} , τ_{23} , τ_{31} and τ_{32} . Six nonlinear algebraic equations of activity coefficients are needed to use for calculation.

G.1 NRTL Model

Function of Broyden’s method for the NRTL equation in MATLAB defines three significant parameters, which consist of equation1, jacob and x.

The first parameter, equation1 is a vector function of x, it has six equations which can be written in expanded form as,

$$\left. \begin{aligned} \text{eq1}(x_1, x_2, x_3, \dots, x_6) &= 0 \\ \text{eq2}(x_1, x_2, x_3, \dots, x_6) &= 0 \\ \text{eq3}(x_1, x_2, x_3, \dots, x_6) &= 0 \\ \text{eq4}(x_1, x_2, x_3, \dots, x_6) &= 0 \\ \text{eq5}(x_1, x_2, x_3, \dots, x_6) &= 0 \\ \text{eq6}(x_1, x_2, x_3, \dots, x_6) &= 0 \end{aligned} \right\} \text{equation1}$$

The second parameter, jacob is the Jacobian matrix of 6×6 obtained from the differential method of each equation, which can be written as,

$$\text{jacob} = \begin{pmatrix} \frac{\partial \text{eq1}}{\partial x_1} & \frac{\partial \text{eq1}}{\partial x_2} & \frac{\partial \text{eq1}}{\partial x_3} & \dots & \frac{\partial \text{eq1}}{\partial x_6} \\ \frac{\partial \text{eq2}}{\partial x_1} & \frac{\partial \text{eq2}}{\partial x_2} & \frac{\partial \text{eq2}}{\partial x_3} & \dots & \frac{\partial \text{eq2}}{\partial x_6} \\ \vdots & \vdots & \vdots & \vdots & \vdots \\ \frac{\partial \text{eq6}}{\partial x_1} & \frac{\partial \text{eq6}}{\partial x_2} & \frac{\partial \text{eq6}}{\partial x_3} & \dots & \frac{\partial \text{eq6}}{\partial x_6} \end{pmatrix}$$

And the last parameter, x is the initial values of six interaction parameters, $x_1 = \tau_{12}$, $x_2 = \tau_{13}$, $x_3 = \tau_{21}$, $x_4 = \tau_{23}$, $x_5 = \tau_{31}$ and $x_6 = \tau_{32}$. Broyden's method for the NRTL equation was written in MATLAB function as below,

```
function [x f I] = BM(equation1,jacob,x)
```

```
maxiter = 5000;
```

```
%First Iteration
```

```
I = 1;
```

```
xold = x;
```

```
B0 = feval(jacob,xold);
```

```
f = feval(equation1,xold);
```

```
invB0 = B0.^-1;
```

```
deltax = -invB0*f;
```

```
%deltax = xnew-xold
```

```
xnew = xold + (deltax.*0.25);
```

```
AbsTol = 1.6e-5;
```

```

while norm(deltax) > AbsTol & I < maxiter

    norm(deltax)

    fold = feval(equation1,xold);

    fnew = feval(equation1,xnew);

    y = fnew - fold;

    s = deltax;

    Bold = feval(jacob,xold);

    invBold = Bold.^-1;

    invBnew = invBold + (((s-(invBold*y))*(s'*invBold))./(s'*invBold*y));

    xold = xnew;

    f = feval(equation1,xold);

    deltax = -invBnew*f;

    xnew = xold + (deltax.*0.25);

    I=I+1;

end

norm(deltax)

if I > maxiter

    disp('divergence')

    return

end

x=xnew;

f=feval(equation1,x);

I;

```

G.2 UNIQUAC Model

In the same way for Broyden's method of UNIQUAC equation, three significant parameters compose of equation, jacob and x. Function of Broyden's method for UNIQUAC equation in MATLAB can be written as,

```
function [x f I] = BM(equation,jacob,x)
```

```
maxiter = 5000;
```

```
%First Iteration
```

```
I = 1;
```

```
xold = x;
```

```
B0 = feval(jacob,xold);
```

```
f = feval(equation,xold);
```

```
invB0 = B0.^-1;
```

```
deltax = -invB0*f;
```

```
%deltax = xnew-xold
```

```
xnew = xold + (deltax.*0.30);
```

```
AbsTol = 5.5e-6;
```

```
while norm(deltax) > AbsTol & I < maxiter
```

```
    norm(deltax)
```

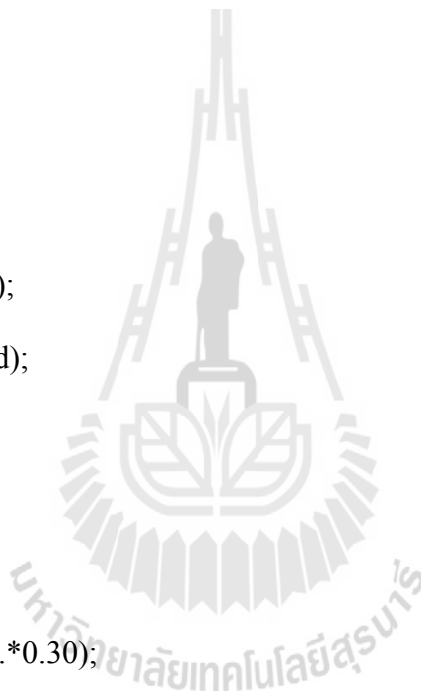
```
    fold = feval(equation,xold);
```

```
    fnew = feval(equation,xnew);
```


```
    y = fnew - fold;
```

```
    s = deltax;
```

```
    Bold = feval(jacob,xold);
```



```
invBold = Bold.^-1;
invBnew = invBold + (((s-(invBold*y))*(s'*invBold))./(s'*invBold*y));
xold = xnew;
f = feval(equation,xold);
deltax = -invBnew*f;
xnew = xold + (deltax.*0.30);
I=I+1;
end
norm(deltax)
if I > maxiter
    disp('divergence')
    return
end
x=xnew;
f=feval(equation,x);
I;
```



BIOGRAPHY

Miss Wanida Potong was born on August 31, 1984 in Rayong Province, Thailand. She received her Bachelor's Degree in Engineering (Chemical Engineering) from Suranaree University of Technology in 2008. During her bachelor degree study in 2007, she participated in the Cooperative Education Program for four months in field of chemical engineering at PTT Public Co., Ltd. Chonburi Pipeline Operation Center with the topic of risk study of internal corrosion factor affected on offshore natural gas pipeline system (eastern seashore). After graduation, she continued study in master degree in the Chemical Engineering Program, Institute of Engineering, Suranaree University of Technology. Her master thesis is financially supported by the Industry/University Cooperative Research Center (I/UCRC) in HDD Component, the Faculty of Engineering, Khon Khaen University and National Electronics and Computer Tecnology Center (NECTEC), National Science and Technology Development Agency (NSTDA). During her master degree study, she has been the teacher assistant scholarship in faculty of chemical engineering.